

UNIVERSITÄT
BAYREUTH

Soil erosion and conservation potential of row crop farming in mountainous landscapes of South Korea

Dissertation

to attain the academic degree of Doctor of Natural Science (Dr. rer. nat.)
of the Bayreuth Graduate School of Mathematical and Natural Sciences (BayNAT)
of the University of Bayreuth

presented by
Sebastian Arnhold
born 21 August 1982
in Erlabrunn (Germany)

Bayreuth, October 2012

This doctoral thesis was prepared at the Department of Soil Physics, University of Bayreuth, between March 2009 and October 2012. It was supervised by Prof. Dr. Bernd Huwe, Prof. Dr. Thomas Koellner, and Dr. Christopher L. Shope.

This is a full reprint of the dissertation submitted to attain the academic degree of Doctor of Natural Science (Dr. rer. nat.) and approved by the Bayreuth Graduate School of Mathematical and Natural Sciences (BayNAT) of the University of Bayreuth.

Date of submission: 10 October 2012

Date of scientific colloquium: 22 January 2013

Acting director:

Prof. Dr. Franz X. Schmid

Doctoral committee:

Prof. Dr. Stefan Peiffer (chairman)

Prof. Dr. Bernd Huwe (first reviewer)

Prof. Dr. John Tenhunen (second reviewer)

Prof. Dr. Thomas Koellner

Abstract

Soils play an essential role for mankind because they provide fundamental ecosystem services required for human life, primarily for the production of food by providing the environment for plant growth. However, soils worldwide became highly threatened by human induced degradation, especially as a consequence of accelerated erosion by water during recent decades. In consideration of climate change and an increasing food demand of a rising population, there is an urgent need to conserve the soil resources by implementing effective erosion control measures for agricultural production. The effective implementation of those measures strongly depends on the specific conditions of particular regions and requires the analysis of the existing farming systems and their capability for erosion control.

Objective of this thesis is the analysis of the major agricultural practices applied for row crop cultivation in mountainous watersheds of South Korea with respect to water erosion and the identification of their conservation potential. Our first two studies analyze the subsurface flow processes, the runoff patterns, and the associated erosion rates of the widely applied plastic covered ridge-furrow system (plastic mulch), and our third study investigates the impact of herbicide applications on erosion associated with conventional and organic farming. To analyze the flow processes induced by the plastic mulch cultivation, we conducted four irrigation experiments on potato fields that represent a smooth surface, uncovered ridges, and plastic covered ridges with and without a developed crop canopy. With an automatic sprinkler, we irrigated small plots with a dye tracer solution of *Brilliant Blue* and *potassium iodide*, collected surface runoff, and excavated soil profiles to visualize the subsurface flow patterns, which were subsequently analyzed by image index functions. We found that the ridge-furrow system, especially when ridges are covered with plastic, decreased infiltration and generated high amounts of surface runoff, whereas a developed crop canopy increased infiltration due to interception and stem flow. The analyses of the subsurface flow patterns show that the plastic covered ridge-furrow system induces preferential infiltration in furrows and planting holes due to its topography and the impermeable covers, but that the impact on flow processes in the soils is relatively small compared to the impact on runoff generation. To identify the patterns of overland flow and the erosion rates associated with the plastic mulch system, we installed runoff collectors to monitor runoff and sediment transport of two potato fields with concave and convex topographies, and we applied the EROSION 3D model to compare the plastic covered ridge-furrow system to uncovered ridges and a smooth surface. We found that plastic mulch cultivation considerably increases soil erosion compared to uncovered ridges as a consequence of high amounts of surface runoff. Our results show that the ridge-furrow system concentrated overland flow on the concave field, resulting in severe gully erosion, but prevented flow accumulation and reduced erosion on the convex field, which demonstrates that the effect of this cultivation strategy is primarily controlled by the field topography and its orientation. To analyze the effects of conventional and organic farming on water erosion, we measured multiple vegetation parameters of crops and weeds of conventional and organic farms cultivating bean, potato, radish, and cabbage, and we simulated long-term soil loss rates with the Revised Universal Soil Loss Equation (RUSLE). We found that organic farming reduced erosion for radish, as a result of an increased weed biomass due to the absence of herbicides, but that it increased erosion for potato due to lower crop coverage, presumably as a consequence of crop-weed competition or herbivory associated with the absence of agricultural chemicals. Although we demonstrated that a developed weed cover in the furrows can potentially decrease the erosion risk for row crops, our results show that the average annual erosion rates of both farming systems exceed by far any tolerable soil loss.

In consideration of the generally high soil loss found in our studies, we conclude that the applied farming practices are not capable for effective erosion control and soil conservation in this region. However, based on our findings, we

could identify possible modifications of those practices that can help to reduce the risk of erosion in the future. We recommend perforated plastic covers for ridges to reduce runoff generation, and the orientation of the ridge-furrow system along the contours or towards field edges to prevent flow accumulation and gully formation. Additionally, we suggest residue mulching of furrows to protect the soil surface from overland flow, and the cultivation of winter cover crops after harvest to maintain a better soil cover throughout the year.

Zusammenfassung

Böden spielen eine entscheidende Rolle für die Menschheit durch die Bereitstellung von grundlegenden Ökosystem-Dienstleistungen, insbesondere für die Produktion von Nahrungsmitteln. Dennoch sind Böden weltweit einer zunehmenden Zerstörung ausgesetzt, die hauptsächlich durch vom Menschen intensivierte Erosion verursacht wird. Vor dem Hintergrund von Klimawandel und dem steigenden Nahrungsmittelbedarf einer wachsenden Weltbevölkerung, ist die Erhaltung der Bodenressourcen, durch die Umsetzung effektiver Erosionsschutzmaßnahmen, unumgänglich. Die Wirksamkeit dieser Maßnahmen hängt jedoch stark von den lokalen Gegebenheiten in den verschiedenen Regionen der Welt ab und erfordert eine intensive Untersuchung der landwirtschaftlichen Praktiken und deren Eignung zur Erosionsminderung.

Ziel dieser Arbeit ist die Analyse der vorherrschenden Ackerbauverfahren für Reihenkulturen in den Bergregionen von Südkorea, in Hinblick auf Bodenerosion sowie deren Potenzial für den Erosionsschutz. In den ersten beiden Studien dieser Arbeit untersuchten wir den verbreiteten Reihenanbau mit Folienabdeckung (Plastic Mulch) und die dadurch hervorgerufenen Fließprozesse im Boden, Abflussmuster und Erosionsraten, und in der dritten Studie analysierten wir den Einfluss von Herbizid-Einsatz auf Erosion im Zusammenhang mit konventioneller und biologischer Landwirtschaft. Um die Fließprozesse im Boden zu untersuchen, wurden vier Beregnungsexperimente durchgeführt, die verschiedene Anbauverfahren und Vegetationsstadien repräsentierten. Mithilfe eines automatischen Beregners besprühten wir die Bodenoberfläche mit einer Tracer-Lösung mit *Brilliant Blue* und *Kaliumiodid*, bestimmten die Abflussmengen und legten anschließend Profile frei, um die unterirdischen Fließwege zu visualisieren, die dann mit Bild-Indizes analysiert wurden. Wir fanden heraus, dass der Reihenanbau, insbesondere mit Folienabdeckung, die Infiltration herabsetzte und zu erhöhter Abflussbildung führte, während ein ausgebildeter Pflanzenbestand durch Interzeption und Stammabfluss die Infiltration begünstigte. Die Analysen der Fließwege zeigten, dass der Reihenanbau durch seine Oberflächenform und die Wasserundurchlässigkeit der Folie präferenzielle Infiltration induziert, die Fließprozesse im Boden allerdings nur geringfügig beeinflusst. Um die Fließmuster des Oberflächenabflusses und die damit verbundene Erosion zu untersuchen, wurden Abfluss-Kollektoren auf zwei Feldern mit konkaver und konvexer Topographie installiert, um Abfluss und Sedimenttransport zu messen. Mithilfe des Modells EROSION 3D haben wir anschließend den Reihenanbau mit Folienabdeckung mit anderen Anbauverfahren verglichen. Wir fanden heraus, dass durch die verstärkte Abflussbildung infolge der Abdeckung die Erosion deutlich erhöht wurde. Unsere Ergebnisse zeigten, dass der Reihenanbau auf dem konkaven Feld den Abfluss konzentrierte und zu starker Gully-Erosion führte, während er auf dem konvexen Feld Abflussakkumulation verhinderte und damit die Erosion verringerte, was verdeutlicht, dass der Effekt dieses Anbauverfahrens in erster Linie von Topographie und Reihenausrichtung bestimmt wird. Um den Einfluss von konventioneller und biologischer Landwirtschaft auf die Bodenerosion zu analysieren, wurden verschiedene Vegetationsmerkmale von Feldfrüchten und Unkräutern von konventionellen und biologischen Betrieben gemessen und die langjährigen Abtragsraten mithilfe der Revised Universal Soil Loss Equation (RUSLE) simuliert. Wir fanden heraus, dass durch den Verzicht auf Herbizide, der eine erhöhte Unkrautentwicklung zur Folge hatte, der biologische Anbau von Rettich die Erosion minderte. Bei Kartoffeln hingegen wurde durch den biologischen Anbau aufgrund eines geringer entwickelten Pflanzenbestandes die Erosion erhöht, was wahrscheinlich eine Folge von Konkurrenz mit Unkräutern oder Fraßschäden war. Obwohl wir gezeigt haben, dass eine höhere Bodenbedeckung durch Unkräuter das Erosionsrisiko senken kann, verdeutlichen unsere Ergebnisse auch, dass die jährlichen Erosionsraten beider Anbaustrategien bei weitem den tolerierbaren Bodenabtrag übersteigen.

In Anbetracht der generell hohen Erosionsraten in unseren Studien, stellen wir fest, dass die angewandten landwirtschaftlichen Praktiken in dieser Region nicht für einen effizienten Erosionsschutz geeignet sind. Dennoch konnten wir aufgrund unserer Ergebnisse mögliche Nachbesserungen identifizieren, die dabei helfen können, das Erosionsrisiko zu mindern. Wir empfehlen den Einsatz von perforierter Folie zur Reihenabdeckung, um die Abflussbildung zu reduzieren, und die Ausrichtung der Reihen entlang von Höhenlinien oder in Richtung der Feldränder, um Abflussakkumulation und Gully-Bildung zu verhindern. Darüberhinaus schlagen wir das Mulchen mit Pflanzenrückständen vor, um die Furchen vor Oberflächenabfluss zu schützen, sowie den Anbau von Wintergetreide nach der Ernte, um eine bessere Bodenbedeckung über das Jahr zu gewährleisten.

Acknowledgements

I would like to thank everyone who supported me in my work on this thesis, especially the people who helped me with my research with their experience and advices and by working together with me in the field and laboratory, but also those who were there to encourage me to meet the various challenges that came up during the last years.

I am sincerely grateful to my advisers Prof. Bernd Huwe, Prof. Thomas Koellner, and Dr. Christopher Shope as well as Dr. Christina Bogner for their guidance, their good ideas and useful critiques, and the uncountable helpful comments concerning our field work designs, modeling strategies, and data analysis problems, but also for their valuable help with writing and editing the individual manuscripts of this thesis.

I would like to thank Prof. John Tenhunen and all my colleagues of the TERRECO-IRTG, who became close friends during the last years, especially Steve Lindner, Marianne Ruidisch, and Svenja Bartsch for the excellent cooperation, the fruitful discussions, and for the moments we shared together in Bayreuth and Haean. My special thanks go to Bora Lee and Eunyoung Jung for their substantial efforts in translation and for negotiating our working permissions with the local farmers, and to Bumsuk Seo for his invaluable help with programming R algorithms and for finding solutions for numerous GIS problems.

I wish to give my great appreciation also to Andreas Kolb for his powerful support during the field installations and his experience in solving unexpected technical problems, and to Margarete Wartinger and Iris Schmiedinger for their outstanding help in the laboratory.

Finally, I would like to express my special thanks to Heera Lee, not only for her support in organizing our experiments and her help on data management, but also for being always around to listen to my problems, and for giving me motivation and new energy for my work. I also want to thank my brother Daniel and my parents Ute and Hans-Jürgen for their support, their understanding, and encouragement, without which I would not have been able to accomplish this thesis.

Table of contents

Abstract.....	i
Zusammenfassung	iii
Acknowledgements.....	v
Table of contents	vi
List of figures.....	ix
List of tables	xi
List of abbreviations	xii
List of symbols	xiv

Chapter 1

Synopsis	1
1.1 Introduction	1
1.1.1 Soil ecosystem services, soil erosion, and conservation	1
1.1.2 Objectives and state of knowledge	3
1.2 Materials and methods	7
1.2.1 Research area and study sites	7
1.2.2 Analysis of flow processes of plastic covered ridge-furrow cultivation	9
1.2.3 Analysis of runoff patterns and soil erosion of plastic covered ridge-furrow cultivation	10
1.2.4 Analysis of soil erosion and conservation potential of conventional and organic row crop cultivation	12
1.3 Results and discussion	14
1.3.1 Flow processes of plastic covered ridge-furrow cultivation.....	14
1.3.2 Runoff patterns and soil erosion of plastic covered ridge-furrow cultivation	15
1.3.3 Soil erosion and conservation potential of conventional and organic row crop cultivation	16
1.4 Conclusions and recommendations.....	19
1.5 List of manuscripts and specification of individual contributions	24
1.6 References	25

Chapter 2

Effects of ridge tillage on flow processes in the Haean catchment, South Korea.....	31
Abstract.....	31
2.1 Introduction	32
2.2 Materials and methods	33
2.2.1 Study site.....	33
2.2.2 Experimental set-up	33
2.2.3 Statistical analysis	35
2.2.4 Image processing.....	35
2.2.5 Image index functions	35
2.3 Results and discussion	38

2.3.1 Water balance and water content.....	38
2.3.2 Analysis of flow patterns.....	39
2.3.3 The effect of tillage management on flow processes and its ecological implications	42
2.4 Conclusions	43
2.5 Acknowledgements.....	43
2.6 References	44

Chapter 3

Plastic covered ridge-furrow systems on mountainous farmland: runoff patterns and soil erosion rates	46
Abstract.....	46
3.1 Introduction	47
3.2 Materials and methods	48
3.2.1 Study area.....	48
3.2.2 Observation of runoff and soil erosion.....	49
3.2.3 Simulation of runoff and soil erosion.....	51
3.3 Results and discussion	54
3.3.1 Observed runoff and soil erosion	54
3.3.2 Simulated runoff and soil erosion	54
3.4 Summary and conclusions	60
3.5 Acknowledgements.....	61
3.6 References	61

Chapter 4

Conventional and organic farming: soil erosion and conservation potential for row crop cultivation.....	64
Abstract.....	64
4.1 Introduction	65
4.2 Materials and methods	66
4.2.1 Study area.....	66
4.2.2 Erosion simulation with the Revised Universal Soil Loss Equation	68
4.2.2.1 Rainfall and runoff erosivity factor (<i>R</i>)	68
4.2.2.2 Soil erodibility factor (<i>K</i>)	69
4.2.2.3 Slope length and steepness factors (<i>L</i> and <i>S</i>), and support practice factor (<i>P</i>)	69
4.2.2.4 Cover-management factor (<i>C</i>)	71
4.2.2.5 Calculation of soil erosion rates	74
4.2.3 Model plausibility	74
4.3 Results and discussion	74
4.3.1 Rainfall and runoff erosivity factor (<i>R</i>).....	74
4.3.2 Soil erodibility factor (<i>K</i>).....	76
4.3.3 Slope length and steepness factors (<i>L</i> and <i>S</i>), and support practice factor (<i>P</i>).....	77
4.3.4 Cover-management factor (<i>C</i>).....	78
4.3.5 Soil erosion rates	83

4.3.6 Model plausibility	84
4.4 Summary and conclusions	85
4.5 Acknowledgements.....	86
4.6 References	87
Appendix	
List of other publications	90
Declaration / Erklärung.....	91

List of figures

Figure 1.1 Location of the study area (Haean-Myeon catchment) on the Korean peninsula (a) and within the watershed of the Soyang Reservoir (b) with the locations of the experimental sites selected for the three studies of this thesis (c). The study on flow processes were conducted at site F1 and F2 (chapter 2), runoff patterns and erosion at site M1 and M2 (chapter 3), and the impact of the farming systems at the sites 01 to 25 (chapter 4)	8
Figure 1.2 Irrigation experiment with dye tracer <i>Brilliant Blue FCF</i> and <i>potassium iodide</i> . Automatic sprinkler spraying tracer solution on the field plot with plastic covered ridges and furrows (a) and excavated soil profile for visualizing the subsurface flow patterns (b)	9
Figure 1.3 Runoff sampler for measuring runoff volume and sediment mass according to Bonilla <i>et al.</i> (2006). Runoff collectors (a) and multislot flow divider according to Pinson <i>et al.</i> (2004) (b).....	11
Figure 2.1 Images processing from a) rectified dye tracer image to b) background image, and c) binary image used to calculate image indices	35
Figure 2.2 Left to right: example of a binary image and three index functions: dye coverage I_D , fragmentation I_F and metric entropy I_{MES} . The gray background represents the soil profile and the dye stained patterns are shown in black. For explanation of circles and arrows see section 2.2.5	38
Figure 2.3 The dynamics of water content in different depths during the irrigation experiments CT, RT, and RT_{pm} . The grey area indicates the time of irrigation.....	39
Figure 2.4 Example images of excavated soil profiles and their binary images. From left to right: CT, RT, RT_{pm} , and $RT_{pm+crops}$. Note that the slope orientation differs between field site 1 (CT and RT, slope oriented to the left) and field site 2 (RT_{pm} and $RT_{pm+crops}$, slope oriented to the right). In the color image of $RT_{pm+crops}$, the white feature on the right hand ridge is a potato cut in half.....	41
Figure 2.5 Image index functions and their 25% and 75% quantiles (colored areas)	42
Figure 3.1 Location of the Haean-Myeon catchment on the Korean peninsula (a) and within the Soyang Lake watershed (b) with locations of the experimental sites conducted for this study (c) (“seminatural areas” include grassland, field margins, riparian areas, small roads and channels)	49
Figure 3.2 Experimental design to measure runoff and soil erosion by installation of three runoff collectors (RC) on field 1 and field 2. Field’s topography and runoff collector drainage areas were calculated based on surface elevation measurements and generation of digital terrain models of both fields.....	50
Figure 3.3 Daily precipitation on field 1 and field 2 during the observation time from 5 July to 9 August 2010. The arrows indicate the sampling dates for the associated rainfall periods.....	51
Figure 3.4 Simulated and observed runoff for field 1 (a) and field 2 (b).....	55
Figure 3.5 Simulated and observed soil loss for field 1 (a) and field 2 (b).....	56
Figure 3.6 Simulated runoff for all rainfall periods for field 1 (a) and field 2 (b) for different management practices (RP: ridges with plastic cover, RU: uncovered ridges, SS: smooth soil surface).....	57
Figure 3.7 Simulated soil loss for all rainfall periods for field 1 (a) and field 2 (b) for different management practices (RP: ridges with plastic cover, RU: uncovered ridges, SS: smooth soil surface).....	58
Figure 3.8 Simulated sediment concentration over all rainfall periods for field 1 and field 2 for different management practices including main flow directions (RP: ridges with plastic cover, RU: uncovered ridges, SS: smooth soil surface).....	59
Figure 3.9 Observed erosion rill formed by ridge breakovers and concentrated flow in the depression line in the center of field 1	59
Figure 4.1 Location of the study area (Haean-Myeon catchment) on the Korean peninsula (a) and within the watershed of the Soyang Lake (b) with the locations of the weather stations and 25 experimental sites (01 to 25) selected for this study (c). The sites M1 and M2 indicate the position of two additional fields where soil loss was measured in 2010, which was used to evaluate model plausibility	67

Figure 4.2 Correlation between rainstorm erosivity calculated on the basis of 1 hour and 30 minutes resolution rainfall records of nine weather stations in the Haean catchment from May 2009 to December 2011. The solid line shows the line of the linear regression through the origin, and the 1:1 line (dotted) is included as reference	75
Figure 4.3 Annual rainfall and <i>R-factor</i> for the Haean catchment for the years 1999 to 2011	75
Figure 4.4 Temporal distribution of rainstorm erosivity (percentage of the half-month period erosivity) within the individual years from January to December for 1999 to 2011	76
Figure 4.5 Growth charts of the four major row crops, bean (a), potato (b), radish (c), and cabbage (d) with crop and weed biomass density (left), and crop cover, weed cover, and canopy height (right). The lower segment of the biomass density plot shows the development of the different crop components and the upper segment shows the development of the associated weeds.....	79
Figure 4.6 Vegetation parameters of crops and weeds measured before harvest for conventional and organic farming of four major row crops. Crop and weed biomass density (a and b), crop and weed cover (c and d), and canopy height (e). The bars show the mean value and the error bars the standard deviation of the associated field sites	81
Figure 4.7 Variation of the <i>C-factor</i> between 1999 and 2011 for conventional (conv.) and organic farming (org.) of the four major row crops, bean (a), potato (b), radish (c), and cabbage (d) for a low degree of disturbance (left) and a high degree of disturbance at harvest (right), and variable planting and harvest times. Early planting means two weeks before, and late planting two weeks after the observed planting and harvest dates of 2009	83

List of tables

Table 2.1 Soil physical properties of the experimental sites	34
Table 2.2 Total amount of irrigation and its partitioning into surface runoff and infiltration.....	38
Table 3.1 Soil and surface parameter values used for the EROSION 3D simulations, divided into uncovered parts of the field (soil surface) and covered parts (plastic film). The third row shows the horizon names of the soil profiles of both fields (according to FAO, 2006)	53
Table 3.2 Observed data for field 1 and field 2. Rainfall characteristics, runoff volume, and sediment mass measured by the runoff collectors (RC 1, RC 2, RC 3), and derived mean runoff and soil loss rates of the whole field.....	54
Table 4.1 Soil characteristics (organic matter and texture) and topography (slope angle and slope length) of the 25 field sites with the calculated <i>K-factors</i> , <i>L-factors</i> , <i>S-factors</i> , and contouring <i>P-factors</i> for the Revised Universal Soil Loss Equation.....	77
Table 4.2 Simulated average annual soil loss for conventional and organic farming of the four major row crops in the Haeon catchment. Mean, maximum, and minimum refer to the simulated soil loss over all 25 field sites.....	84
Table 4.3 Rainfall erosivity, factors for the Revised Universal Soil Loss Equation, and simulated soil loss for the sites M1 and M2 in comparison to the observed soil loss measured during the monsoon season of 2010	85

List of abbreviations

Abbreviation	Meaning
^{137}Cs	caesium-137
Ap	soil A horizon (ploughed)
Apb	soil A horizon (ploughed, buried)
ASABE	American Society of Agricultural and Biological Engineers
Bw	soil B horizon (developed color or structure)
Bwb	soil B horizon (developed color or structure, buried)
BwC	soil transitional horizon between Bw and C
C	soil C horizon
CH_4	methane
CO_2	carbon dioxide
conv.	conventional
CT	conventional tillage
DEM	digital elevation model
DFG	Deutsche Forschungsgemeinschaft
DTM	digital terrain model
FAO	Food and Agriculture Organization of the United Nations
FDR	frequency domain reflectometry
GIS	geographical information system
GLEAMS	Groundwater Loading Effects of Agricultural Management Systems
HSI	hue, saturation, intensity color space
InVEST	Integrated Valuation of Ecosystem Services and Tradeoffs
IPCC	Intergovernmental Panel on Climate Change
IRTG	International Research Training Group
ISELE	International Symposium on Erosion and Landscape Evolution
IUSS	International Union of Soil Sciences
KOSEF	Korea Science and Engineering Foundation
KRF	Korea Research Foundation
LiDAR	light detection and ranging
LISEM	Limburg Soil Erosion Model
N_2O	nitrous oxide
NAAS	National Academy of Agricultural Science
NRCS	National Resources Conservation Service
OECD	Organization for Economic Cooperation and Development
org.	organic
PVC	polyvinyl chloride
RC	runoff collector
RGB	red, green, blue color space

RP	ridges with plastic
RT	ridge tillage
RT _{pm}	ridge tillage with plastic mulch
RT _{pm+crops}	ridge tillage with plastic mulch and developed crop canopy
RU	uncovered ridges
RUSLE	Revised Universal Soil Loss Equation
SI	système international d'unités
SS	smooth surface
SWAT	Soil and Water Assessment Tool
TERRECO	Complex Terrain and Ecological Heterogeneity
USDA	United States Department of Agriculture
USGS	United States Geological Survey
USLE	Universal Soil Loss Equation
WEPP	Water Erosion Prediction Project
WRB	World Reference Base for Soil Resources

List of symbols

Symbol	Definition	Unit
A	average annual soil loss	[t ha ⁻¹ yr ⁻¹]
b	surface cover coefficient	[-]
B_{ur}	mass density of live and dead roots	[g m ⁻²]
B_{us}	mass density of incorporated surface residue	[g m ⁻²]
C	bucket sediment concentration	[kg L ⁻¹]
C_b	effectiveness of subsurface residue in consolidation	[-]
CC	canopy cover subfactor	[-]
C_f	surface-soil consolidation factor	[-]
C -factor	cover-management factor	[-]
c_{uf}, c_{ur}, c_{us}	subsurface residue coefficients	[-]
e	unit energy of rainfall	[MJ ha ⁻¹ mm ⁻¹]
EI	percentage of rainfall erosivity	[%]
EI_{30}	rainfall erosivity	[MJ mm ha ⁻¹ h ⁻¹]
F_c	fraction of land area covered by canopy	[-]
h	information content	[-]
H	average information content (Shannon's entropy) (<i>chapter 2</i>)	[-]
H	raindrop fall height from canopy (<i>chapter 4</i>)	[m]
H_b	height to canopy bottom	[m]
H_t	height to canopy top	[m]
i	rainfall intensity	[mm h ⁻¹]
I_C	contiguity	[-]
I_D	dye coverage	[-]
I_E	Euler number	[-]
I_F	fragmentation	[-]
I_{MAX}	maximum run length	[-]
I_{MES}	metric entropy ($L = 8$)	[-]
I_{MEL}	metric entropy	[-]
K -factor	soil erodibility factor	[t h MJ ⁻¹ mm ⁻¹]
L	length of sequences ("words")	[-]
L -factor	slope length factor	[-]
m	row length of binary image	[-]
M	product of primary particle size fractions	[-]
n	number of events (<i>chapter 2</i>)	[-]
n	Manning's roughness coefficient (<i>chapter 3</i>)	[s m ^{-1/3}]
NSE	Nash-Sutcliffe efficiency	[-]
OM	organic matter content	[%]
p	probability (<i>chapter 2</i>)	[-]

p	soil permeability code (<i>chapter 4</i>)	[-]
P_0	on-grade contouring support practice factor	[-]
$PBIAS$	percent bias	[-]
P -factor	support practice factor	[-]
PLU	prior land use subfactor	[-]
\bar{r}	row of binary image	[-]
R	total runoff volume	[L]
R_l	function calculating sequence of run lengths	[-]
R^2	coefficient of determination	[-]
R -factor	rainfall and runoff erosivity factor	[MJ mm ha ⁻¹ h ⁻¹ yr ⁻¹]
r_i	pixel value of binary image row	[-]
$RMSE$	root mean square error	[-]
RSR	$RMSE$ -observation standard deviation ratio	[-]
R_U	surface roughness	[cm]
s	soil structure code	[-]
S	total sediment mass	[kg]
$sand$	percentage of sand	[%]
SC	surface cover subfactor	[-]
S -factor	slope steepness factor	[-]
$silt$	percentage of silt	[%]
SLR	soil loss ratio	[-]
SM	soil moisture subfactor	[-]
S_p	percentage of land area covered by surface cover	[%]
SR	surface roughness subfactor	[-]
\bar{u}	point coordinates on original image	[-]
\bar{v}	point coordinates on corrected image	[-]
V	bucket runoff volume	[L]
vfs	percentage of very fine sand	[%]
\bar{w}	sequence of pixels of binary image (“words”)	[-]
W_L	sliding window extracting sequences (“words”)	[-]
x	outcome of random variable X	[-]
X	random variable	[-]
β	ratio of rill to interrill erosion	[-]
θ	slope angle	[°]
θ_f	slope angle along furrows	[°]
θ_v	volumetric water content	[cm ³ cm ⁻³]
κ	magnitude of radial distortion	[-]
λ	slope length	[m]

Chapter 1

Synopsis

1.1 Introduction

1.1.1 Soil ecosystem services, soil erosion, and conservation

Soils are an important component of the economics of nations because they provide a series of fundamental ecosystem services (Daily *et al.*, 1997). Ecosystem services are the conditions and processes, through which natural ecosystems sustain and fulfill human life (Daily, 1997). The Millennium Ecosystem Assessment (2005) divide ecosystem services into provisioning services, regulating services, and cultural services that directly affect people, and supporting services, which are needed to maintain the other services. According to Dominati *et al.* (2010), soils provide provisioning, regulating, and cultural services. Presumably the most important provisioning service for human life supplied by soils is the production of food. Agriculture uses 11% of the world's land surface for crop production (FAO, 2011b). Essential functions, necessary for food production, provided by soils are the physical support of plants by the provision of an environment for seed germination and root growth, and the retention and delivery of nutrients (Daily *et al.*, 1997, Powlson *et al.*, 2011). Furthermore, soils provide the pathways, through which water and nutrients move to the roots, they are the matrix for nutrient transformations, and the environment for microorganisms and fauna (Powlson *et al.*, 2011). Regulatory services supplied by soils are flood mitigation due to storage and retention of water, filtering of nutrients because of their ability to absorb and retain solutes, biological control of pests and diseases by providing habitat to beneficial species, and the recycling of wastes and detoxification by the decomposition by soil biota and the absorption and destruction of harmful substances (Dominati *et al.*, 2010). Additionally, soils play an important role in regulating the emissions of greenhouse gases, such as carbon dioxide (CO₂), methane (CH₄), and nitrous oxide (N₂O) due to their high storage capacity of carbon and nitrogen (Daily *et al.*, 1997, Dominati *et al.*, 2010). Soils, as part of the landscape that support vegetation, provide a place to bury deceased persons, and supply the foundation and material to build houses, provide aesthetic, spiritual, and cultural benefits through cultural services (Dominati *et al.*, 2010). Soils are essential for sustaining human life (Daily *et al.*, 1997) and they are a limited and practically a non-renewable resource (Lal, 1994). The U.S. president Franklin D. Roosevelt already described the importance of soils, not only for food production, but for the future of mankind: “*The nation that destroys its soils, destroys itself*” (Powlson *et al.*, 2011).

However, soil resources worldwide became highly threatened by human induced degradation. Soil degradation is the decline in the capacity of soils to produce goods to humans (Lal, 1994). According to Oldeman *et al.* (1990), about 17% of the vegetated land surface has been exposed to human induced degradation since 1945 (Daily *et al.*, 1997). Almost 40% of the agricultural land has been affected by soil degradation and more than 6% is degraded to a degree that restoration to its original productivity is only possible with tremendous investments (Oldeman, 1994). By far the most important type of soil degradation worldwide is soil erosion by water (Oldeman, 1994). Water erosion consists of the detachment of soil particles by rainsplash and runoff, and the transport and deposition of these particles (Morgan, 2005). It is a natural process operating for millions of years, but has been strongly accelerated by human activities (Toy *et al.*, 2002). The loss of protective vegetation through deforestation, over-grazing, fire, and excessive cultivation makes soils highly vulnerable to erosion (Mermut, 2008). Cropland is most susceptible to erosion because the soil is frequently tilled and left without a protective vegetation cover (Pimentel *et al.*, 1995). The worldwide average annual erosion rate from cropland is about 30 t ha⁻¹ yr⁻¹, resulting in about 30% of arable land that has already become unproductive during

the last 40 years (Pimentel, 2006). The degraded crop productivity of eroded soils is a consequence of the reduction of cultivable soil depth and a reduced fertility due to losses of organic matter and nutrients (Morgan, 2005). Soil organic matter, which facilitates the formation of aggregates, increases porosity, and improves soil structure (Pimentel, 2006), and basic plant nutrients, such as nitrogen, phosphorus, potassium, and calcium, which are essential for crop production, are removed by erosion (Pimentel *et al.*, 1995). Additionally, soils can be enriched in coarse particles when fine particles are washed away, which reduces the water-holding capacity that can adversely affect plant growth when water becomes a limiting factor (Toy *et al.*, 2002). In order to maintain the productivity of the agricultural land and to slow down its degradation, additional efforts are necessary and high costs must be paid. Pimentel *et al.* (1995) estimated that about 10% of the energy used in the U.S. agriculture is spent to compensate for the losses of nutrients, water, and crop productivity caused by erosion. In other parts of the world where irrigation is not possible or fertilizers are too expensive, the price of erosion is paid by reduced food production (Pimentel *et al.*, 1995). Erosion will raise the costs for optimizing agricultural management until they become prohibitive, which makes it impossible to sustain production levels (Larson *et al.*, 1983). Accelerated erosion does not only produce enormous problems on the agricultural areas where it occurs (on-site damages) but also negatively affects the surrounding environment (off-site damages) (Pimentel *et al.*, 1995). Off-site damages result from the sedimentation of the eroded soil material downstream, which reduces the capacity of rivers and channels, enhances the risk of flooding, and influences the function of reservoirs, for example hydro-electricity generation (Morgan, 2005). Furthermore, sediment contains adsorbed chemicals, such as fertilizers and pesticides that degrade water quality in streams and lakes (Toy *et al.*, 2002). The total cost of erosion from agricultural land in the United States including on-site and off-site damages is about 44 billion dollars per year, increasing the actual production costs by about 25% (Pimentel *et al.*, 1995). Different studies indicate that rainfall intensity and the variability and frequency of extreme precipitation events increase as a consequence of climate change (IPCC Working Group I, 2001, Zhai *et al.*, 2005), which would result in a further acceleration of global soil erosion (Nearing *et al.*, 2005). As a consequence, we can expect that the costs of erosion and the degradation of the worldwide soil resources will progressively increase in the future.

Although the soils' ecosystem services are already highly degraded as a consequence of the accelerated erosion, the rising population is expected to result in a 70% increase in global demand for agricultural production by 2050 (FAO, 2011b). However, the world land surface for crop production is limited. The remaining potentially cultivatable areas in the world are marginal for agricultural use because most of the land is either inaccessible or severely constrained by steep terrain, shallow rooting depth, extreme moisture or temperature regimes, or it is located in ecologically sensitive regions (Lal, 1994). Therefore, the intensification of crop production will be required in more marginal production areas with less reliable conditions, lower soil quality, limited access to water, and less favorable climates (FAO, 2011a). To accommodate future food demands, it is inevitable to protect the existing agricultural areas from continuing soil degradation. The FAO (2011a) proposed a sustainable crop production intensification that produces more food from the same area of land while reducing negative environmental impacts (Godfray *et al.*, 2010). This implies primarily the implementation of conservation measures that effectively control soil erosion on agricultural land. Erosion control on agricultural land depends primarily on good management measures, which implies the establishment of sufficient ground cover and the selection of appropriate tillage practices supported by additional mechanical measures (Morgan, 2005). There is a variety of different control measures, which can be classified into active control measures that aim on minimizing the on-site damages by reducing the detachment of soil particles, and passive control measures that aim on reducing off-site damages by retaining detached particles before entering surface water bodies (Schmidt and von Werner, 2000). Standard guidelines such as the *National Conservation Practice Standards* available from the National

Resources Conservation Service (NRCS) describe the design and the application of the different erosion control measures for example contour farming, residue mulching, or filter strips. The effectiveness of the different management measures strongly depends on site specific conditions, such as soil, slope, and topography (Wolfe *et al.*, 2002). Furthermore, conservation measures are often associated with additional costs, labor, and use restrictions. Therefore, effective soil conservation planning requires not only individual treatments depending on the local conditions, but they must be also socially and economically acceptable to the farmers (Morgan, 2005). In order to reduce the costs and to increase the acceptability of control measures, the existing farming systems of the specific regions should be analyzed and integrated in conservation plans, instead of implementing entirely new techniques from outside (Morgan, 2005).

1.1.2 Objectives and state of knowledge

The objective of this thesis is the quantification of soil erosion of farming systems applied in mountainous watersheds in South Korea and the identification of their conservation potential. The agricultural areas in many Korean watersheds are highly susceptible to soil degradation by water erosion due to steep slopes and intense monsoonal rainfall events during the summer months. These rain events in combination with an intensive agriculture do not only produce high amounts of soil loss (Choi *et al.*, 2010, Lee *et al.*, 2010a), but they also contribute to eutrophication problems in many Korean reservoirs due to phosphorus loaded eroded sediments (Kim *et al.*, 2001a). The annual total precipitation has increased as a consequence of the intensification of heavy rain events during the last decades (Choi *et al.*, 2008) and it is expected that the frequency and intensity of heavy rainfall on the Korean peninsula will further increase (Boo *et al.*, 2006). This development implicates higher future erosion risks for mountainous watersheds in South Korea and demonstrates the need for effective control measures. Focus of this thesis is, therefore, the analysis of the dominant farming practices to investigate their effects on soil erosion and their capability for erosion control and soil conservation in Korean watersheds.

The cultivated areas in South Korea can be grouped into rice paddy fields, which are primarily located in the flat areas within the watersheds for example in the valleys and floodplains, and dryland fields, which are often located on the surrounding hillslopes. Because erosion rates from flat terraced paddy fields are expected to be negligible compared to those from the sloping dryland areas, we focused in our studies only on the cultivation practices on dryland fields. The dominant farmland practice on dryland fields in South Korea is the cultivation of row crops, predominantly cabbage, radish, and potato (Kim *et al.*, 2007, Lee *et al.*, 2010a), embedded in a plastic covered ridge-furrow system (plastic mulch). At the beginning of the growing season (usually between April and May, depending on the crop type) mineral fertilizer is applied to the soil surface, fields are plowed and subsequently ridges are created. The distance between two ridges is approximately 70 cm and the ridges are usually between 30 to 40 cm wide and 15 cm higher than the furrows. Ridges are covered with a black polyethylene film with regularly spaced planting holes of 5 cm diameter. The polyethylene film is buried several centimeters deep on either side of the ridge. It has been reported that plastic mulch increases crop yields, reduces evaporation losses and nutrient leaching, and helps to control weeds (Lament Jr., 1993). However, the surface topography caused by ridges and furrows and the water-impermeable plastic covers can highly influence flow processes occurring on the surface and the underlying soil profile. It has been identified in different studies that tillage operations and the use of machinery substantially affect water infiltration and flow processes in agricultural soils as a consequence of a modified soil structure and surface topography by inducing non-uniform flow (Petersen *et al.*, 2001, Kulli *et al.*, 2003, Bogner *et al.*, 2012). Non-uniform or preferential flow is the movement of water along certain pathways, while bypassing a fraction of the porous matrix, leading to increased flow velocities and water quantities at certain locations compared to other parts in the soil profile (Hendrickx and Flury,

2001). Preferential flow can, therefore, result in rapid movement of water compared to uniform matrix flow (Bogner *et al.*, 2010) and accelerate the transport of agricultural chemicals, such as fertilizers or pesticides (Šimůnek *et al.*, 2003). The modified infiltration patterns and velocity distribution of subsurface water flow can additionally influence the generation of surface runoff of the ridge-furrow system and may, therefore, affect the amount of soil detachment on the surface. During intense rain events, non-uniform infiltration, caused for example by the drainage of surface water from ridges into furrows, can produce concentrated overland flow with higher erosive power (Wan and El-Swaify, 1999). Although the plastic cover protects the surface from raindrop impacts and minimizes ridge erosion, the remaining exposed soil surface in the furrows is more vulnerable to erosion due to the elevated runoff amounts (Wolfe *et al.*, 2002). When surface runoff occurs, the ridge-furrow system additionally changes its flow direction and distribution over the field site. Ridges are predominantly oriented perpendicular to the main slope direction, but often not parallel with the contours. On fields with complex topographies, which dominate the Korean watersheds, the orientation of the ridge-furrow system can, therefore, affect the amount of erosion losses. Runoff flows along the furrows where ridge breakovers occur (Renard *et al.*, 1997), which can result in higher erosion damages compared to fields without ridges (Stocking, 1972, Wischmeier and Smith, 1978, El-Swaify *et al.*, 1982, Haggmann, 1996). Additionally, the cultivation of row crops in general produces more serious erosion problems due to the higher percentage of bare ground compared, for instance, to many cereal crops with higher plant densities, especially in early stages of crop growth (Morgan, 2005). The intensive use of agricultural chemicals in South Korea (Kang and Kim, 2000, Kim and Kim, 2004), especially the application of herbicides may, therefore, contribute to the high erosion losses. Brock (1982), for example, reported that the use of herbicides for weed control significantly increases soil loss from agricultural fields. A well developed weed cover, however, can help to reduce erosion (Weil, 1982, Afandi *et al.*, 2002, García-Orenes *et al.*, 2009, Blavet *et al.*, 2009). Environmentally friendly farming systems (organic farming and no-chemical farming), which rely on the minimization of chemical use, became more popular in Korea (Kim *et al.*, 2001b, Choo and Jamal, 2009). Since the number of organic farms has been strongly increased within recent years (Kim and Kim, 2004, Kim *et al.*, 2012), those farming systems may, therefore, play an additional role in erosion control. However, organic farming can also lead to reduced crop yields due to crop-weed competition and herbivory, which would have contrary effects.

In the first two studies of this thesis, we focused on the plastic covered ridge-furrow system namely on the effect on subsurface flow processes (chapter 2) and their impact on the runoff patterns and soil erosion rates (chapter 3). The third study (chapter 4) analyzes the soil erosion and conservation potential of conventional and organic farming. The following three sections summarize the previous research and the state of knowledge, related to these topics and introduce our objectives and hypotheses for each of the studies.

Study 1: flow processes of plastic covered ridge-furrow cultivation

The effect of the ridge-furrow system on flow processes in soils has been investigated in different studies. Saffigna *et al.* (1976) analyzed the infiltration patterns induced by ridge cultivation of potatoes using dye tracer irrigation. They found a non-uniform infiltration with a deep dye movement, preferentially around potato stems and in the furrows caused by surface runoff from the ridges. In another study, Bargar *et al.* (1999) used soil moisture sensors to investigate the infiltration patterns and flow processes in uncropped ridge-furrow fields. They also reported that infiltration occurred primarily in furrows than in the ridge positions. Furthermore, they found that water subsequently moved laterally from furrows to ridges minimizing vertical water flow below the ridges. Also Leistra and Boesten (2010) reported surface runoff from ridges to the furrows in their study. They analyzed pesticide leaching using irrigation experiments on a potato field and found that pesticide transport for ridge-furrow cultivation can be substantially higher

than that for fields with a smooth soil surface. These studies demonstrate that the ridge-furrow system can strongly influence the infiltration and flow patterns and the transport of chemicals in agricultural soils. However, most of the previous studies concentrated on the soil water dynamics of uncovered ridge-furrow systems. The impact of plastic covered ridge-furrow cultivation on water flow processes in soils has not been investigated so far.

The objectives of this study were to compare infiltration and surface runoff for the plastic covered ridge-furrow system, to investigate its effects on the subsurface flow patterns, and to evaluate the environmental impact in terms of agricultural pollutant transport. For this study, we formulated the following hypotheses:

- 1) The plastic covered ridge-furrow system constrains infiltration and increases the amount of surface runoff compared to non-covered ridges and a smooth soil surface
- 2) The plastic covered ridge-furrow system induces typical infiltration and flow patterns as a consequence of the topography and the impermeable cover of ridges
- 3) During monsoonal rainstorm events, preferential macropore flow in the soil is responsible for a rapid transport of agricultural chemicals to the groundwater

Therefore, we conducted different dye tracer irrigation experiments to compare the plastic covered ridge-furrow system to non-covered ridges and a smooth surface cultivation. We measured infiltration, runoff, and the soil moisture development, and we analyzed the subsurface flow patterns visualized by the applied tracers.

Study 2: runoff patterns and soil erosion of plastic covered ridge-furrow cultivation

Several studies have previously investigated the effect of plastic covered ridge-furrow systems on runoff and soil erosion for a variety of different crops. In rainfall simulator experiments on pineapple plantations, Wan and El-Swaify (1999) found substantially higher runoff and soil erosion under plastic mulch plots relative to bare plots. However, in combination with a developed vegetative crown, plastic mulch can reduce runoff and soil loss, because water is ponded by the canopy and funneled into the planting holes. Rice *et al.* (2001) reported higher runoff and a three times higher soil loss from tomato plots with plastic mulch compared to vegetative mulch. In another example, Gascuel-Oudou *et al.* (2001) also found higher runoff and a four times higher erosion rate for corn cultivation with plastic mulch than without plastic covers. In contrast to these studies, Stevens *et al.* (2009) could not identify large differences in surface runoff for strawberry cultivation for plastic mulch and uncovered management. Moreover, they found that plastic mulch even significantly reduced soil erosion. Lee *et al.* (2010b) found in lysimeter plots studies with cabbage and potato cultivation a reduction of both runoff and erosion by plastic mulch. These studies show that plastic mulch can have contrary effects on runoff and erosion, which may be a consequence of the different crop type or the design of the ridge-furrow system, but also of the different experimental designs, particularly plot size and ridge orientation. However, all of these studies used plots or delimited sections of field sites with a defined dimension and uniform topographical conditions. The combination of the ridge-furrow system with the internal topography of agricultural fields in complex terrain has not been investigated.

The objectives of this study were the quantification of runoff and soil erosion produced by the plastic covered ridge-furrow system on two mountainous agricultural fields with different topographical characteristics and the analysis of the generated runoff flow patterns and their effects on the soil loss rate from the entire field. For this study, we formulated the following hypotheses:

- 1) The plastic covered ridge-furrow system increases soil erosion compared to non-covered ridges and a smooth soil surface as a consequence of an increased surface runoff
- 2) The field topography controls the runoff flow patterns generated by the ridge-furrow system and its effects on soil loss from the field

Therefore, we measured runoff and soil erosion from two agricultural fields and applied a model to simulate the response of the same fields without plastic cover and ridges. We implemented a measurement method, which is not limited to defined plot dimensions and can better represent the complex topography of those fields. We used a process-based erosion model, which can describe the spatial patterns of runoff and erosion affected by the terrain and the topography of ridges and furrows.

Study 3: soil erosion and conservation potential of conventional and organic row crop cultivation

The role of organic farming in erosion control has been studied already by many authors using various methods with different results. Lockeretz *et al.* (1981), for instance, modeled soil erosion from organic and conventional farms and found about one-third less erosion for organic farming due to a different crop rotation. Reganold *et al.* (1987) studied the long-term effects of the farming systems by comparing erosion measurements and the top soil thickness of two farms and found an almost four times lower erosion on the organic farm as a consequence of a different crop rotation and less tillage operations. Fleming *et al.* (1997) calculated the soil erodibility from soil samples taken from conventional and organic farms and reported a potential erosion reduction for some of the soils. Also Siegrist *et al.* (1998) found in a long-term field experiment an increased aggregate stability of the soil under organic management but no significant reduction in erosion. In another field experiment, Eltun *et al.* (2002) observed lower erosion on plots with organic arable crops, but higher erosion on plots with organic forage crops. Auerswald *et al.* (2003) found in a modeling study based on cropping statistics of conventional and organic farms slightly lower soil erosion for organic farming, but also a high variability between both farming systems. In contrast to most of the previous work, Pacini *et al.* (2003) found in another modeling study a strong increase of erosion for organic farms as a result of different crops and more intense tillage operations, but Kuhn *et al.* (2012) recently reported again a lower erosion rate from organic compared to conventional soils. Although many of the previous studies describe a potential erosion control of organic farming as a result of a reduced soil erodibility and crop composition, a general conclusion can still not be drawn. The soil stabilization might be an effect of long-term organic farming and may not apply for recently established organic farms. Furthermore, large differences between both farming systems were primarily reported, when different crops were cultivated and tillage operations applied. The impact of weed coverage as a consequence of the application or absence of herbicides associated with the two farming systems for the same crop condition has still not been investigated.

The objectives of this study were the analysis of the crop and weed development on row crop fields from different conventional and organic farms, the quantification of soil loss from those fields, and the identification of the erosion control potential of both farming systems. For this study, we formulated the following hypotheses:

- 1) Organic farming increases weed coverage compared to conventional farming as a consequence of the absence of herbicides
- 2) Organic farming reduces soil erosion because of the protective effect of weeds and can be used to effectively control soil erosion

Therefore, we measured multiple vegetation parameters of crops and weeds on conventional and organic row crop fields and used an erosion model, which can simulate the amount of soil loss associated with different plant properties and surface conditions. In order to take into account the temporal variability of the monsoonal rainstorm events on the Korean peninsula (Choi *et al.*, 2008, Kim *et al.*, 2009) in combination with different growth schedules and harvest operations, we used long-term weather station data sets and simulated a range of scenarios representing different planting times and levels of soil disturbance.

All three studies of this thesis were carried out within the framework of the International Research Training Group TERRECO (Complex Terrain and Ecological Heterogeneity) (Kang and Tenhunen, 2010), which aims at the assessment of ecosystem services derived from mountainous landscapes that play an essential role in providing freshwater for large parts of the human population (Liniger *et al.*, 1998). The TERRECO-IRTG consists of a large group of scientists from different fields, who investigate processes related to soils, hydrology, water yield and water quality, agricultural and forest production, biodiversity, and the associated economic gains and losses obtained from those landscapes. The general goal of the research group is the development of an assessment framework that allows the quantitative evaluation of shifts in ecosystem services due to future changes in climate, land use, and human population. Such an assessment framework requires tools that are suitable to describe the complexity of processes regulating ecosystem services at a landscape level and to transform them into economically interpretable values. Large-scale simulation models, such as SWAT (Soil and Water Assessment Tool) (Gassman *et al.*, 2007) and InVEST (Integrated Valuation of Ecosystem Services and Tradeoffs) (Tallis and Polasky, 2011) combine multiple processes and can provide the basis for such tools. However, those models often apply highly simplified approaches to describe certain processes and require comprehensive modifications and adaptations to adequately reflect regional conditions. The individual research studies of the TERRECO-IRTG, therefore, contribute not only to a better understanding of processes occurring in mountainous landscapes, but they also help to develop and improve the models that are required for ecosystem service assessment. In addition to erosion control and soil conservation issues, the three studies of this thesis describe important processes and driving factors related to water movement and particle transport of agricultural soils in mountainous landscapes of Korea. The results of our work provide information that can be used for the parameterization of simulation models like SWAT and InVEST, with respect to erosion prediction, and can, therefore, contribute to evaluate ecosystem services related to agricultural production and water quality in this region.

1.2 Materials and methods

1.2.1 Research area and study sites

The studies were conducted in the Haean-Myeon catchment in the Kangwon Province located in the northeast of South Korea (128°08' E, 38°17' N) (Figure 1.1). The catchment is part of the watershed of the Soyang Lake, which is the largest reservoir in South Korea (Kim *et al.*, 2000). The Haean catchment is a major agricultural hotspot that substantially affects the trophic state of the reservoir (Park *et al.*, 2010). The total catchment area is 64 km² with 58% of the catchment classified as forested mountains and 30% as agricultural areas (22% dryland fields and 8% rice paddy fields). The remaining 12% are residential and seminatural areas including grassland, field margins, riparian areas, channels, and farm roads. The topography of the research area is characterized by flat areas and moderately steep slopes in the center of the catchment and steep slopes at the forest edges. The terrain is highly complex with a variety of different hillslopes and flow directions. The soil landscape is dominated by *Cambisols* formed from weathered granite.

Soils are highly influenced by human disturbances. Especially dryland fields are modified by the replenishment of excavated materials from nearby mountain slopes in order to compensate annual erosion losses (Park *et al.*, 2010). The average annual temperature of the Haeon catchment is 8.5°C and the average annual precipitation is 1599 mm (13 years average from 1999 to 2011), of which more than 65% are concentrated in July, August, and September.

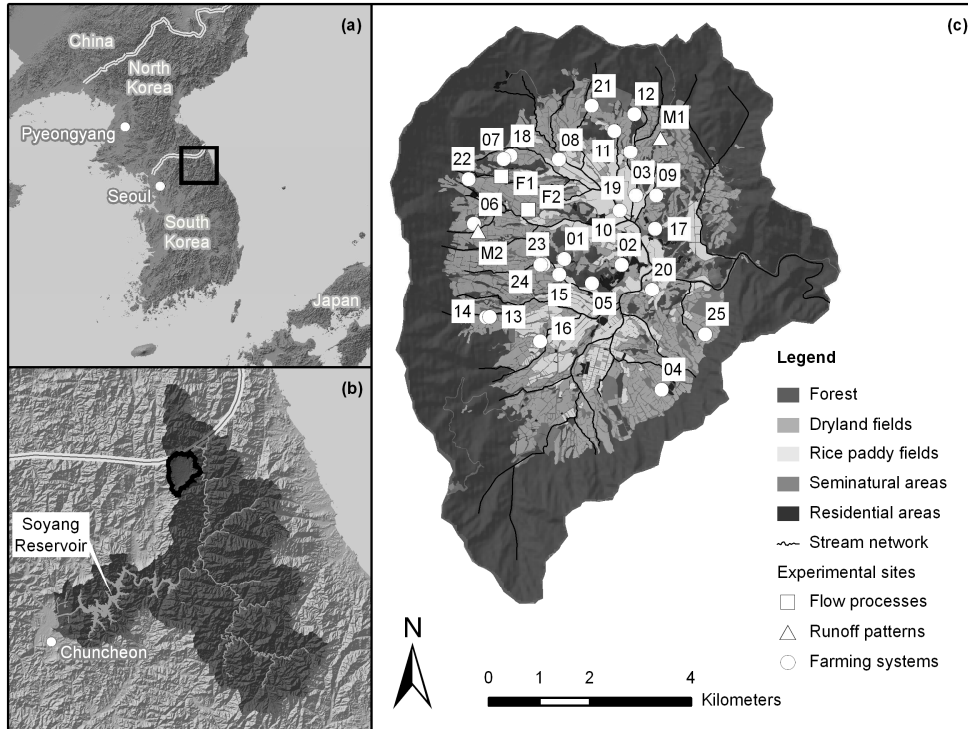


Figure 1.1 Location of the study area (Haeon-Myeon catchment) on the Korean peninsula (a) and within the watershed of the Soyang Reservoir (b) with the locations of the experimental sites selected for the three studies of this thesis (c). The study on flow processes were conducted at site F1 and F2 (chapter 2), runoff patterns and erosion at site M1 and M2 (chapter 3), and the impact of the farming systems at the sites 01 to 25 (chapter 4)

For analyzing the flow processes of the plastic covered ridge-furrow system (chapter 2), we selected two study sites (F1 and F2, in chapter 2 indicated as site 1 and site 2) cultivated with potato (*Solanum tuberosum*). Both field sites were located on sloping terrain with slopes of 8° and 6° for site F1 and F2, respectively. The soil type of site F1 was a *terric Cambisol* (Ap-2Apb-Bwb) and the soil of site F2 was a *terric Anthrosol over haplic Cambisol* (Ap1-Ap2-Ap3-2Apb-2Bwb), both highly influenced by erosion and repeated soil replenishments. Table 2.1 (chapter 2) contains detailed information on the soil parameters of both fields.

For the analysis of the runoff patterns and soil erosion associated with the plastic covered ridge-furrow system (chapter 3), we selected two additional study sites (M1 and M2, in chapter 3 indicated as field 1 and field 2), which were also cultivated with potato (*Solanum tuberosum*). The topography of site M1 was concave, characterized by a depression line going through the field center, and site M2 was convex without topographical depressions. The average slope of both fields was estimated with about 9°. An automatic approach for calculating slope length and steepness revealed slightly different values between both fields (M1 with 9.6° and M2 with 8.1°, see chapter 4). The soil type of site M1 was a *haplic Cambisol* (Ap-Bw-BwC-C) and the soil of site M2 was a *leptic terric Cambisol* (Ap-2Apb-2Bwb-2C). Table 3.1 (chapter 3) contains detailed information on the soil parameters.

For analyzing soil erosion and the conservation potential of the two farming systems (chapter 4), we selected 25 fields sites (01 to 25) including the four major dryland row crops: bean (*Glycine max*), potato (*Solanum tuberosum*),

radish (*Raphanus sativus*), and cabbage (*Brassica rapa* and *Brassica oleracea*), cultivated by conventional and organic farmers. The field sites were distributed over the entire Haean catchment representing the variety of different field sizes, hill slopes, and soil conditions of the agricultural areas. Table 4.1 (chapter 4) shows the soil properties and topographical parameters for the 25 sites. For the erosion model, we used the recorded precipitation and temperature data of ten automatic weather stations installed in the Haean catchment. Additionally, we also used the sites M1 and M2 in this study to evaluate the performance of the erosion model.

1.2.2 Analysis of flow processes of plastic covered ridge-furrow cultivation

To analyze the flow processes associated with the plastic covered ridge-furrow system on dryland fields, we conducted four irrigation experiments using dye tracers to measure infiltration and runoff and to visualize the subsurface flow patterns (Figure 1.2). The experiments 1 and 2 were carried out on site F1 and experiments 3 and 4 on site F2. Experiment 1 was conducted after plowing before ridges were created, representing a smooth soil surface tillage, as it is usually applied for cereal crop cultivation in many countries. Experiment 2 was done when ridges and furrows were created. Experiment 3 was carried out after the ridge-furrow system was covered with plastic and seed potatoes were recently sown. The last experiment (experiment 4) was done in the later growing season when potato canopy and root system were well developed. Before we started the irrigation, we installed soil moisture sensors in 5 and 20 cm depth from the soil surface (experiment 1) and from the top of the ridges and furrows (experiment 2 and 3) in order to record soil water content during the experiments with 2 minutes resolution. We irrigated an area of 1 by 2 m by using an automatic sprinkler and a tracer solution of 5 g L^{-1} of *Brilliant Blue FCF* and additionally 5 g L^{-1} *potassium iodide* for experiment 1 and 3. In order to quantify the amount of runoff and infiltration, we installed a frame around the irrigated area and collected the surface runoff. After one day, we excavated 8 to 10 soil profiles of 1 by 2 m, which were equipped with a metallic frame, photographed, and sampled. We removed soil material of *Brilliant Blue* stained and non-stained components from different profiles and subsequently measured soil texture and bulk density in order to investigate the effect of these soil properties on the flow patterns.

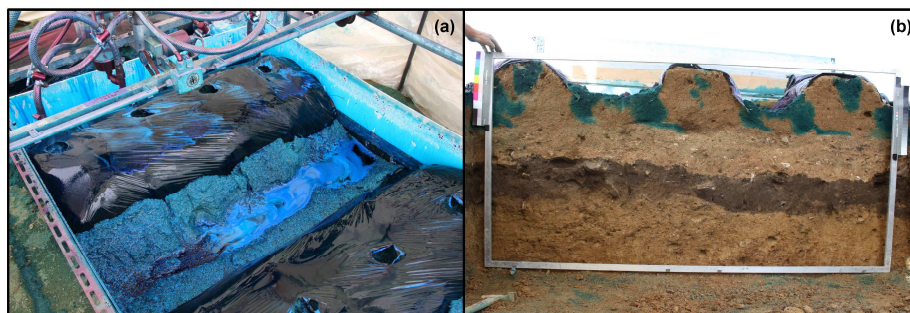


Figure 1.2 Irrigation experiment with dye tracer *Brilliant Blue FCF* and *potassium iodide*. Automatic sprinkler spraying tracer solution on the field plot with plastic covered ridges and furrows (a) and excavated soil profile for visualizing the subsurface flow patterns (b)

The photos taken from each of the profiles were corrected for perspective and radial distortion in such a way that they correspond to images taken by an ideal camera looking exactly perpendicular onto the profiles. Subsequently, we transformed the images from RGB into HSI (hue, saturation, intensity) color space and created binary images that classified the profiles into *Brilliant Blue* stained (black) and non-stained (white) parts (Bogner *et al.*, 2010, Trancón y Widemann and Bogner, 2012). For the experiments 2, 3, and 4, we additionally created a second binary background image containing the soil (black) and the background between ridges (white). Image correction and color segmentation

were performed by the Halcon software (ver. 10.0). To analyze the flow patterns in those binary images, we calculated different image index functions described by Trancón y Widemann and Bogner (2012), which summarize different features of the binary image row by row and emphasize the vertical configuration of patterns in the profile. In the following section, we briefly describe the individual functions and their interpretation. The detailed mathematical descriptions are provided in chapter 2 and by Trancón y Widemann and Bogner (2012).

The first image index function we used is the *dye coverage* (I_D), which shows the proportion of stained pixels in each row. It simply describes the quantity of staining, but without consideration of the patterns of stained objects in the soil profile (Trancón y Widemann and Bogner, 2012). The second function is the *Euler number* (I_E) that calculates the number of runs (contiguous sequence of stained pixels) divided by the number of possible runs in each row. It is a measure for the number of separated stained objects in the profile. The third function (I_{MAX}) gives the *maximum run length* in each row normalized by the row length and is, therefore, a measure for the maximum size of stained objects. The fourth function we used is the *fragmentation* (I_F), which is defined as $1 - I_C$, where I_C is the *contiguity* function. The *contiguity* is calculated as the inner product of the run length sequence divided by the squared number of stained pixels in each row. It is a measure of the connectivity of stained pixels, and the *fragmentation*, therefore, describes how strongly stained objects are interrupted by non-stained parts in the profile. The fifth index function we used for analyzing the patterns is the *metric entropy* (I_{MEL}). It is a generalization of the Shannon's entropy for sequences ("words") of stained or non-stained pixels with a defined length L (in this study 8 pixels), normalized by L (Trancón y Widemann and Bogner, 2012). The Shannon's entropy (Shannon, 1948) describes the average information content (or the uncertainty) of the outcome of a random variable. In our case, the outcomes of the random variable are the different possible "words" within each row of the binary image. If only a small number of different "words" occur within a row, for example when the profile is dominated only by a few large contiguous objects or repeating patterns of stained and non-stained parts, the *metric entropy* is low. Whereas, if a high number of different "words" occur, for example when the patterns are highly diverse with combinations of different large and small objects, the *metric entropy* rises to its maximum. It can be interpreted as a measure of the variability or diversity of patterns within the profile. All image index functions were calculated using the R programming language.

1.2.3 Analysis of runoff patterns and soil erosion of plastic covered ridge-furrow cultivation

To identify the patterns of surface runoff within the field and to quantify the associated erosion rates, we first measured runoff volume and sediment mass, which were subsequently used to calibrate the erosion model that visualized the runoff patterns and computed soil loss for the alternative tillage practices. On each of the two field sites M1 and M2, we installed three runoff samplers designed according to Bonilla *et al.* (2006) (Figure 1.3). Each sampler consisted of a runoff collector connected to a multislot flow divider developed by Pinson *et al.* (2004). They were installed at locations within the field sites where we expected large amounts of runoff, without an artificial enclosure of the contributing area. The flow divider consisted of wooden boxes including four 20-Liter buckets with divider crowns resulting in a total runoff sampling capacity of 144 m³ of each collector. Excessive water was removed at the bottom of the boxes to the field edges. After seven rainfall periods within the monsoon season between 5 July and 9 August 2010, we measured the water level and calculated the runoff volume for each bucket. We took samples from each of the buckets and determined the sediment concentration. Subsequently, we calculated the total runoff volume and the total sediment mass of each collector. The according equations are described in chapter 3 and by Bonilla *et al.* (2006). In order to transform the measured sediment mass to the associated rate of soil loss, it was necessary to define the size of the drainage areas of the collectors. Therefore, we used a tachymeter to develop a mesh of elevation points distributed

over the entire field area and we counted the number of ridges and furrows and measured their orientation and dimensions. The elevation points were interpolated to create surfaces representing the basic field topography and subsequently the ridges were added. We created two digital terrain models with 0.25 m spatial resolution for the fields, one representing the basic topography with a smooth soil surface and one representing the actual field shape with ridges and furrows. The latter were used to delineate the drainage area of each collector and to calculate the size. A detailed description of the measurement design including the drainage areas of the collectors is given in Figure 3.2 (chapter 3). Runoff and soil loss per unit area were calculated as the quotient of the measured runoff volume and sediment mass and the drainage area of each collector. The mean runoff and soil loss from each field site was then calculated as the average of the three collectors weighted to their drainage area size.

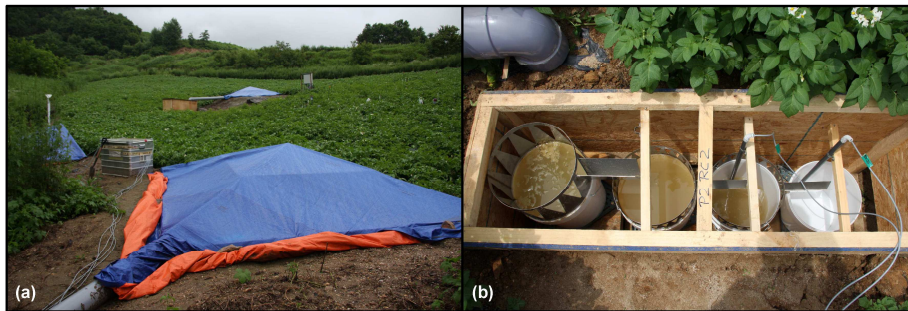


Figure 1.3 Runoff sampler for measuring runoff volume and sediment mass according to Bonilla *et al.* (2006). Runoff collectors (a) and multislot flow divider according to Pinson *et al.* (2004) (b)

We used the EROSION 3D model (Schmidt, 1991, von Werner, 1995) to compare runoff and erosion for the plastic covered ridge-furrow system to runoff and erosion for uncovered ridges and a smooth soil surface cultivation. EROSION 3D is a process-based and spatially distributed model, which can describe the overland flow distribution and diversion as affected by the terrain topography and the associated erosion and sediment transport. It requires only a small number of input parameters (Wickenkamp *et al.*, 2000), but the relatively simple physical approach leads to some limitations, for instance the assumption of constant erodibility and roughness during rain events (Wickenkamp *et al.*, 2000) and the non-consideration of rill detachment processes that can cause an overestimation of erosion rates at small spatial scales (von Werner, 1995). The EROSION 3D input parameters can be grouped into three groups: relief parameters, precipitation parameters, and soil-surface parameters (Schmidt *et al.*, 1999). For relief parameters, we used the previously developed digital terrain models of the field sites with ridges and furrows and the base terrain model to represent the smooth soil surface cultivation. Precipitation parameters were obtained from two rain gauges installed on the field sites that recorded rainfall during the observation period with 10 minutes resolution. The soil surface-parameters were primarily obtained from field observations, photographs (soil layer thickness, percentage cover) and laboratory analyses of soil samples (texture, bulk density, organic carbon content). Additionally, we used simulations with the HYDRUS 2D/3D model (Šimůnek *et al.*, 2011) carried out on the same field sites (Ruidisch *et al.*, 2012) to derive the initial soil moisture at the beginning of each rainfall period. The surface roughness (Manning's n) was derived from the literature (Chow, 1959, Montes, 1998, Vieux, 2001, Chanson, 2004), and allocated separately to the soil surface and the polyethylene cover of ridges. Table 3.1 (chapter 3) contains the soil-surface parameters used for the EROSION 3D simulations of the two field sites. The model was calibrated to the observed runoff and erosion rates for the plastic covered ridge-furrow system (by optimizing the skin factor and erodibility) and subsequently used to simulate runoff and erosion for uncovered ridges and a smooth surface. We used three performance statistics as

evaluation criteria for the quality of model calibration: the Nash-Sutcliffe efficiency (*NSE*), the *RMSE*-observation standard deviation ratio (*RSR*), and the percent bias (*PBIAS*).

1.2.4 Analysis of soil erosion and conservation potential of conventional and organic row crop cultivation

To determine the amount of soil erosion and to identify the conservation potential of conventional and organic farming, we used the Revised Universal Soil Loss Equation (RUSLE) (Renard *et al.*, 1997) and applied it to 25 fields (site 01 to 25) of conventional and organic farms in the Haean catchment. RUSLE is a widely used erosion model based on the Universal Soil Loss Equation (USLE) (Wischmeier and Smith, 1978) and provides the possibility to enter multiple parameters, that can be measured in the field, to describe crop conditions and surface properties associated with specific management practices, such as conventional and organic farming systems. RUSLE calculates the average annual soil erosion as the product of five factors: the rainfall and runoff erosivity factor (*R*), the soil erodibility factor (*K*), the slope length factor (*L*) and the slope steepness factor (*S*), the cover management factor (*C*), and the support practice factor (*P*) (Renard *et al.*, 1997). The following section gives a short summary of the RUSLE factors and briefly describes their determination. The equations of the individual factors are given in chapter 4 and the original mathematical description using U.S. customary units is provided by Renard *et al.* (1997).

The *R-factor* quantifies the effect of raindrop impact and reflects the amount and rate of runoff associated with the rainfall (Wischmeier and Smith, 1978, Renard *et al.*, 1997) and is calculated from weather station records as the product of the kinetic energy of erosive rainstorm events and their maximum 30-minute intensity (Renard *et al.*, 1997). A total of 13 years of recorded precipitation and temperature data were available from ten weather stations located in the Haean catchment. One weather station in the center of the catchment recorded precipitation and temperature from January 1999 to May 2009 with 1 hour resolution, and in May 2009, nine additional weather stations were installed providing weather data with 30 minutes resolution until December 2011. We developed an algorithm using the R programming language that automatically identifies erosive rain events from these weather station data sets and calculated *R-factor* and the temporal distribution of rainfall erosivity for every half-month period from 1999 to 2011. The *R-factors* derived from the weather station record from 1999 to 2009 were subsequently corrected, as the maximum 30-minute intensity is underestimated using 1 hour resolution data. The correction factor was derived from the slope of the linear regression line between rainfall erosivity calculated on 30 minutes resolution and aggregated 1 hour resolution data sets from 2009 to 2011. The average annual *R-factor* for the Haean catchment was calculated as the mean of the 13 years individual *R-factors*. The *K-factor* represents the effects of soil properties and soil profile characteristics on soil erosion (Renard *et al.*, 2011). It is a function of the soil texture, the organic matter content, and the soil structure and permeability (Wischmeier *et al.*, 1971). To calculate the *K-factor* for the 25 field sites, we took samples of top soils (0 to 30 cm depth) and determined soil texture and organic matter contents in the laboratory. The soil structure and permeability codes were estimated from field observations, profile descriptions, and the results of the dye tracer experiments (chapter 2) on dryland fields in the Haean catchment. The *L-factor* and *S-factor* describe the effect of the hillslope topography on erosion. The *L-factor* considers the higher soil loss potential with increasing slope length and the *S-factor* reflects the influence of the slope steepness (Renard *et al.*, 1997). The topography of the ridge-furrow system can be regarded as contouring support practice and is described with the *P-factor*, which reflects the positive impact through the control of surface runoff (Renard *et al.*, 2011). The effectiveness of contouring is controlled by the field slope steepness and the angle along the furrows because the ridges are often not parallel to the contours. For the highly complex terrain with various flow paths and directions (see section 1.2.1), it is difficult to identify the representing hillslope profile and to determine slope lengths and slope angles. We developed an algorithm using the R programming language that

automatically identifies all possible flow paths within each of the 25 sites and extracts the mean slope length and slope angles, which were used to calculate *L-factor*, *S-factor*, and *P-factor*. Data basis for the algorithm were three 0.25 m resolution ArcGIS raster grids (the depression-filled elevation raster, the flow direction raster, and the flow accumulation raster) of each field, which were developed from an available 30 m resolution digital elevation model of the Haean catchment. The *C-factor* represents the effects of crops and the management practices on erosion (Renard *et al.*, 1997) and is, therefore, the critical factor in this study for describing conventional and organic farming. Because vegetation and soil surface conditions change over the course of the year, a time varying *C-factor* approach is used in RUSLE based on half-month time steps (Renard *et al.*, 1997). For each half-month period within the year, a soil loss ratio (*SLR*) is calculated as the product of five subfactors (Renard *et al.*, 1997): the prior land use subfactor (*PLU*) describing the effect of soil consolidation and the biomass density of roots and residues, the canopy cover subfactor (*CC*) describing the effect of the vegetation coverage and height, the surface cover subfactor (*SC*) describing the effect of the residue and other materials covering the soil surface, the surface roughness subfactor (*SR*) describing the effect of the soil surface microtopography, and the soil moisture subfactor (*SM*). To obtain the parameters for calculating the soil loss ratios for each half-month period, we first measured biomass density of the different vegetation components, the canopy cover, and the height of crops and the associated weeds of the four major row crops during the growing season of 2009 on four of the 25 field sites and developed individual growth charts for each crop. Subsequently, we measured the same parameters on the remaining 21 field sites including organic and conventional farming before harvest, and adjusted the growth charts based on the average yield, cover, and canopy height for the two farming systems to obtain growth charts for conventional and organic bean, potato, radish, as well as conventional cabbage cultivation. For the time prior to planting, we assumed a bare soil surface and the absence of roots and residue, because we had no information of previous crops. The amount of residue and coverage after harvest was depending on the crop type and the disturbance and mixing of the surface-soil during harvesting. For bean, almost the whole plant biomass remains in the field, for potato, the above-ground parts remain, whereas for radish, most of the biomass is removed, and for cabbage, everything except roots and outer leaves are harvested. For bean and cabbage, soil disturbance and mixing is minimized due to the above-ground harvesting and more of the remaining residue covers the soil surface. For potato and radish, harvesting requires a higher degree of disturbance because of the below-ground crop components resulting in less residue remaining on the surface. Based on these assumptions, we calculated the soil loss ratios and weighted them by the percentages of the associated rainfall erosivities (see *R-factor*) to obtain the *C-factors* for the four major row crops and both farming systems. In order to account for different harvesting techniques and machinery applied by the farmers, we simulated two scenarios representing a low and a high level of soil disturbance. Furthermore, we simulated two additional scenarios to include early and late planting and harvesting schedules over the different years by shifting all *SLR* values to the previous and the next half-month time step, respectively.

There were only a few field measurements on soil erosion in the Haean catchment that we could use to verify the model performance. First, we used the erosion rates of the sites M1 and M2 measured with the runoff collectors in 2010 (chapter 3) and compared them to the soil loss we calculated for the two sites with RUSLE, using the methods described above. Second, we compared the average annual soil loss rates of the 25 field sites computed with RUSLE to long-term erosion estimations using the fallout radionuclide caesium-137 (^{137}Cs) for two sloping fields in the Haean catchment (Meusburger *et al.*, 2012). Additionally, we used literature values from other soil erosion studies conducted in the Kangwon Province and compared them to our results.

1.3 Results and discussion

1.3.1 Flow processes of plastic covered ridge-furrow cultivation

The analyses of the flow processes produced by the plastic covered ridge-furrow cultivation yielded the following results. Regarding the water balance, we found the highest infiltration on the smooth surface cultivation (79%) compared to the ridge-furrow system (62%) and the ridges with plastic cover (50%), which showed the highest amount of runoff due to the surface topography and the impermeable polyethylene film. For the plastic covered ridges in combination with the developed potato canopy, however, infiltration is increased (69%), which might have been a consequence of interception and stem flow leading to local infiltration around the stems into the planting holes, as previously described by Saffigna *et al.* (1976), Jefferies and MacKerron (1985), and Leistra and Boesten (2010). The soil water content, measured during the irrigation, gradually increased with irrigation time under the smooth soil surface, with higher values in the downslope part of the inclined irrigated area. For the ridge-furrow system, the soil water content rapidly increased already at the beginning of the experiment in the furrows and then, delayed, also in the ridges, due to the routing of runoff from the ridges and accumulation in the furrows, which was also reported by Saffigna *et al.* (1976) and Leistra and Boesten (2010). For the plastic covered ridge-furrow system, the water content in the furrows increased more rapidly than without plastic, whereas the covered ridges stayed dry throughout the irrigation. Only the deeper parts of the ridges showed a very slight increase in water content, probably as a consequence of lateral water movement from the furrows to the ridges (Bargar *et al.*, 1999) along the tillage pan or as a result of pressure head gradients between dryer ridges relative to the furrows.

The flow patterns visualized with the dye tracer showed that the soil surface topography and the covering created by the different tillage practices control the occurrence of preferential flow, because they produce zones where infiltration preferentially appears, namely furrows and planting holes, and zones where no infiltration occurs, namely the plastic covered ridges. The patterns in the profiles also revealed that the tillage pan is the most important feature for controlling the flow processes by inhibiting the water movement to deeper layers. In none of the four experiments, we identified dye (neither *Brilliant Blue* nor *potassium iodide*) deeper than the operation depth of 25 to 35 cm, which may be explained by the significantly higher bulk density and the textural difference below the tillage pan. Also a vertical propagation to deeper soil layers via macropores could not be detected with either tracer. The effect of the topography of the ridge-furrow system and the polyethylene cover on the subsurface flow patterns is well reflected by the different image index function. Both I_F and I_{ME8} were higher for the ridge-furrow system compared to the smooth surface and reflect a higher fragmentation and diversity of stained objects as produced by preferential infiltration in furrows and planting holes due to the surface topography. I_{MAX} was highest for the smooth soil surface, but also within the uppermost cm of the uncovered ridge-furrow system indicating a uniform matrix flow within the top soil horizon, which produced only one large contiguous stained object. Also I_D showed its maximum for the smooth soil surface and the uncovered ridges as a result of the uniform infiltration at the soil surface. However, the presence of the plastic cover strongly reduced both I_{MAX} and I_D near the soil surface because of the restricted infiltration in the ridges (except for planting holes). For the plastic covered ridge-furrow system, both I_D and I_{MAX} were highest approx. 20 cm deeper in the furrows, where accumulated surface runoff from the impermeable ridges produced preferential infiltration and lateral water flow. The developed crop canopy under the plastic covered ridge-furrow system lead to stem flow effects funneling additional irrigation water into the planting holes, as previously described (Saffigna *et al.*, 1976, Jefferies and MacKerron, 1985, Leistra and Boesten, 2010). The water was subsequently preferentially channeled along living roots resulting in maximum values of I_D and I_{MAX} in the root zone depth. Furthermore, we observed from the dye patterns an increased

lateral water flow from the furrows to the ridges as a consequence of a high pressure head gradient between the dry, covered ridges, where additionally root water uptake occurred, and wet furrows. However, one very important feature that strongly influences the subsurface water flow, regardless of ridges and covers, is the top soil horizon itself, which was created by the deposition of sandy soil material to compensate erosion losses (Park *et al.*, 2010). It consists of structureless, non-cohesive, and coarse material that strongly differs from the characteristics of the soil horizons below. I_E showed relatively low values for all four experiments representing a small number of stained objects that resulted from uniform dye propagation, producing only a few large contiguous stained areas within the topsoil horizon. As shown before, the dense, cohesive, and finer textured subsoil horizons below, do not considerably contribute to water flow, also due to the absence of fissures, cracks, or earthworm burrows that can act as preferential flow paths (Weiler and Naef, 2003, Bachmair *et al.*, 2009, Bogner *et al.*, 2012). Our results indicate that the subsurface flow processes in agricultural fields in the Haean catchment are primarily constricted to the top soil above the tillage pan and that the vertical propagation of agricultural chemicals to the groundwater is generally relatively low. However, the rapid lateral downslope water movement above the tillage pan, plays, therefore, the crucial role for transporting chemicals to adjacent surface water bodies, especially during monsoonal rainstorm events. Although we found that a developed crop canopy can reduce the downslope water flow due to high pressure head gradients induced by root water uptake, the risk of chemical transport to surface waters is still high, especially in early growth stages when fertilizers are recently applied and plants are juvenile.

Generally, our results show that the ridge-furrow system induces preferential infiltration in furrows and planting holes and creates zones without infiltration (plastic covered ridges), but they demonstrate that its impact on the subsurface flow processes is relatively small compared to the impact on runoff generation. The ridge-furrow system, especially when covered with plastic, increases the risk of surface water pollution especially due to the high amounts of surface runoff, which can potentially produce accelerated soil erosion rates and increase particulate phosphorus transport.

1.3.2 Runoff patterns and soil erosion of plastic covered ridge-furrow cultivation

The analyses of the field site runoff patterns and erosion rates associated with the plastic covered ridge-furrow system for the two field sites yielded the following results. The observed runoff and soil loss was highly variable during the observation period and varied strongly between both fields. The total recorded precipitation on site M1 was 165.2 mm and on site M2 242.7 mm. The highest amount of runoff and sediment was concentrated in two of seven rainfall periods whereas two other periods did not produce any appreciable runoff and erosion. The total observed runoff over all seven rainfall periods for site M1 and M2 were 80.3 L m⁻² and 94.1 L m⁻², respectively. Although precipitation and rainfall intensity was higher on site M2, the observed erosion was much higher on site M1 throughout all seven rainfall periods. The total soil loss for M1 and M2 were 3636.7 kg ha⁻¹ and 626.5 kg ha⁻¹, respectively.

The comparison between the observed and simulated runoff and erosion for the optimized parameters (skin factor and erodibility) showed acceptable results. The *NSE* ranged from 0.914 to 0.943 for runoff and from 0.803 to 0.976 for soil loss, and the *RSR* ranged from 0.239 to 0.293 and 0.154 to 0.444 for runoff and soil loss, respectively. The *PBIAS* showed an overestimation of runoff for both field sites (-13.462 to -1.275) and an overestimation of soil loss for M1 (-14.571) and an underestimation for M2 (12.879). However, for both sites, the *EROSION 3D* model achieved satisfactory representations for runoff and soil loss (Moriassi *et al.*, 2007). We found the highest simulated runoff for both sites for the plastic covered ridge-furrow system, with 81.3 L m⁻² for M1 and 106.8 L m⁻² for M2. Without plastic cover, runoff could be reduced to 52.1 L m⁻² and 60.2 L m⁻² for M1 and M2, respectively. The higher runoff amounts

for plastic covered ridges are a direct result of the large field area associated with impermeable polyethylene film, which was also found by the HYDRUS 2D/3D simulations (Ruidisch *et al.*, 2012). The effect of the plastic cover on runoff generation correlated negatively with the rainfall intensity. For small intensities lower than the soils infiltration capacity, the impermeable plastic cover largely increases runoff, whereas for high intensities exceeding the soils infiltration capacity, the effect is much smaller due to low infiltration and high runoff on both soil and plastic (Wolfe *et al.*, 2002). For the smooth surface cultivation, EROSION 3D simulated the same amount of runoff than for the uncovered ridges, because due to the same soil properties, the model estimated the same hydraulic conductivity. Only the runoff distribution was changed due to different surface conditions. The highest soil loss for both field sites was also simulated for the plastic covered ridge-furrow system, with 4178.1 kg ha⁻¹ for M1 and 545.8 kg ha⁻¹ for M2. Without plastic cover, the soil loss could be reduced to 2469.9 kg ha⁻¹ and 371.7 kg ha⁻¹ for M1 and M2, respectively. The higher soil loss rate of the plastic covered ridges is a consequence of the higher concentrated flow in the furrows due to elevated runoff amounts resulting in a higher erosive power (Wan and El-Swaify, 1999, Wolfe *et al.*, 2002). For the smooth surface cultivation, we found contrary effects between the two field sites. The model predicted an additional soil loss reduction for site M1 to 1017.3 kg ha⁻¹, but an increase for M2 to 467.5 kg ha⁻¹ compared to uncovered ridges.

Due to field topography and orientation of the ridges, both sites show entirely different flow characteristics, which caused the different soil loss rates between the ridges and smooth surface cultivation. The runoff flow direction of the ridge cultivation is primarily controlled by the orientation of the ridges on the field site. Water is routed in the furrows parallel to the ridges instead of moving along the steepest flow paths. It flows along furrows until it reaches the field edge or a topographical depression. On site M1, the runoff is accumulated in such depressions due to the field concavity and is routed across the ridges. For those concentrated flow lines, especially in the center of site M1, the model predicted much higher erosion than for the surrounding areas resulting in higher total soil loss from the field. During our field measurements, we observed at the same location ridge breakovers caused by concentrated flow, which formed a permanent gully through the center of M1. On site M2, accumulated runoff flow and ridge breakovers did not occur as a consequence of its convex shape, which resulted in the lower total soil loss compared to M1. The smooth soil surface cultivation entirely changes the flow patterns because runoff is routed directly along the steepest flow paths and solely controlled by the field terrain. For M1, the absence of ridges led to a more evenly distributed runoff flow and a reduced flow concentration with less erosive power. In contrast, for M2 the smooth surface resulted in runoff routing along a steeper slope and accumulation at the field's lower edge where higher erosion was predicted.

Our results demonstrate that the plastic covered ridge-furrow system considerably increases surface runoff and erosion due to a lower permeability and that the runoff flow patterns generated by the ridge-furrow system and their effects on erosion is controlled by the field topography. On site M1, the ridge-furrow system generated a 140% higher soil loss because of its concave shape, and on M2, the ridge-furrow system separated runoff, constrained it to the furrows and prevented flow accumulation due to its convex shape.

1.3.3 Soil erosion and conservation potential of conventional and organic row crop cultivation

The analyses of soil loss and erosion control associated with conventional and organic farming yielded the following results for our study sites regarding the individual RUSLE factors. The rainfall and runoff erosivity of the Haeen catchment, calculated on the basis of 30 minutes resolution weather station records from May 2009 to December 2011, was higher than the aggregated 1 hour resolution data sets, by the factor 1.391 (slope of the regression line), which was used for correcting the *R-factors* from January 1999 to May 2009. The average annual rainfall and runoff erosivity was 6599.1 MJ mm ha⁻¹ h⁻¹ yr⁻¹ with a strong variability over the 13 years, but also within individual years, which showed

highly diverse rainstorm peak distributions. The dryland soils within the study area were characterized by high sand contents (texture was predominantly sandy loam and loamy sand) and low organic matter contents (0 to 2%) resulting in an average soil erodibility among the 25 field sites of $0.0211 \text{ t h MJ}^{-1} \text{ mm}^{-1}$. The *K-factor* for the organic fields ($0.0199 \text{ t h MJ}^{-1} \text{ mm}^{-1}$) was slightly lower than that of conventionally managed fields ($0.0219 \text{ t h MJ}^{-1} \text{ mm}^{-1}$), which was a result of the spatial variation of soil properties, and not the consequence of improved soil characteristics by organic management (Erhart and Hartl, 2010), which may take many years to develop. The various slope lengths and steepness of the 25 fields represented the topographical variability of the farmland in the Haean catchment. The slope lengths ranged from 4.7 to 124.6 m, resulting in *L-factors* between 0.380 and 2.479, and the slope angles varied from 0.0° to 14.9° with *S-factors* between 0.030 and 3.828. Despite the ridge-furrow system on all field sites, the slope angle along the furrows was still relatively high, which resulted in high *P-factors* between 0.730 and 1.148, showing that the contouring control effect is not very effective because ridges are usually not oriented along the contours. The vegetation measurements of the four major row crops revealed highly different growth charts, most notably the duration of the individual growing periods (bean with 157 days, potato with 123 days, radish with 82 days, and cabbage with 61 days), but also regarding the development of biomass, canopy cover, and height. The highest leaf biomass density at the end of the growing period was observed for bean (253.3 g m^{-2}) and cabbage (134.0 g m^{-2}), resulting in a higher crop cover compared to potato and radish, for which the largest portion of crop biomass is represented by their below-ground parts. For potato, after the first half of the growing period, we observed a strong decrease in leaf biomass and crop cover, associated with an increased development of weeds, compared to the other three crops, which showed only negligible weed biomass and coverage. The yield measurements for both farming systems before harvest showed a higher crop biomass density for conventional bean (1205.5 g m^{-2}) and potato (1976.0 g m^{-2}) than for organic bean (995.3 g m^{-2}) and potato (1270.9 g m^{-2}), resulting, for potato, also in a higher crop cover for conventional (26.8%) compared to organic (12.1%) management. In contrast, radish showed a higher crop biomass density for organic (669.7 g m^{-2}) than conventional (568.0 g m^{-2}) farming, resulting also in a higher crop cover for organic (71.2%) compared to conventional (61.7%) radish. The weed biomass density and cover was consistently higher for organic than conventional farming, except for bean, which shows similar values under both farming systems. For potato, the mean weed biomass was 96.1 g m^{-2} for conventional and 127.2 g m^{-2} for organic farming and the weed cover was 21.3% and 43.0%, respectively. For radish, the difference in weed biomass was much higher with 19.1 g m^{-2} for conventional and 127.1 g m^{-2} for organic farming and weed covers of 3.3% and 14.0%, respectively. Conventionally grown cabbage showed the lowest values for weed biomass and cover among all four crops. These results demonstrate that weed biomass and especially the ground cover provided by weeds can be highly increased by the absence of herbicides associated with organic farming. However, our results also show that organic farming can result in a lower crop yield and crop cover, which might be a consequence of crop-weed competition or herbivory due to the absence of herbicides and pesticides. The computed *C-factors* for the four crops and the two management systems showed a high variability over the 13 years and for the scenarios of soil disturbance and timing of planting and harvesting. Bean showed maximum values for years with early rain events, especially for late planting and harvest, but no considerable differences for the two levels of soil disturbance, as bean fields are more susceptible to erosion prior to planting than after harvest when the monsoon season is already over. Bean did not show different *C-factors* for conventional and organic farming, because crop and weed coverage was similar for both farming systems. Potato showed maximum *C-factors* for years, when rain events occurred late in the season and for a high level of soil disturbance especially for the early planting and harvesting scenario, as potato field are more susceptible after harvest when soils are barely covered and disturbed. Potato showed higher *C-factors* for organic than conventional farming as a consequence of the

lower crop biomass and surface cover by crop residue, which has a stronger effect than the higher weed coverage provided by the organic management. The difference between both farming systems was higher for the low disturbance scenario, as less crop residue, which can act as surface cover, is incorporated. Radish showed its maximum *C-factors* for years with early rain events for late planting and harvesting and for years with late rain events for the early planting and harvesting scenario and for a high level of soil disturbance. Radish fields are susceptible to erosion for both conditions prior to planting and after harvest due to the relatively short growing period compared to bean and potato. For radish, we computed lower *C-factors* for organic than conventional farming as a consequence of the higher weed coverage but also the slightly higher crop yield for the organic system. The difference between both farming systems was considerably higher for a high level of disturbance in combination with early planting and harvesting due to high amounts of incorporated weed biomass and a higher proportion of surface cover by residues when plastic is removed. Cabbage also showed its maximum *C-factors* for years with early rain events for late planting and harvest and for years with late rain events for the early planting and harvest scenario, because the very short growing period makes cabbage also susceptible to rainstorms occurring prior to planting as well as after harvest. Also for cabbage, the higher level of disturbance resulted in higher *C-factors* due to the reduced surface cover. The average annual *C-factor* computed over all 13 years and different scenarios was highest for radish with 0.202 for conventional, and 0.166 for organic farming. The *C-factors* for bean were 0.121 and 0.120 for conventional and organic farming, respectively, and for potato 0.113 for conventional and 0.141 for organic management. The average annual *C-factor* for conventional cabbage was 0.128.

The average annual erosion rate over all 25 field sites was also highest for radish due to the relatively short growing period in combination with the high disturbance and the low amount of crop residue remaining in the field after harvest compared to the other three crops. Organic farming reduced soil erosion for radish by 18% ($45.5 \text{ t ha}^{-1} \text{ yr}^{-1}$) compared to conventional farming ($54.8 \text{ t ha}^{-1} \text{ yr}^{-1}$) as a result of the higher weed biomass density and cover at the end of the growing season. However, our results show that the protective effect of weeds can not sufficiently counteract the negative effects of the short growing period, low residue, and high disturbance, because the erosion rate of organic radish is still higher than those of the other three crops. For potato, organic farming increased soil erosion by 25% ($38.2 \text{ t ha}^{-1} \text{ yr}^{-1}$) compared to conventional farming ($30.6 \text{ t ha}^{-1} \text{ yr}^{-1}$) due to the reduced crop biomass and cover, but the erosion rate is still lower than those of radish. For bean, we could not identify considerably different erosion rates for organic ($32.5 \text{ t ha}^{-1} \text{ yr}^{-1}$) and conventional ($32.8 \text{ t ha}^{-1} \text{ yr}^{-1}$) farming. The average annual soil loss for conventional cabbage was $34.7 \text{ t ha}^{-1} \text{ yr}^{-1}$. The highest erosion rates among the 25 field sites were computed for steep hillslopes at the forest edges with maximum values of $93.0 \text{ t ha}^{-1} \text{ yr}^{-1}$ (conventional potato) and $166.4 \text{ t ha}^{-1} \text{ yr}^{-1}$ (conventional radish), and the lowest erosion rates were found on flat fields in the catchment center with 0.4 and $0.7 \text{ t ha}^{-1} \text{ yr}^{-1}$.

The comparison of the RUSLE simulations to the measured erosion rates for sites M1 (3.65 t ha^{-1}) and M2 (0.63 t ha^{-1}) during the monsoon season of 2010 revealed a strong underestimation for site M1 (1.27 t ha^{-1}), although the erosion rate of M2 was acceptably reflected by the model (0.71 t ha^{-1}). The insufficient performance for M1 might be explained by the runoff generation and flow accumulation associated with the plastic covered ridge system producing breakovers and gully erosion (chapter 3), which cannot be adequately modeled by RUSLE. However, the simulated soil erosion in this study reflects the average soil loss rate estimated by ^{137}Cs ($41.8 \text{ t ha}^{-1} \text{ yr}^{-1}$) for a long-term agricultural hillslope in the Haean catchment (Meusburger *et al.*, 2012). Also the comparison to other erosion studies on dryland fields in the Kangwon Province (Jung *et al.*, 2003, Choi *et al.*, 2005) show that the long-term erosion rates produced by RUSLE are plausible.

1.4 Conclusions and recommendations

In three different studies, this thesis analyzed the major factors and processes that control soil erosion related to typical farming practices on dryland fields of a mountainous landscape in South Korea. The focus of the first two studies was the widely applied plastic covered ridge-furrow system and its effects on subsurface water flow, infiltration, runoff generation, and associated erosion rates. In the third study, we focused on the impact on erosion and the conservation potential of organic farming systems, which became an important management practice in the Korean agriculture during recent years. The following three sections summarize the main conclusions of the three studies related to the initially stated hypotheses (section 1.1.2), present their limitations, and give recommendations for future research.

Study 1: flow processes of plastic covered ridge-furrow cultivation

In our first study, we analyzed the flow processes affected by the plastic covered ridge-furrow system using dye tracer irrigation experiments. We found that the ridge-furrow system, especially when ridges are covered with plastic, increase the amount of surface runoff due to the topography and the impermeable polyethylene film. We can, therefore, conclude that our first hypothesis formulated for this study can be confirmed. Our results show that the plastic covered ridge-furrow system induces preferential infiltration in furrows and planting holes due to the topography and plastic cover. We can, therefore, also confirm the second hypothesis. However, the results also demonstrate that the impact on the subsurface flow processes is relatively small. The flow processes are primarily constricted to the sandy topsoil horizon, which shows highly different soil physical properties than the subsoil horizons below the tillage pan. Preferential macropore flow could not be identified in our experiments. Therefore, the third hypothesis formulated for this study must be rejected, and we can conclude that agricultural chemicals are primarily transported laterally along the tillage pan to surface water bodies.

However, our dye irrigation experiments were conducted only on two field sites, which may not represent the whole variety of soil conditions in this region. Own soil surveys in the Haean catchment demonstrated that not all agricultural soil profiles are characterized by replenished sandy top soil horizons and that the subsoil can have highly variable properties depending on previous land use and management conditions. Nevertheless, our observations show that most of the profiles feature a clear separation between relatively coarse, incoherent top soil material and the underlying cohesive finer-textured subsoil layers. Although our experimental sites can not cover the whole variety of soil characteristics, we can assume that they reflect the basic physical properties controlling subsurface water flow and that the observed flow patterns apply for most of the dryland fields in the Haean catchment. An additional simplification was given by the automatic sprinkler used for the irrigation experiments, which could not completely reflect heavy monsoonal rainstorm events. The amounts of irrigated water during the experiments (37 to 45 mm) reflect only moderate monsoonal storms in this region. Extreme events with long duration and high intensities presumably change the proportion of infiltration and runoff, as affected by the plastic covered ridge-furrow system, and influence the subsurface flow patterns, for example the effects induced by the root system. Furthermore, the impacts of real raindrops could not be accurately simulated by the sprinkler, because drop size and fall height were very small resulting in a low kinetic energy (Bogner *et al.*, 2012). Rain splash, soil particle transport, and deposition on the surface may additionally affect infiltration patterns and runoff amounts as a consequence of a changing microtopography, soil sealing, and crust formations. Nevertheless, our experiments revealed the basic infiltration patterns and subsurface flow processes as affected by the ridge-furrow system and polyethylene mulch, which are responsible for pollutant transport, runoff generation, and soil erosion on the agricultural fields in the Haean catchment.

Our findings may be complemented by additional research studies to fully understand all different processes related to plastic covered ridge-furrow systems under monsoonal climate conditions. During our irrigation experiments, we additionally monitored the soil surface development using a stereo system consisting of four single-lens reflex cameras. The stereo images can be used in further studies to develop digital terrain models of the soil surface to analyze the interactions between surface soil redistribution processes and subsurface flow (Bogner *et al.*, 2012). In order to reproduce real rainfall characteristics and the variability of monsoonal storm events, we suggest the improvement of our experimental design by the development of an integrated rainfall simulator, which allows us to control rainfall intensity and drop size, combined with dye tracer application and the stereo camera system.

Study 2: runoff patterns and soil erosion of plastic covered ridge-furrow cultivation

In our second study, we analyzed the effect of the plastic covered ridge-furrow system on runoff patterns and erosion rates in combination with the farmland topography using field observations and the EROSION 3D model. The results of this study show that the plastic covered ridge-furrow system generates higher amounts of surface runoff due to a lower permeability, which leads to a considerably increased soil erosion. Furthermore, our results demonstrate that the runoff flow patterns generated by the ridge-furrow system and their effects on erosion, is controlled by the field topography. We can therefore conclude that both hypotheses formulated for this study can be confirmed.

However, in our study, we could not consider the effects of rainfall interception and stem flow on runoff generation, because we did not have quantitative information about the infiltration amounts caused by stem flow under plastic mulch conditions. After plant emergence, stem flow can lead to local infiltration of the above-crop rainfall around the stems into the planting holes (Saffigna *et al.*, 1976, Jefferies and MacKerron, 1985, Leistra and Boesten, 2010), which was also observed in our first study (chapter 2). As a consequence, stem flow effects during the mature crop stage could potentially result in higher infiltration rates and in lower soil erosion in the furrows (Wan and El-Swaify, 1999). Therefore, the effects of plastic mulch on runoff generation may be overestimated for the rainfall periods throughout this study. Nevertheless, stem flow is only relevant for infiltration and runoff generation, when a high covering crop canopy is developed. For the time periods between seedbed preparation and plant maturity and after senescence, stem flow effects on runoff generation can be considered as negligible. We, therefore, believe that our model assumptions were reasonable for evaluating the elementary effects of plastic mulch on runoff and erosion for potato cultivation over the season. However, other crop types cultivated in our study area, such as bean, radish, and cabbage, are characterized by entirely different structural conditions and canopy development over time, which may result in diverse effects on infiltration and runoff generation caused by interception and stem flow throughout the growing season. Additionally, our experiments were conducted only on two field sites with a specific topography and ridge orientation. On the basis of these sites, we could demonstrate the importance of the landscape topography in combination with the orientation of ridges and furrows on erosion rates, but our study cannot represent the variety of different fields and topographical conditions within the complex terrain of Korean watersheds. In order to assess soil erosion and sediment transport within those complex landscapes, it may be necessary to identify general patterns related to topography and tillage orientation, which can be used for large-scale model applications. Watershed-scale models, such as SWAT and InVEST generally work on the basis of coarse digital elevation models that cannot adequately represent those cropping systems and their orientation, which can result in strong over- and underestimations of erosion rates.

To better understand the hydraulics of overland flow as affected by plastic covered ridge-furrow systems and its impact on soil erosion rates, we suggest additional modeling studies that cover a broader variety of different field topographies occurring in complex mountainous watersheds and that account for various ridge-furrow configurations.

The development of required high resolution digital terrain models based on tachymeter measurements may not be applicable for a large number of field sites and could be replaced by the LiDAR (light detection and ranging) technology that can be used to develop high resolution topographical data over large areas (James *et al.*, 2007). The results of those studies can help to develop correction factors for large-scale models to improve their erosion prediction for mountainous watersheds. Additionally, we recommend further research focusing on crop canopy interception and stem flow under plastic mulch cultivation to fully understand the processes of runoff generation. Comprehensive lysimeter studies, such as those of the National Academy of Agricultural Science of Korea (NAAS) (e.g. Jung *et al.*, 2003) can be conducted to directly compare infiltration and runoff amounts of plastic covered to non-covered cultivation for different growth stages of various dryland crops. The findings of these studies can be also implemented for the application of watershed-scale models for a better representation of runoff generation for different crop types over the season.

Study 3: soil erosion and conservation potential of conventional and organic row crop cultivation

In our third study, we analyzed the impact of conventional and organic farming on soil erosion and their conservation potential for row crop cultivation using measured vegetation parameters and the Revised Universal Soil Loss Equation (RUSLE). The results of this study demonstrate that weed biomass and especially the ground cover provided by weeds can be highly increased by the absence of herbicides associated with organic farming. We can, therefore, conclude that our first hypothesis formulated for this study can be confirmed. The erosion simulations, however, showed that the soil loss rates of both management systems exceed, by far, any tolerable limits. The OECD (2001) defined soil loss as tolerable when it is below $6.0 \text{ t ha}^{-1} \text{ yr}^{-1}$, and severe when it exceeds $33.0 \text{ t ha}^{-1} \text{ yr}^{-1}$. The average annual erosion rate of all four row crops in this study was at least at the limit to severe erosion, and in many cases highly above. Neither organic nor conventional farming can sufficiently lower the amount of soil erosion for row crop cultivation to an acceptable level. We can, therefore, conclude that our second hypothesis must be rejected, and that organic farming alone cannot be used to effectively control soil erosion on mountainous farmland in South Korea.

However, this study was based on crop and weed properties, which were measured within one season only. The effects of crop rotation on the soil and surface conditions of the agricultural fields were not considered. We have shown that different crop types can produce strongly different above-ground and below-ground biomass densities at the end of the growing season, which may affect the biomass pool of the soil of the following season. Based on crop price fluctuations and governmental subsidies, conventional and organic farmers may have different strategies for crop selection, which can result in different sequences of cultivated crop types. Specific configurations of crops over many years may have long-term effects on the soil conditions and, as a consequence, on the erosion rates, which could not be covered with our study. We additionally assumed that both conventional and organic farmers apply the same techniques for soil management, namely the annual tillage before seedbed preparation. In fact, in some cases, we observed that organic farmers in the Haean catchment planted crops (i.e. bean) in already existing ridge-furrow systems of the previous season without additional tillage. Such temporary no-till cultivation may considerably reduce the soil loss rate of the associated field sites and can strongly contribute to erosion control for organic farming systems. Nevertheless, this cultivation strategy was only rarely observed and may, so far, only play a marginal role for erosion prevention in the study area.

In order to understand also the long-term effects of both farming systems on soil erosion, additional modeling studies may be conducted, which consider crop sequences over many years and potential differences in the tillage management. RUSLE and RUSLE2 (USDA, 2008) can be applied to run different scenarios of crop rotation by using

the biomass conditions at the end of one season as initial conditions for the following season. The required information about crop selection and applied soil management can be obtained by additional questionnaires of local farmers or from crop statistics provided from agricultural agencies. Furthermore, we recommend that these studies are supported by additional field measurements of crop and weed biomass beyond the crop growing season to obtain information about the weed development after harvest and decomposition rates of the plant residues. The findings of these measurements could also be used to further develop and update current USLE factors for different crops and management strategies, which can help for improving soil erosion predictions of SWAT and InVEST on the watershed-scale.

Although our studies were subject to different limitations and simplifications, we could identify the major processes and factors controlling water flow, runoff generation, and soil erosion, as affected by the dominant dryland farming practices of a mountainous watershed in South Korea. Soil replenishment and tillage operations lead to lateral water flow and transport of agricultural chemicals. Ridge-furrow cultivation with polyethylene cover supports the generation of surface runoff and increases soil erosion. Furthermore, the ridge-furrow system can generate concentrated runoff flow resulting in severely accelerated erosion by gully formation, depending on the field topography and the ridge orientation. The absence of agricultural chemicals in organic farming systems supports the development of weed coverage in the furrows, but does not sufficiently reduce soil loss from the field sites. Based on the generally high soil erosion rates on dryland fields in the study area, we can conclude that the applied management practices are not capable for effective erosion control and soil conservation.

However, based on our findings, we could identify different measures of modification of the current management practices, which can help to reduce the erosion risk, without implementing entirely new conservation techniques. The first measure addresses the reduction of runoff generation caused by the plastic covered ridge-furrow system. Instead of using impermeable polyethylene covers of the ridges, we would recommend the application of perforated plastic sheets for row crop cultivation. The plastic perforation can help to increase infiltration rates into the ridges and reduce runoff accumulation in the furrows. As a consequence, the erosion risk and also the transport of agricultural chemicals could be diminished, especially in early growth stages before high canopy covers are established. At the same time, the benefits of plastic mulch for example for crop yield and weed control (Lament Jr., 1993) can be maintained. The second measure targets a well-directed construction of ridges and furrows within the individual field sites. In a complex mountainous landscape with a highly variable topography, the ridge-furrow cultivation should be performed carefully in order to prevent severe erosion damages. We recommend that ridges are located preferably parallel with the contours, or, if not applicable, oriented towards the field edges in order to drain surface runoff away from depressions and to prevent concentrated flow within the fields. However, when draining overland flow towards field edges, the transition zones between the field and the surrounding margins require special consideration. In order to prevent erosion damages caused by accumulated runoff along the edges, overland flow should be drained preferably from the individual furrows directly into adjacent buffers or filter strips. In any case, the slope angles along the ridge-furrow system should be minimized to avoid high flow velocities of surface runoff and detachment of soil particles. The third measure integrates practices aiming at a better protection of the soils within the furrows from erosion by overland flow. Rice *et al.* (2007) suggested the establishment of vegetated covered furrows, for example by cereal grass cultivation, which act as “in-field-buffers” that increase infiltration capacity and reduce flow velocity due to a higher surface roughness. However, the cultivation of cover crops during the growing season could involve competition with the main crop, which could potentially result in lower yields. Another very effective measure for erosion prevention is mulching with plant residues (Morgan, 2005) that may be used for furrow protection instead of cover crop cultivation. After the growing season, soils

are more susceptible to erosion due to low ground covers and disturbances during harvest activities. The cultivation of winter cover crops, for example ryegrass, can be used to protect soils for the time period after harvest (Kim *et al.*, 2007) and may also help to reduce soil erosion by early rainstorms in the following year. We, therefore, recommend residue mulching of furrows during the growing season in combination with winter cover crop cultivation after harvest to provide a better protection of the soil surface throughout the year. The presented management measures are based on modifications of the existing row crop farming practices to make them more capable for erosion control. Before implementing new technologies that may imply additional costs and use restrictions for farmers, these measures may be considered for designing land use plans for soil conservation in the Haean catchment and other Korean mountainous watersheds.

However, all three studies of this thesis focused only on the on-site factors and processes of runoff and soil erosion and did not address the fate of eroded sediments outside of the agricultural fields. Since particulate phosphorus is a major source of eutrophication, it is essential to control also the transfer of sediment from the agricultural field to the downstream water bodies (Duzant *et al.*, 2011). The degree of sediment delivery to downstream locations is highly dependent on the land use and land cover patterns of the landscape (Conte *et al.*, 2011). When sediments leave the edge of the field sites, they generally pass other landscape elements, such as field margins, riparian forests, farm roads, and also adjacent field sites, before entering surface water bodies. In a comprehensive study using the EROSION 3D model, Stöckler (2012) identified the location of erosion hotspots and the pathways of transported soils within the entire Haean catchment. This study provides valuable information about the function of the different landscape elements for sediment retention and their contribution to water quality conservation. Especially field margins, which can act as vegetative buffers, can play an important role in controlling the off-site damages of erosion by slowing down surface runoff and retaining sediment, nutrients, and other agricultural chemicals. An essential role for the effectiveness of such vegetative buffers plays the architecture of the vegetation and the plant species composition (Duzant *et al.*, 2011). In 2012, a research study was initiated in the Haean catchment focusing on the vegetation structure of existing field margins and their capability for sediment retention (Hamada Elsayed Ali and Björn Reineking, personal communication). The outcome of this study can give important insights into the role of field margins for erosion control and may provide important additional information for future conservation planning for the agricultural areas of mountainous landscapes in South Korea.

1.5 List of manuscripts and specification of individual contributions

The three studies described in this thesis refer to three different manuscripts. One manuscript is in review for the ISELE 2011 Special Collection of the *Transactions of the ASABE*, one is submitted to *Hydrological Processes* and one to *Geoderma*. The following list specifies the contributions of the individual authors to each manuscript.

Manuscript 1

Authors	Marianne Ruidisch, Sebastian Arnhold, Bernd Huwe, Christina Bogner	
Title	Effects of ridge tillage on flow processes in the Haean catchment, South Korea	
Journal	<i>Hydrological Processes</i>	
Status	submitted	
Contributions	M. Ruidisch	idea, methods, data collection, data analysis, modeling, manuscript writing, figures, discussion, manuscript editing, corresponding author
	S. Arnhold	data collection, data analysis, discussion, manuscript editing
	B. Huwe	idea, discussion, manuscript editing
	C. Bogner	idea, discussion, manuscript writing, manuscript editing

Manuscript 2

Authors	Sebastian Arnhold, Marianne Ruidisch, Svenja Bartsch, Christopher L. Shope, Bernd Huwe	
Title	Plastic covered ridge-furrow systems on mountainous farmland: runoff patterns and soil erosion rates	
Journal	<i>Transactions of the ASABE</i> (ISELE 2011 Special Collection)	
Status	in review	
Contributions	S. Arnhold	idea, methods, data collection, data analysis, modeling, manuscript writing, figures, discussion, manuscript editing, corresponding author
	M. Ruidisch	data collection, data analysis, discussion
	S. Bartsch	data collection, discussion
	C. L. Shope	idea, discussion, manuscript editing
	B. Huwe	idea, discussion, manuscript editing

Manuscript 3

Authors	Sebastian Arnhold, Steve Lindner, Bora Lee, Emily Martin, Janine Kettering, Trung Thanh Nguyen, Thomas Koellner, Yong Sik Ok, Bernd Huwe	
Title	Conventional and organic farming: soil erosion and conservation potential for row crop cultivation	
Journal	<i>Geoderma</i>	
Status	submitted	

Contributions	S. Arnhold	idea, methods, data collection, data analysis, modeling, manuscript writing, figures, discussion, manuscript editing, corresponding author
	S. Lindner	data collection, data analysis, discussion
	B. Lee	data collection, data analysis, discussion
	E. Martin	data collection, discussion
	J. Kettering	data collection, data analysis
	T. T. Nguyen	idea, discussion
	T. Koellner	idea, discussion, manuscript editing
	Y. S. Ok	discussion, manuscript editing
	B. Huwe	idea, discussion, manuscript editing

1.6 References

- Afandi, G., Manik, T. K., Rosadi, B., Utomo, M., Senge, M., Adachi, T., Oki, Y., 2002. Soil erosion under coffee trees with different weed managements in humid tropical hilly area of Lampung, South Sumatra, Indonesia. *Journal of the Japanese Society of Soil Physics* **91**, 3-14.
- Auerswald, K., Kainz, M., Fiener, P., 2003. Soil erosion potential of organic versus conventional farming evaluated by USLE modelling of cropping statistics for agricultural districts in Bavaria. *Soil Use and Management* **19**, 305-311.
- Bachmair, S., Weiler, M., Nützmann, G., 2009. Controls of land use and soil structure on water movement: lessons for pollutant transfer through the unsaturated zone. *Journal of Hydrology* **369**(3-4), 241-252.
- Bargar, B., Swan, J. B., Jaynes, D., 1999. Soil water recharge under uncropped ridges and furrows. *Soil Science Society of America Journal* **63**, 1290-1299.
- Blavet, D., De Noni, G., Le Bissonnais, Y., Leonard, M., Maillou, L., Laurent, J. Y., Asseline, J., Leprun, J. C., Arshad, M. A., Roose, E., 2009. Effect of land use and management on the early stages of soil water erosion in French Mediterranean vineyards. *Soil and Tillage Research* **106**(1), 124-136.
- Bogner, C., Gaul, D., Kolb, A., Schmiedinger, I., Huwe, B., 2010. Investigating flow mechanisms in a forest soil by mixed-effects modelling. *European Journal of Soil Science* **61**(6), 1079-1090.
- Bogner, C., Mirzaei, M., Ruy, S., Huwe, B., 2012. Microtopography, water storage and flow patterns in a fine-textured soil under agricultural use. *Hydrological Processes*, DOI: 10.1002/hyp.9337.
- Bonilla, C. A., Kroll, D. G., Norman, J. M., Yoder, D. C., Molling, C. C., Miller, P. S., Panuska, J. C., Topel, J. B., Wakeman, P. L., Karthikeyan, K. G., 2006. Instrumentation for measuring runoff, sediment, and chemical losses from agricultural fields. *Journal of Environmental Quality* **35**, 216-223.
- Boo, K., Kwon, W., Baek, H., 2006. Change of extreme events of temperature and precipitation over Korea using regional projection of future climate change. *Geophysical Research Letters* **33**(1), L01701.
- Brock, B. G., 1982. Weed control versus soil erosion control. *Journal of Soil and Water Conservation* **37**(2), 73-76.
- Chanson, H., 2004. *The hydraulics of open channel flow. An introduction*, second ed. Elsevier Butterworth Heinemann, Oxford.
- Choi, G., Kwon, W., Boo, K., Cha, Y., 2008. Recent spatial and temporal changes in means and extreme events of temperature and precipitation across the Republic of Korea. *Journal of the Korean Geographical Society* **43**(5), 681-700.
- Choi, J., Choi, Y., Lim, K., Shin, Y., 2005. Soil erosion measurement and control techniques, in: Chung, N., Kim, W., Kim, H., Kim, J., Eom, K., Lee, I. (Eds.), *Proceedings of the International Workshop on Newly Developed Innovative Technology for Soil and Water Conservation*. Rural Development Administration.

- Choi, J., Lee, H., Park, S., Won, C., Choi, Y., Lim, K., 2010. Sediment control practices in sloping highland fields in Korea, in: Gilkes, R. J., Prakongkep, N. (Eds.), *Proceedings of the 19th World Congress of Soil Science. Soil solutions for a changing world*. International Union of Soil Sciences, pp. 132-135.
- Choo, H., Jamal, T., 2009. Tourism on organic farms in South Korea: a new form of ecotourism? *Journal of Sustainable Tourism* **17**(4), 431-454.
- Chow, V. T., 1959. *Open-channel hydraulics*. McGraw-Hill, New York.
- Conte, M., Ennaanay, D., Mendoza, G., Walter, M. T., Wolny, S., Freyberg, D., Nelson, E., Solorzano, L., 2011. Retention of nutrients and sediment by vegetation, in: Kareiva, P., Tallis, H., Ricketts, T. H., Daily, G. C., Polasky, S. (Eds.), *Natural capital. Theory and practice of mapping ecosystem services*. Oxford University Press, Oxford, pp. 89-110.
- Daily, G. C., 1997. Introduction: what are ecosystem services?, in: Daily, G. C. (Ed.), *Nature's services. Societal dependence on natural ecosystems*. Island Press, Washington D.C., pp. 1-10.
- Daily, G. C., Matson, P. A., Vitousek, P. M., 1997. Ecosystem services provided by soil, in: Daily, G. C. (Ed.), *Nature's services. Societal dependence on natural ecosystems*. Island Press, Washington D.C., pp. 113-132.
- Dominati, E., Patterson, M., Mackay, A., 2010. A framework for classifying and quantifying the natural capital and ecosystem services of soils. *Ecological Economics* **69**(9), 1858-1868.
- Duzant, J. H., Morgan, R. P. C., Wood, G. A., Deeks, L. K., 2011. Modelling the role of vegetated buffer strips in reducing transfer of sediment from land to watercourses, in: Morgan, R. P. C., Nearing, M. A. (Eds.), *Handbook of erosion modelling*. Wiley-Blackwell, Chichester, pp. 249-262.
- El-Swaify, S. A., Dangler, E. W., Armstrong, C. L., 1982. *Soil erosion by water in the tropics*. College of Tropical Agriculture and Human Resources, University of Hawaii, Honolulu.
- Eltun, R., Korsæth, A., Nordheim, O., 2002. A comparison of environmental, soil fertility, yield, and economical effects in six cropping systems based on an 8-year experiment in Norway. *Agriculture, Ecosystems and Environment* **90**, 155-168.
- Erhart, E., Hartl, W., 2010. Soil protection through organic farming: a review, in: Lichtfouse, E. (Ed.), *Sustainable agriculture reviews. Organic farming, pest control and remediation of soil pollutants*. Springer, Dordrecht, pp. 203-226.
- Fleming, K. L., Powers, W. L., Jones, A. J., Helmers, G. A., 1997. Alternative production systems' effects on the K-factor of the Revised Universal Soil Loss Equation. *American Journal of Alternative Agriculture* **12**(2), 55-58.
- Food and Agriculture Organization of the United Nations (FAO), 2011a. *Save and grow. A policymaker's guide to the sustainable intensification of smallholder crop production*. Food and Agriculture Organization of the United Nations, Rome.
- Food and Agriculture Organization of the United Nations (FAO), 2011b. *The state of the world's land and water resources for food and agriculture. Managing systems at risk*, first ed. Food and Agriculture Organization of the United Nations, Rome.
- García-Orenes, F., Cerdà, A., Mataix-Solera, J., Guerrero, C., Bodí, M. B., Arcenegui, V., Zornoza, R., Sempere, J. G., 2009. Effects of agricultural management on surface soil properties and soil-water losses in eastern Spain. *Soil and Tillage Research* **106**(1), 117-123.
- Gascuel-Oudou, C., Garnier, F., Heddadj, D., 2001. Influence of cultural practices on sheetflow, sediment and pesticide transport: the case of corn cultivation under plastic mulching, in: Stott, D. E., Mohtar, R. H., Steinhardt, G. C. (Eds.), *Sustaining the global farm. Selected papers from the 10th International Soil Conservation Organization Meeting*. International Soil Conservation Organization, pp. 300-304.
- Gassman, P. W., Reyes, M. R., Green, C. H., Arnold, J. G., 2007. The Soil and Water Assessment Tool: historical development, applications, and future research directions. *Transactions of the ASABE* **50**(4), 1211-1250.
- Godfray, H. C. J., Beddington, J. R., Crute, I. R., Haddad, L., Lawrence, D., Muir, J. F., Pretty, J., Robinson, S., Thomas, S. M., Toulmin, C., 2010. Food security: the challenge of feeding 9 billion people. *Science* **327**(5967), 812-818.
- Hagmann, J., 1996. Mechanical soil conservation with contour ridges: cure for, or cause of, rill erosion? *Land Degradation and Development* **7**, 145-160.

- Hendrickx, J. M. H., Flury, M., 2001. Uniform and preferential flow mechanisms in the vadose zone, in: Council, N. R. (Ed.), *Conceptual models of flow and transport in the fractured vadose zone*. National Academy Press, Washington D.C., pp. 149-187.
- Intergovernmental Panel on Climate Change (IPCC) Working Group I, 2001. *Climate change 2001. The scientific basis*. Cambridge University Press, Cambridge.
- James, L. A., Watson, D. G., Hansen, W. F., 2007. Using LiDAR data to map gullies and headwater streams under forest canopy: South Carolina, USA. *Catena* **71**(1), 132-144.
- Jefferies, R. A., MacKerron, D. K. L., 1985. Stemflow in potato crops. *Journal of Agricultural Science* **105**, 205-207.
- Jung, K., Son, Y., Hur, S., Ha, S., Jang, Y., Jung, P., 2003. *Estimation of nationwide soil loss with soil type*. National Academy of Agricultural Science (NAAS), Research Report.
- Kang, J., Kim, C., 2000. Technical change and policy implications for developing environmentally-friendly agriculture in Korea. *Journal of Rural Development* **23**, 163-182.
- Kang, S., Tenhunen, J., 2010. Complex Terrain and Ecological Heterogeneity (TERRECO): evaluating ecosystem services in production versus water quantity/quality in mountainous landscapes. *Korean Journal of Agricultural and Forest Meteorology* **12**(4), 307-316
- Kim, B., Choi, K., Kim, C., Lee, U., Kim, Y., 2000. Effects of the summer monsoon on the distribution and loading of organic carbon in a deep reservoir, Lake Soyang, Korea. *Water Research* **34**(14), 3495-3504.
- Kim, B., Park, J., Hwang, G., Jun, M., Choi, K., 2001a. Eutrophication of reservoirs in South Korea. *Limnology* **2**(3), 223-229.
- Kim, C., Jeong, H., Moon, D., 2012. *Production and consumption status and market prospects for environment-friendly agri-foods*. Korea Rural Economic Institute (KREI), Research Report.
- Kim, C., Kim, T., 2004. Economics of conversion to environmentally friendly practices of rice production. *Journal of Rural Development* **27**, 91-112.
- Kim, M., Flanagan, D. C., Frankenberger, J. R., Meyer, C. R., 2009. Impact of precipitation changes on runoff and soil erosion in Korea using CLIGEN and WEPP. *Journal of Soil and Water Conservation* **64**(2), 154-162.
- Kim, P., Chung, D., Malo, D., 2001b. Characteristics of phosphorus accumulation in soils under organic and conventional farming in plastic film houses in Korea. *Soil Science and Plant Nutrition* **47**(2), 281-289.
- Kim, S., Yang, J., Park, C., Jung, Y., Cho, B., 2007. Effects of winter cover crop of ryegrass (*Lolium multiflorum*) and soil conservation practices on soil erosion and quality in the sloping uplands. *Journal of Applied Biological Chemistry* **55**(1), 22-28.
- Kuhn, N. J., Armstrong, E. K., Ling, A. C., Connolly, K. L., Heckrath, G., 2012. Interrill erosion of carbon and phosphorus from conventionally and organically farmed Devon silt soils. *Catena* **91**, 94-103.
- Kulli, B., Gysi, M., Flühler, H., 2003. Visualizing soil compaction based on flow pattern analysis. *Soil and Tillage Research* **70**(1), 29-40.
- Lal, R., 1994. Sustainable land use systems and soil resilience, in: Greenland, D. J., Szabolcs, I. (Eds.), *Soil resilience and sustainable land use. Proceedings of a symposium held in Budapest, 28 September to 2 October 1992, including the Second Workshop on the Ecological Foundations of Sustainable Agriculture (WEFSA II)*. CAB International, Wallingford, pp. 41-67.
- Lament Jr., W. J., 1993. Plastic mulches for the production of vegetable crops. *HortTechnology* **3**(1), 35-39.
- Larson, W. E., Pierce, F. J., Dowdy, R. H., 1983. The threat of soil erosion to long-term crop production. *Science* **219**(4584), 458-465.
- Lee, G., Lee, J., Ryu, J., Hwang, S., Yang, J., Joo, J., Jung, Y., 2010a. Status and soil management problems of highland agriculture of the main mountainous region in the South Korea, in: Gilkes, R. J., Prakongkep, N. (Eds.), *Proceedings of the 19th World Congress of Soil Science. Soil solutions for a changing world*. International Union of Soil Sciences, pp. 154-157.
- Lee, G., Lee, J., Ryu, J., Zhang, Y., Jung, Y., 2010b. Loss of soil and nutrient from different soil managements in highland agriculture, in: Gilkes, R. J., Prakongkep, N. (Eds.), *Proceedings of the 19th World Congress of Soil Science. Soil solutions for a changing world*. International Union of Soil Sciences, pp. 78-81.

- Leistra, M., Boesten, J. J. T. I., 2010. Pesticide leaching from agricultural fields with ridges and furrows. *Water, Air and Soil Pollution* **213**(1-4), 341-352.
- Liniger, H. P., Weingartner, R., Grosjean, M., 1998. *Mountains of the world - water towers for the 21st century*. Centre for Development and Environment, Bern.
- Lockeretz, W., Shearer, G., Kohl, D. H., 1981. Organic farming in the Corn Belt. *Science* **211**, 540-547.
- Mermut, A. R., 2008. Understanding soils within the context of earth surface systems, in: Dazzi, C., Costantini, E. A. C. (Eds.), *The soils of tomorrow. Soils changing in a changing world*. Catena, Reiskirchen, pp. 1-11.
- Meusburger, K., Jeong, J., Mabit, L., Park, J., Sandor, T., Alewell, C., 2012. Effect of deforestation on soil erosion rates using fallout radionuclides - a case study in a mountainous catchment, South Korea, *in preparation*.
- Millennium Ecosystem Assessment, 2005. *Ecosystems and human well-being. Synthesis*. Island Press, Washington D.C.
- Montes, S., 1998. *Hydraulics of open channel flow*. ASCE Press, Reston.
- Morgan, R. P. C., 2005. *Soil erosion and conservation*, third ed. Blackwell, Malden.
- Moriasi, D. N., Arnold, J. G., van Liew, M. W., Bingner, R. L., Harmel, R. D., Veith, T. L., 2007. Model evaluation guidelines for systematic quantification of accuracy in watershed simulations. *Transactions of the ASABE* **50**(3), 885-900.
- Nearing, M. A., Jetten, V., Baffaut, C., Cerdan, O., Couturier, A., Hernandez, M., Le Bissonnais, Y., Nichols, M. H., Nunes, J. P., Renschler, C. S., Souchère, V., van Oost, K., 2005. Modeling response of soil erosion and runoff to changes in precipitation and cover. *Catena* **61**(2-3), 131-154.
- Oldeman, L. R., 1994. The global extent of soil degradation, in: Greenland, D. J., Szabolcs, I. (Eds.), *Soil resilience and sustainable land use. Proceedings of a symposium held in Budapest, 28 September to 2 October 1992, including the Second Workshop on the Ecological Foundations of Sustainable Agriculture (WEFSA II)*. CAB International, Wallingford, pp. 99-118.
- Oldeman, L. R., van Engelen, V., Pulles, J., 1990. The extent of human-induced soil degradation, Annex 5, in: Oldeman, L. R., Hakkeling, R. T. A., Sombroek, W. G. (Eds.), *World map of the status of human-induced soil degradation: an explanatory note*, second ed. International Soil Reference Information Centre, Wageningen.
- Organization for Economic Cooperation and Development (OECD), 2001. *Environmental indicators for agriculture*. OECD Publications, Paris.
- Pacini, C., Wossink, A., Giesen, G., Vazzana, C., Huirne, R., 2003. Evaluation of sustainability of organic, integrated and conventional farming systems: a farm and field-scale analysis. *Agriculture, Ecosystems and Environment* **95**(1), 273-288.
- Park, J., Duan L., Kim, B., Mitchell, M. J., Shibata, H., 2010. Potential effects of climate change and variability on watershed biogeochemical processes and water quality in Northeast Asia. *Environment International* **36**, 212-225.
- Petersen, C. T., Jensen, H. E., Hansen, S., Bender Koch, C., 2001. Susceptibility of a sandy loam soil to preferential flow as affected by tillage. *Soil and Tillage Research* **58**(1-2), 81-89.
- Pimentel, D., 2006. Soil erosion: a food and environmental threat. *Environment, Development and Sustainability* **8**(1), 119-137.
- Pimentel, D., Harvey, C., Resosudarmo, P., Sinclair, K., Kurz, D., McNair, M., Crist, S., Shpritz, L., Fitton, L., Saffouri, R., Blair, R., 1995. Environmental and economic costs of soil erosion and conservation benefits. *Science* **267**(5201), 1117-1123.
- Pinson, W. T., Yoder, D. C., Buchanan, J. R., Wright, W. C., Wilkerson, J. B., 2004. Design and evaluation of an improved flow divider for sampling runoff plots. *Applied Engineering in Agriculture* **20**(4), 433-438.
- Powlson, D. S., Gregory, P. J., Whalley, W. R., Quinton, J. N., Hopkins, D. W., Whitmore, A. P., Hirsch, P. R., Goulding, K. W. T., 2011. Soil management in relation to sustainable agriculture and ecosystem services. *Food Policy* **36**, 72-87.
- Reganold, J. P., Elliott, L. F., Unger, Y. L., 1987. Long-term effects of organic and conventional farming on soil erosion. *Nature* **330**, 370-372.

- Renard, K. G., Foster, G. R., Weesies, G. A., McCool, D. K., Yoder, D. C., 1997. *Predicting soil erosion by water. A guide to conservation planning with the Revised Universal Soil Loss Equation (RUSLE)*. Agriculture Handbook 703. USDA, Washington D.C.
- Renard, K. G., Yoder, D. C., Lightle, D. T., Dabney, S. M., 2011. Universal Soil Loss Equation and Revised Universal Soil Loss Equation, in: Morgan, R. P. C., Nearing, M. A. (Eds.), *Handbook of erosion modelling*. Wiley-Blackwell, Chichester, pp. 137-167.
- Rice, P. J., Harman-Fetcho, J. A., Sadeghi, A. M., McConnell, L. L., Coffman, C. B., Teasdale, J. R., Abdul-Baki, A. A., Starr, J. L., McCarty, G. W., Herbert, R. R., Hapeman, C. J., 2007. Reducing insecticide and fungicide loads in runoff from plastic mulch with vegetative-covered furrows. *Journal of Agricultural and Food Chemistry* **55**(4), 1377-1384.
- Rice, P. J., McConnell, L. L., Heighton, L. P., Sadeghi, A. M., Isensee, A. R., Teasdale, J. R., Abdul-Baki, A. A., Harman-Fetcho, J. A., Hapeman, C. J., 2001. Runoff loss of pesticides and soil: a comparison between vegetative mulch and plastic mulch in vegetable production systems. *Journal of Environmental Quality* **30**, 1808-1821.
- Ruidisch, M., Kettering, J., Arnhold, S., Huwe, B., 2012. Modeling water flow in a plastic mulched ridge cultivation system on hillslopes affected by South Korean summer monsoon. *Agricultural Water Management*, in press.
- Saffigna, P. G., Tanner, C. B., Keeney, D. R., 1976. Non-uniform infiltration under potato canopies caused by interception, stemflow, and hilling. *Agronomy Journal* **68**(2), 337-342.
- Schmidt, J., 1991. A mathematical model to simulate rainfall erosion, in: Bork, H. R., De Ploey, J., Schick, A. P. (Eds.), *Erosion, transport and deposition processes. Theories and models*. Catena Supplement 19. Catena, Cremlingen, pp. 101-109.
- Schmidt, J., von Werner, M., 2000. Modeling the sediment and heavy metal yields of drinking water reservoirs in the Osterzgebirge region of Saxony (Germany), in: Schmidt, J. (Ed.), *Soil erosion. Application of physically based models*. Springer, Berlin, pp. 93-108.
- Schmidt, J., von Werner, M., Michael, A., 1999. Application of the EROSION 3D model to the CATSOP watershed, The Netherlands. *Catena* **37**, 449-456.
- Shannon, C. E., 1948. A mathematical theory of communication. *Bell System Technical Journal* **27**(3), 379-423.
- Siegrist, S., Schaub, D., Pfiffner, L., Mäder, P., 1998. Does organic agriculture reduce soil erodibility? The results of a long-term field study on loess in Switzerland. *Agriculture, Ecosystems and Environment* **69**, 253-264.
- Šimůnek, J., Jarvis, N. J., van Genuchten, M. T., Gärdenäs, A., 2003. Review and comparison of models for describing non-equilibrium and preferential flow and transport in the vadose zone. *Journal of Hydrology* **272**, 14-35.
- Šimůnek, J., Šejna, M., van Genuchten, M. T., 2011. *The HYDRUS software package for simulating two- and three-dimensional movement of water, heat, and multiple solutes in variably-saturated media*. Technical manual, version 2.0. PC Progress, Prague.
- Stevens, M. D., Black, B. L., Lea-Cox, J. D., Sadeghi, A. M., Harman-Fetcho, J. A., Pfeil, E., Downey, P., Rowland, R., Hapeman, C. J., 2009. A comparison of three cold-climate strawberry production systems: environmental effects. *HortScience* **44**(2), 298-305.
- Stocking, M. A., 1972. Aspects of the role of man in erosion in Rhodesia. *Zambezia* **2**(2), 1-10.
- Stöckler, E., 2012. Prozessbasierte Modellierung zur Untersuchung der Bodenerosion in einem bergigen Einzugsgebiet in Südkorea. *MSc Thesis*. University of Bayreuth, Department of Soil Physics.
- Tallis, H., Polasky, S., 2011. Assessing multiple ecosystem services: an integrated tool for the real world, in: Kareive, P., Tallis, H., Ricketts, T. H., Daily, G. C., Polasky, S. (Eds.), *Natural capital. Theory and practice of mapping ecosystem services*. Oxford University Press, Oxford, pp. 34-50.
- Toy, T. J., Foster, G. R., Renard, K. G., 2002. *Soil erosion. Processes, prediction, measurement, and control*. John Wiley and Sons, New York.
- Trancón y Widemann, B., Bogner, C., 2012. Image analysis for soil dye tracer infiltration studies, in: *Proceedings of the 3rd International Conference on Image Processing Theory, Tools and Application*, in press.
- United States Department of Agriculture (USDA), 2008. *Revised Universal Soil Loss Equation version 2. Science documentation*. USDA, Washington D.C.

- Vieux, B. E., 2001. *Distributed hydrologic modeling using GIS*. Kluwer Academic Publishers, Dordrecht.
- von Werner, M., 1995. GIS-orientierte Methoden der digitalen Reliefanalyse zur Modellierung von Bodenerosion in kleinen Einzugsgebieten. *PhD Thesis*. Free University of Berlin, Department of Earth Sciences.
- Wan, Y., El-Swaify, S. A., 1999. Runoff and soil erosion as affected by plastic mulch in a Hawaiian pineapple field. *Soil and Tillage Research* **52**, 29-35.
- Weil, R. R., 1982. Maize-weed competition and soil erosion in unweeded maize. *Tropical Agriculture (Trinidad)* **59**(3), 207-213.
- Weiler, M., Naef, F., 2003. An experimental tracer study of the role of macropores in infiltration in grassland soils. *Hydrological Processes* **17**(2), 477-493.
- Wickenkamp, V., Duttmann, R., Mosimann, T., 2000. A multiscale approach to predicting soil erosion on cropland using empirical and physically based soil erosion models in a geographic information system, in: Schmidt, J. (Ed.), *Soil erosion. Application of physically based models*. Springer, Berlin, pp. 109-134.
- Wischmeier, W. H., Johnson, C. B., Cross, B. V., 1971. A soil erodibility nomograph for farmland and construction sites. *Journal of Soil and Water Conservation* **26**(5), 189-193.
- Wischmeier, W. H., Smith, D. D., 1978. *Predicting rainfall erosion losses. A guide to conservation planning*. Agriculture Handbook 537. USDA, Washington D.C.
- Wolfe, M. L., Ross, B. B., Diem, J. F., Dillaha, T. A., Flahive, K. A., 2002. *Protecting water quality: best management practices for row crops grown on plastic mulch in Virginia*. Virginia Cooperative Extension, Blacksburg.
- Zhai, P., Zhang, X., Wan, H., Pan, X., 2005. Trends in total precipitation and frequency of daily precipitation extremes over China. *Journal of Climate* **18**(7), 1096-1108.

Chapter 2

Effects of ridge tillage on flow processes in the Haeon catchment, South Korea

Marianne Ruidisch ¹, Sebastian Arnhold ¹, Bernd Huwe ¹, Christina Bogner ²

¹ Department of Soil Physics, University of Bayreuth, Universitätsstraße 30, 95447 Bayreuth, Germany

² Department of Ecological Modelling, University of Bayreuth, Dr.-Hans-Frisch-Straße 1-3, 95448 Bayreuth, Germany

Abstract

The intense agricultural land use has a considerable impact on water quality worldwide. A detailed understanding of the transport of agrochemicals requires knowledge about flow processes and how they are affected by agricultural management operations like tillage. This is especially important in regions influenced by extreme rainstorm events. We carried out four dye tracer experiments on two sloped agricultural dryland fields in South Korea to compare flow processes under (i) conventional tillage, (ii) ridge tillage, (iii) ridge tillage with plastic mulch, and (iv) plastic mulched ridge tillage with well developed potato crops. We found that the ridge topography enhanced the infiltration in depression zones like furrows and planting holes. Deeper in the soil, the water flow was funneled preferentially above the tillage pan, however, preferential macropore flow to greater depths was absent. Furthermore, we found substantially higher surface runoff under ridge tillage with plastic mulch before the crop canopy was developed. Therefore, to reduce surface runoff, we suggest to encourage crop production in ridge cultivation with perforated plastic mulch. Additionally, to reduce the leaching risk of agrochemicals and fertilizers via subsurface flow above the tillage pan, we propose the establishment of riparian buffer zones between dryland fields and the river network.

Keywords: *Agricultural soils, Dye tracers, Preferential flow, Flow patterns, Ridge cultivation, Tillage management*

2.1 Introduction

Worldwide, intense agriculture is accompanied by increasing use of fertilizers, pesticides and herbicides to meet the food demand of a growing population. This trend has a considerable impact on ecosystem services. In regions like East Asia that are characterized by seasonal extreme rainstorm events, leaching of agrochemicals plays a key role in pollution of freshwater resources. Over the last decades, a substantial increase of extreme rainfall during the summer monsoon has been observed for western, southwestern, and southern parts of China and South Korea (Park *et al.*, 2010, Zhai *et al.*, 1999, 2005). Non-point-source pollution like intensified export of sediments and nutrients from agricultural land in combination with these increasing amounts and intensities of precipitation strongly affects the fresh water resources of lakes and reservoirs and results in water quality degradation in these regions (Park *et al.*, 2010, Zhang *et al.*, 1996).

To determine the pathways of agricultural pollutants, we have to identify the dominant flow processes in agricultural soils. In general, two major types of water flow in soils can be distinguished: uniform and non-uniform (i.e. preferential) flow. The latter is characterized by water and solute movements bypassing a fraction of the porous soil matrix and can further be classified into a) macropore flow occurring in root channels, earthworm burrows, fissures or cracks, b) unstable flow induced by textural layering, water repellency, air entrapment, or continuous non-ponding infiltration and c) funnel flow describing lateral redirection and funneling of water caused by textural boundaries (Hendrickx and Flury, 2001). Preferential flow paths are responsible for rapid water movement and solute transport to greater soil depths or groundwater (Bogner *et al.*, 2010, Gish *et al.*, 1998, Šimůnek *et al.*, 2003). Their occurrence in soils depends on soil texture, soil structure, topography, surface microrelief, and management as well as on the initial soil water content and the intensity and duration of rainfall (Bachmair *et al.*, 2009, Jarvis, 2007).

Preferential flow is all the more important when intense agriculture is practiced under the influence of monsoon climate. In South Korea, for instance, a considerable amount of chemical fertilizer of up to 450 kg ha⁻¹ is applied yearly on dryland farming fields (Statistics of Korea). Although high rainfall intensities strongly support preferential flow in macropores, the leaching of a particular agrochemical agent depends on its sorption characteristics, nature of biological transformations and the form of its application (Jarvis, 2007).

Agricultural management practices like ploughing, harrowing, drilling, and wheel traffic have been identified to strongly affect water flow and infiltrability (Bogner *et al.*, 2012, Kulli *et al.*, 2003, Petersen *et al.*, 2001). Both Bogner *et al.* (2012) and Petersen *et al.* (2001) found that the tillage pan could initiate water funneling and disconnect macropores situated below from processes in the ploughed horizon. Furthermore, Kulli *et al.* (2003) noted in their study that wheel traffic caused soil compaction along with decreased permeability and macroporosity and supported water ponding in the compacted parts of the soil.

Ridge cultivation is another common management practice for example in vegetable production and was found to have positive effects on crop yield and weed control when using plastic mulch (Lament Jr., 1993). Its effects on water flow and solute transport, however, has rarely been investigated and most of the studies concentrated on soil water dynamics in ridge cultivation systems without plastic mulch. Leistra and Boesten (2010), for instance, reported that runoff from ridges to furrows (i.e. induced by surface topography) led to higher soil moisture in furrows. Thus, water movement occurred laterally from furrows to ridges and vertical water flow and solute movement under ridges was minimized (Bargar *et al.*, 1999). However, the effect of plastic mulched ridge cultivation systems on non-uniform flow regimes has not been considered in the literature so far.

In our study, we used the food dye tracer *Brilliant Blue FCF* to directly visualize flow patterns in irrigation experiments under (i) flat conventional tillage, (ii) ridge tillage, (iii) ridge tillage with plastic mulch, and (iv) ridge tillage with plastic mulch cropped with potato plants. *Brilliant Blue* is often used in tracer studies in soil hydrology and is well known for its low toxicity, relatively high mobility and good visibility against most soil colors (Flury and Flühler, 1995). Our objectives were (i) to compare infiltration and surface runoff under different tillage management systems, (ii) to investigate the effect of ridge tillage, plastic mulch and the crop root system on flow patterns qualitatively using binary images and index functions, and (iii) to evaluate the sustainability of the ridge cultivation systems in terms of pollutant transport.

2.2 Materials and methods

2.2.1 Study site

The Haean-Myeon catchment, also called Punchbowl, (128°1'33.101'' E, 38°28'6.231'' N) is located in the mountainous northeastern part of South Korea and is approximately 64 km² large. The bowl shape is characteristic and subdivides the catchment into three major land use zones. The steep hillslopes are mostly forested (58%) and the more gentle ones are dominated by dryland farming (22%). Rice paddies (8%) are characteristic for the central area of the catchment and the remainder is occupied by residences, grassland and field margins. The annual precipitation in the Haean catchment is about 1577 mm (11 years average) with 50 to 60% of the annual rainfall occurring during the monsoon season from June to August.

The geology of the catchment is dominated by granite bedrock material, which is strongly weathered due to the high precipitation rates. It constitutes the parent material for *Cambisols* - the most widely spread soil type. As a consequence of extreme rainfall events during the summer monsoon, the upper soil horizons are often eroded. To compensate this high erosion loss, the local farmers commonly bring sandy soil material at the beginning of the growing season from outside of the catchment and distribute it on their fields.

On the dryland fields, agricultural farming usually starts between April and May depending on the crop type. The common procedure is a primary fertilization using mineral fertilizer in form of granules and a subsequent ploughing to mix them into the top soil. Therefore, a tillage pan is characteristic for the most dryland farming soils. Afterwards, ridges (approx. 15 cm height, 30 cm width) are created perpendicularly to the slope with a ridge to ridge spacing of approx. 70 cm. Typically, the ridges are covered with a black plastic mulch (polyethylene) perforated with planting holes (diameter 5 cm) spaced by 25 to 30 cm while the furrows remain uncovered. Depending on the crop type, seeds are sown or juvenile plants are planted after the creation of the ridges. During the growing season, herbicides and pesticides are applied several times and fertilizers spread a second time depending on the crop type. Finally, harvesting usually begins in late August to September.

2.2.2 Experimental set-up

We carried out four irrigation experiments at two potato fields (*Solanum tuberosum*) on hillslopes. Field site 1 (128°6'32.625'' E, 38°18'4.148'' N) was located in a distance of approx. 830 m from field site 2 (128°6'54.803'' E, 38°17'43.254'' N). Both soils can be characterized as strongly anthropologically modified *Cambisols* with eroded A-horizons. Indeed, intense fertilization and application of pesticides and herbicides have altered the soils chemically. Additionally, allocthonous sandy soil material was spread several times on top of the fields. The soils were classified as a *terrlic Cambisol* and a *terrlic Anthrosol over haplic Cambisol* (IUSS Working Group WRB, 2006) with a slope of 8°

and 6° on field site 1 and 2, respectively. We selected these fields because their slope degrees and soil physical properties were comparable (Table 2.1).

Table 2.1 Soil physical properties of the experimental sites

	Horizon (WRB)	Depth ^[a] (cm)	Clay (%)	Silt (%)	Sand (%)	Soil texture class	Bulk density (g cm ⁻³)
Site 1	Ap	0-25	3.2	16.4	80.3	Loamy sand	1.43
	2Apb ^[b]	25-50	20.2	53.4	26.4	Silt loam	1.45
	Bwb	50-100	24.8	46.6	28.6	Loam	1.38
Site 2	Ap1	0-35	1.9	14.5	83.6	Loamy sand	1.41
	Ap2	35-45	8.1	28.9	63.0	Sandy loam	1.66
	Ap3	45-55	7.6	27.9	64.5	Sandy loam	1.61
	2Apb	55-70	20.9	58.2	20.9	Silt loam	1.28
	2Bwb	70-100	13.6	38.9	47.5	Loam	1.56

^[a] approximate depth

^[b] horizon continuous in the second experiment (RT) only

We carried out the first two experiments on field site 1 and the last two at field site 2. The first experiment (CT) took place after ploughing and before ridges were created, so that the soil surface was flat and represented conventional tillage management. The second one (RT) was carried out after the creation of ridges. At field site 2, potato crops were planted in ridges covered with black plastic mulch, and we conducted the third experiment (RT_{pm}) in the early season when seed potatoes were just sown. Finally, the last irrigation (RT_{pm+crops}) followed in the later season when potato crops and their root system were already well developed. In the following, we use CT, RT, RT_{pm} and RT_{pm+crops} to refer to the corresponding experiments or plots.

Before irrigation, we installed soil moisture sensors (Decagon devices, Inc., Pullman, WA-99163, USA) to monitor the volumetric water content θ_v . These sensors measure the dielectric constant based on frequency domain technology. On CT, they were placed in 5 and 20 cm depth from the flat soil surface. In experiments RT and RT_{pm}, two sensors were situated in furrows in 5 and 20 cm depth from the furrow surface and another two in ridges in 5 and 20 cm depth from the ridge surface. Due to technical problems, the fourth experiment was carried out without any soil moisture sensors. We recorded the values of soil moisture in a 2 minutes interval on a data logger (Decagon devices, Inc., Pullman, WA-99163, USA).

We irrigated a surface of 2 m² with a tracer solution containing 5 g L⁻¹ of *Brilliant Blue FCF* using an automated sprinkler. Because this tracer can be retarded compared to infiltrating water (Flury and Flühler, 1995), we added 5 g L⁻¹ *potassium iodide* on plots CT and RT_{pm} as a reference tracer. To calculate the amount of surface runoff the irrigation area was equipped with an infiltration frame. It channeled the surface runoff via internal tubes into buckets outside of the frame. The total time and amount of irrigation varied among experiments due to technical problems with blocked sprinkler jets. However, the experiments were still comparable (Table 2.2).

One day after the irrigation, we excavated 8 to 10 soil profiles of 1 by 2 m spaced by 10 cm on each plot. For visualization of the iodide tracer, an indicator solution with *iron (III) nitrate* and starch was prepared (Lu and Wu, 2003) and sprayed onto the excavated soil profiles. All profiles were equipped with a metallic frame of 2 m² and a Kodak color scale and photographed with a digital single-lens reflex camera (Canon EOS 1000D). Only the parts of the profiles surrounded by the frame were analyzed.

The soil profiles were sampled systematically in *Brilliant Blue* stained and non-stained areas to determine soil physical properties. We carefully scraped soil material from different profiles and analyzed the texture in a laser particle

size analyzer (Mastersizer S 'MAM 5044', Malvern instruments GmbH, Herrenberg, Germany). Additionally, we took undisturbed samples with small soil core rings (diameter 2.8 cm, height 1 cm) in stained and non-stained parts. They were weighted, dried for 24 hours at 105°C in a drying oven and weighed again to calculate the bulk density.

2.2.3 Statistical analysis

The tillage pan was a prominent feature observed on all experimental sites and might influence the soil physical properties. Therefore, we tested whether the bulk density varied significantly above and below the tillage pan. There were no indications that the distribution of the data was non-normal (quantile-quantile plot and the Shapiro-Wilk Test) or that the variance varied from plot to plot (Bartlett's Test). Because the sample size differed between soil horizons, we performed the Welch *t*-Test. All statistical tests were done in R (R Core Team, 2012).

2.2.4 Image processing

We corrected the images for perspective and radial distortion such that they corresponded to pictures taken by an ideal camera looking perpendicularly onto the profiles. The transformation was calculated by:

$$\bar{v} = \frac{1}{1 + \kappa \cdot \langle \bar{u}, \bar{u} \rangle} \cdot \bar{u} \quad (1)$$

where the parameter κ is the magnitude of the radial distortion, \bar{u} are coordinates of a point in the original image and \bar{v} are coordinates in the corrected one and the brackets $\langle \rangle$ indicate the inner product. If κ is negative, the distortion is barrel-shaped, while for positive κ , it is pincushion-shaped (Steger *et al.*, 2008). The parameter κ is obtained in a camera calibration procedure with a special calibration plate. Subsequently, we transformed the images from RGB to HSI (hue, saturation, intensity) color space and classified them into *Brilliant Blue* stained (black) and non-stained (white) parts resulting in a binary image. Indeed, the HSI color space is more suitable for color-based segmentations of images taken under varying illumination. More details on image transformation and classification are given in Bogner *et al.* (2010). For the experiments RT, RT_{pm}, and RT_{pm+crops}, we additionally produced a second binary background image, where soil was coded black and the background between ridges white (Figure 2.1). The correction of distortion and color segmentation were done in Halcon ver. 10.0 (MVTec Software GmbH, Munich, Germany).

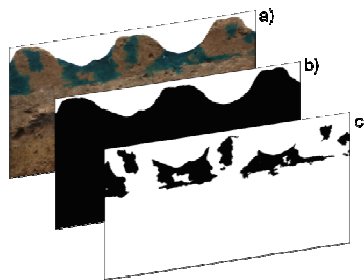


Figure 2.1 Images processing from a) rectified dye tracer image to b) background image, and c) binary image used to calculate image indices

2.2.5 Image index functions

We used the binary images to assess differences between the tillage management systems. The first two experiments (CT and RT) show the influence of soil surface topography on flow patterns in general. By comparing the experiments RT and RT_{pm}, we can infer the effect of plastic mulch. Finally, we can extract information about the impact of the potato root system on flow patterns by comparing the images on plot RT_{pm} with those on RT_{pm+crops}.

To effectively analyze the flow patterns in binary images, we calculate image index functions. An index function is a real-valued function of a row \bar{r} of length m in a binary image (i.e. of a binary vector). These functions are constructed such that they are independent of spatial scale and resolution of the image and confined to the interval $[0, 1]$. They summarize different features of a binary image row by row. Indeed, because the vertical direction is the primary direction of water movement in the vadose zone, these functions summarize the horizontal and emphasize the vertical configuration of patterns. For a detailed mathematical description see Trancón y Widemann and Bogner (2012) who we follow closely in the description of image index functions stated below. In the following, we identify stained pixels with the integer 1 and non-stained with 0.

The *dye coverage* is a well-known index function in dye tracer studies. It shows the proportion of stained pixels:

$$I_D(\bar{r}) = \frac{1}{m} \sum_i r_i \quad (2)$$

We define contiguous sequences of stained pixels as *runs*. Their lengths represent the width of stained objects in an image row and their number is called the *Euler number*. Normalized by the maximum number of possible runs (i.e. $m/2$) gives:

$$I_E(\bar{r}) = \frac{|R_1(\bar{r})|}{\lceil m/2 \rceil} \quad (3)$$

where R_1 is a function that calculates the sequence of run lengths and the brackets $\lceil \rceil$ are the ceiling function that rounds up to the nearest integer. I_E is small, if the patterns are dominated by large stained objects and attains its maximum of 1 for a regular sequence of alternating stained and non-stained pixels.

The distribution of run lengths can be summarized by their minimum, *maximum* and median. In our experiments, however, we only used the *maximum* for the analysis because it was the most suitable index to distinguish between the different tillage managements:

$$I_{MAX} = \frac{1}{m} \max(R_1(\bar{r})) \quad (4)$$

Furthermore, we can measure how *contiguous* the runs are, by defining:

$$I_C(\bar{r}) = \frac{\langle R_1(\bar{r}), R_1(\bar{r}) \rangle}{\left(\sum_i r_i\right)^2} \quad (5)$$

The indeterminate case where there are no stained pixels in a row is set to 1. I_C can be interpreted as the reciprocal of a non-integer measure of the number of stained objects weighted by their size. It behaves differently compared to the other index functions because it is 1 for completely stained and completely non-stained rows. Therefore, for an easier interpretation we used $1 - I_C$ (i.e. we flipped it horizontally) and called this new index function *fragmentation*:

$$I_F(\bar{r}) = 1 - I_C(\bar{r}) \quad (6)$$

In an image row where large stained objects dominate (i.e. contiguous runs), I_F will be smaller compared to an image row with smaller stained objects given the same proportion of staining (i.e. equal I_D). Furthermore, I_F equals 0 for completely stained and non-stained image rows.

Last but not least, we want to assess the information contained in an image row \bar{r} via the metric entropy, a version of the famous Shannon's entropy. Shannon (1948) defined the information content of an outcome x of a discrete random variable as $h(x) = -\log_2 p(x)$, $p(x)$ being the probability of occurrence of the outcome x . It is measured in bits. The average information content (i.e. Shannon's entropy) is defined as:

$$H(X) = - \sum_{x \in X} p(x) \cdot \log_2 p(x) \quad (7)$$

for a set of events X with probability of occurrence $p(x_1), p(x_2), \dots, p(x_n)$. Among all distributions with n possible events, H attains its maximum of $\log_2 n$ for the uniform distribution. This is intuitively clear for the average information content is equivalent to our uncertainty about which event will occur. In other words, Shannon's entropy measures how much information is "produced" by the random variable. For an event that will certainly occur, H is equal to 0.

Now let's consider the staining of a pixel as realization of a binary random variable (i.e. possible outcomes are stained or non-stained). In this case, H is maximum for $p(1) = p(0) = 0.5$ and is called the binary entropy function. Replacing the theoretical probabilities in (7) by empirical frequencies, $p(0)$ and $p(1)$, we can calculate Shannon's entropy via:

$$H(\bar{r}) = -[p(0) \cdot \log_2 p(0) + p(1) \cdot \log_2 p(1)] \quad (8)$$

Often, it is more informative to consider the entropy of substrings or words (\bar{w}) of length L in a binary vector (Ebeling *et al.*, 1995). Normalizing by L yields the metric entropy:

$$I_{MEL}(\bar{r}) = \frac{1}{L} \cdot H(W_L(\bar{w})) \quad (9)$$

where H is the generalization of Shannon's entropy for words of length L . In other words, the random variable X from equation (7) is defined to pick an arbitrary word of length L from \bar{r} . For our images, we chose $L = 8$. W_L is a sliding window function that moves through the image row \bar{r} to produce the different words. The metric entropy gives useful values, only if $m \gg L$. Compared to Shannon's entropy in equation (7), the metric entropy allows to assess the correlation structure inside words. Indeed, metric entropy attains its maximum when single pixels in the words are uncorrelated and decreases for correlated pixels. For binary sequences, I_{MEL} is confined to the interval $[0, 1]$.

Special care should be taken when calculating image index functions for soils with an uneven soil surface. Therefore, to differentiate between soil and non-soil on the ridged surface of RT, RT_{pm}, and RT_{pm+crops}, we used the background binary images (Figure 2.1b). Areas identified as non-soil were omitted. Additionally, we discarded the first and the last profiles completely because of edge effects and used 8 images for CT, RT, and RT_{pm} and 5 images for RT_{pm+crops}. The image index functions were calculated in R (R Core Team, 2012).

The interpretation of differences in tillage management systems is based on median values of image index functions. To better understand which features of flow patterns are reflected by these functions, we first give an example of a single profile from RT_{pm} (Figure 2.2). As indicated by circles and arrows, the index functions are sensible to different relevant features and complement each other. In fact, the dye coverage I_D increases when the stained objects become larger (red arrow), however, it is not sensitive to different pattern configurations. By contrast, I_F increases when smaller stained objects appear and the pattern is fragmented. The metric entropy I_{ME8} indicates that at the scale of 8 pixels we find a strong correlation in our patterns. In other words, there are only few different words of length 8 (namely predominantly those with 1s only or 0s only) because large stained and non-stained areas alternate.

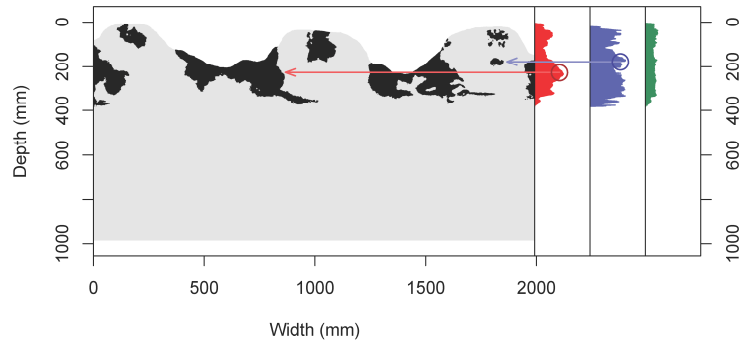


Figure 2.2 Left to right: example of a binary image and three index functions: dye coverage I_D , fragmentation I_F and metric entropy I_{MES} . The gray background represents the soil profile and the dye stained patterns are shown in black. For explanation of circles and arrows see section 2.2.5

2.3 Results and discussion

2.3.1 Water balance and water content

We observed the largest infiltration and the smallest runoff on plot CT (Table 2.2). The amount of infiltrated water decreased and the surface runoff increased from CT to RT and further to RT_{pm} due to the surface topography and plastic mulching of the ridges. In experiment RT_{pm} , approx. 50% of the total amount of irrigation water contributed to the runoff. By contrast, on $RT_{pm+crops}$, the infiltration increased again and the surface runoff decreased to 31% compared to RT_{pm} probably due to the well developed crop canopy. Indeed, interception and throughfall of irrigated water might have reduced the formation of surface runoff. Our results agree well with Saffigna *et al.* (1976) who investigated non-uniform infiltration patterns caused by hilling and potato canopy. These authors also found an increased runoff from ridges.

Table 2.2 Total amount of irrigation and its partitioning into surface runoff and infiltration

Experiment	Total amount of irrigated water		Infiltration		Runoff	
	(L)	(L)	(L)	(%)	(L)	(%)
CT ^[a]	87	69	69	79	18	21
RT ^[b]	74	46	46	62	28	38
RT_{pm} ^[c]	81	41	41	50	41	50
$RT_{pm+crops}$ ^[d]	91	63	63	69	28	31

^[a] Conventional flat tillage

^[b] Ridge tillage

^[c] Ridge tillage with plastic mulch

^[d] Ridge tillage with plastic mulch and potato crops

At the beginning of experiment CT, the water content in 5 cm depth was lower compared to 20 cm depth (Figure 2.3). Approx. 15 minutes after the start of irrigation, the sensors placed in 5 cm depth registered an increase of water content, while the dynamics in 20 cm depth was delayed. Although flat, the soil surface was inclined, which explains larger soil moisture values measured by the FDRs situated downslope (FDR 2 and FDR 4).

On plots RT and RT_{pm} , we found higher water contents in furrows at the beginning of irrigation. This was probably caused by previously preferentially infiltrated water due to topography effects. Indeed, higher soil moisture in furrows due to runoff from ridges was also found by Leistra and Boesten (2010) and Saffigna *et al.* (1976). In 5 cm depth in RT, the water content went up first in furrows, since the runoff from the ridges accumulated here, and then in ridges. It increased only slightly in 20 cm depth.

In experiment RT_{pm} , the dynamics was comparable to RT except on ridges that were covered with plastic mulch. The increase in water content in ridges in 20 cm depth was probably related to water, which infiltrated primarily in the furrows and was subsequently funneled laterally above the tillage pan to the ridges. Furthermore, the initial soil moisture differed between furrows and ridges so that pressure head gradients caused lateral water movement from furrows to ridges (Ruidisch, unpublished data). These findings are in accordance with results by Bargar *et al.* (1999). They investigated soil water recharge and infiltration patterns in an uncropped ridge-furrow formation without plastic mulch and found lateral water flow from furrows to ridges.

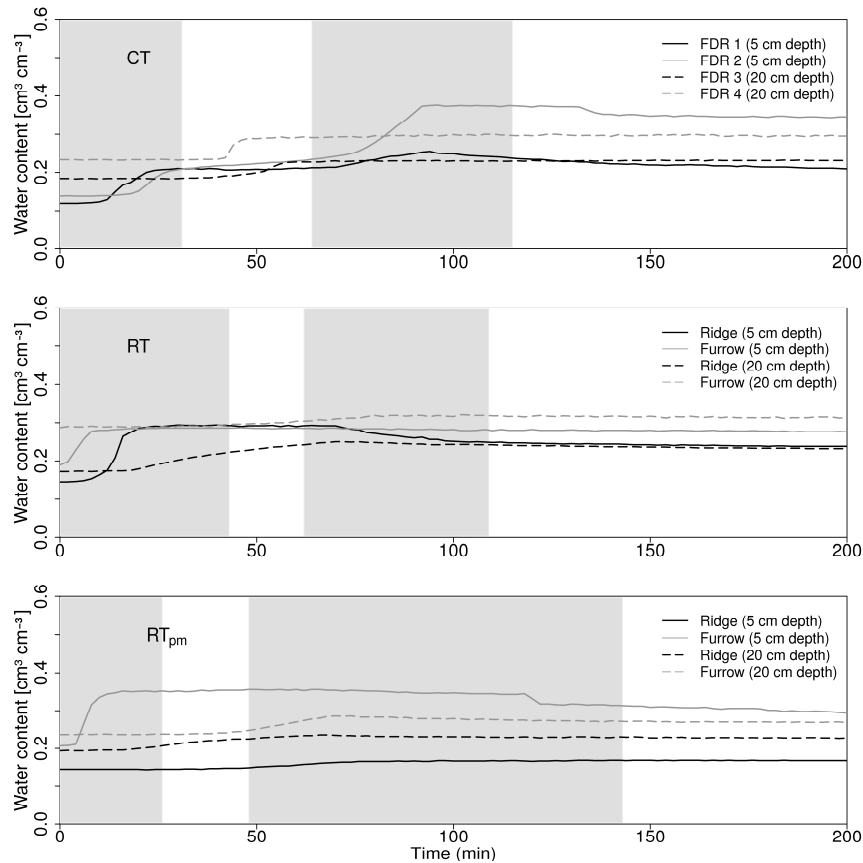


Figure 2.3 The dynamics of water content in different depths during the irrigation experiments CT, RT, and RT_{pm} . The grey area indicates the time of irrigation

2.3.2 Analysis of flow patterns

The experiments revealed that firstly, tillage produced zones of preferential infiltration, namely furrows and planting holes and zones of no infiltration, namely plastic mulched ridges (Figure 2.4). Therefore, the patchiness of the patterns and the occurrence of preferential flow is a result of the soil surface topography. Figure 2.5 shows the image index functions. In all four experiments, I_E was approx. 0.1, which is quite small and reflects the few vertically stained patterns. Secondly, the tillage pan was the most important feature for water movement in these agricultural soils, which was clearly evident by the decrease of all the indices to zero in approx. 25 to 35 cm depth. Furthermore, we found that the bulk density differed significantly ($p < 0.05$) above and below the tillage pan on RT_{pm} and $RT_{pm+crops}$ (i.e. between the horizons Ap and Bwb and between the horizons Ap1 and Ap2, respectively). However, we could not detect any difference ($p > 0.05$) between Ap and 2Apb on RT despite the visible funnel flow (Figure 2.4) due to textural differences (Table 2.1). Thirdly, the shape of the index curves shows that in our experiments water flow occurred in the

topsoil and was funneled preferentially above the tillage pan. Indeed, the vertical propagation to the deeper soil horizons via macropores was absent. This was also confirmed by comparing the *Brilliant Blue* stained patterns to the *iodide* patterns. The propagation of the *iodide* tracer solution was exactly equivalent to that of *Brilliant Blue FCF*. This result contradicts the findings by Flury and Flühler (1995) who reported that *Brilliant Blue FCF* was retarded by a factor of 1.2 compared to the *iodide* tracer. We explain this disagreement by the sandy texture of the top soil and, thus, its large hydraulic conductivity.

The effect of the ridge topography in experiment RT was well represented by the indices I_D , I_F , I_{MES} and I_{MAX} . Both I_F (max = 0.64) and I_{MES} (max = 0.35) were larger on RT compared to CT ($\max(I_F) = 0.48$ and $\max(I_{MES}) = 0.21$), which reflected the typical dye pattern induced by topography effects. Indeed, the alternation between stained furrows, stained inner parts of the ridges due to infiltration in planting holes, and unstained parts on the inner sides of the ridges are the prominent features (Figure 2.4). The index I_{MAX} with a maximum of 1 reflected the homogeneous and continuous infiltration on CT. It remained large down to the depth of the tillage pan indicating homogeneous matrix flow. Similarly, looking at the uppermost cm of RT, where the tracer infiltrated homogeneously as well, we also find a large I_{MAX} (max = 0.75).

The effect of plastic mulch can be best extracted by comparing I_D and I_{MAX} on RT and RT_{pm} . On RT, I_D was largest (max = 1) in the uppermost cm as a result of homogeneous infiltration. In contrast, I_D on RT_{pm} increased to a maximum of 0.53 in 20 cm soil depth reflecting the high surface runoff rates from the plastic mulched ridges into furrows where most of the irrigated water infiltrated preferentially. Additionally, the blockage of tracer infiltration caused by plastic mulch was well mirrored by I_{MAX} . In fact, the homogeneous matrix flow in the upper cm of RT was reflected by a large I_{MAX} (max = 0.75), whereas the largest I_{MAX} (max = 0.22) on RT_{pm} marked the depth of laterally funneled water above the tillage pan.

The effect of the root system on dye patterns was only slightly apparent in larger I_D in approx. 20 cm soil depth on $RT_{pm+crops}$ compared to RT_{pm} . The stem flow funneled the irrigation water to the planting holes and, therefore, caused an additional ponding. After infiltration, the tracer solution was preferentially channeled along living roots, which resulted in a maximum of I_D (0.66) in the root zone depth. In contrast, the maximum of I_D on RT_{pm} without crop roots occurred in the depth of the tillage pan (0.53). Similarly, the largest I_{MAX} on RT_{pm} (0.22) and $RT_{pm+crops}$ (0.25) reflected the funnel flow above the tillage pan under RT_{pm} and the highly stained root zone on $RT_{pm+crops}$, respectively. We observed another important factor, which was best visible in the profile pictures (Figure 2.4). On $RT_{pm+crops}$, water movement in slope direction was not longer pronounced compared to RT_{pm} . Instead, water was primarily redirected from furrows to ridges (i.e. up slope). We attribute this lateral flow to the hydraulic gradient with lowest pressure heads found in the inner part of the plastic mulched ridges where root water uptake took place. A similar phenomenon was observed by Ruidisch (unpublished data) who found that plastic mulched ridge cultivation led to lateral flow driven by a pressure head gradient between furrows and the relatively drier ridges.

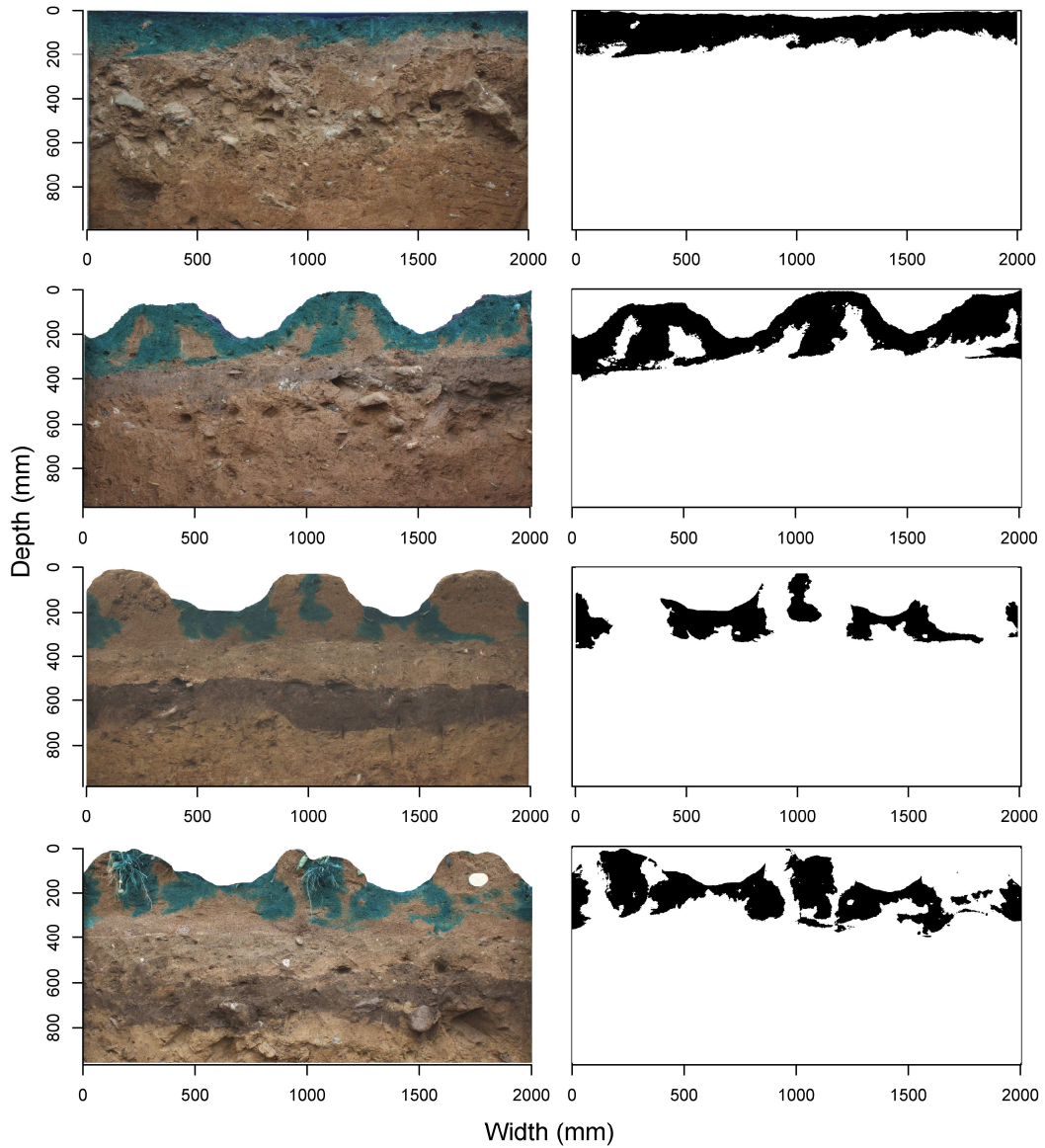


Figure 2.4 Example images of excavated soil profiles and their binary images. From left to right: CT, RT, RT_{pm}, and RT_{pm+crops}. Note that the slope orientation differs between field site 1 (CT and RT, slope oriented to the left) and field site 2 (RT_{pm} and RT_{pm+crops}, slope oriented to the right). In the color image of RT_{pm+crops}, the white feature on the right hand ridge is a potato cut in half

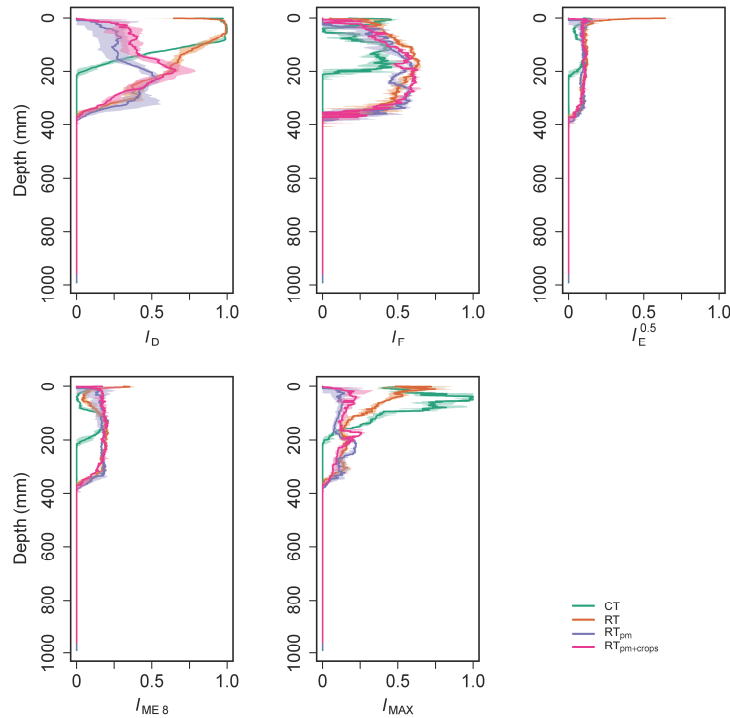


Figure 2.5 Image index functions and their 25% and 75% quantiles (colored areas)

2.3.3 The effect of tillage management on flow processes and its ecological implications

First, we want to highlight the tillage operations, which take place regardless of ridge cultivation with or without plastic mulch, namely the distribution of sandy soil material on agricultural fields prior to planting and the subsequent ploughing. Indeed, the distribution of sandy soil material to counterbalance erosion loss in the Haeen catchment strongly influences the flow processes. This management practice leads to an artificial layering with different soil physical properties. A cohesive, denser, and finer textured subsoil is overlain by a topsoil consisting of a non-cohesive and coarse material. As a result, an important textural boundary is created with clearly contrasting hydraulic conductivities between the horizons above and below it. Additionally, ploughing activities create a tillage pan and, thus, further support the structural differences between the horizons. We identified these structural features to be responsible for the initiation of the rather uniform flow through the sandy toplayer as well as for the funnel flow on the tillage pan.

Several authors reported that fissures, cracks and earthworm burrows could act as preferential flow paths especially in fine textured subsoils (Bachmair *et al.*, 2009, Weiler and Naef, 2003). Although ploughing activities lead to a discontinuity of macropores between topsoil and subsoil (Gjettermann *et al.*, 1997), preferential flow paths in the deeper subsoil can still conduct water (Bogner *et al.*, 2012). In our experiments, we could not detect any macropore flow, neither in the topsoil nor in the subsoil. This can be related to the fact that the non-cohesive sandy toplayer does not have any macropores even before ploughing. Simultaneously, the denser and finer textured subsoil lacked macropores like fissures or cracks, which could initiate preferential flow. Additionally, we did not observe any soil fauna on our field sites, which could build a network of macropores.

Ecologically, our findings imply that the risk of a vertical propagation of agrochemicals to groundwater is generally relatively low. On the other hand, the lateral downhill water flow above the tillage pan seems to be the most crucial process, to which we should pay particular attention. Especially during the East Asian summer monsoon, when rain events can reach more than 100 mm per day, the fast flow through a coarse textured topsoil laterally down the slope

seems to play a key role in the transport of agrochemicals. Therefore, the field sites, which are located next to the river system, should be recognized as critical locations for pollutants entering the water bodies.

Additionally, the temporal aspect plays an important role. We found that in the later season the developed potato crop canopy decreased surface runoff due to interception and throughfall. Additionally, a developed root system has the potential to interrupt the subsurface funnel flow above the tillage pan, because root water uptake induced pressure head gradients and therefore influenced water movement. Hence, the leaching risk via surface runoff and subsurface water flow is reduced in the adult stage of the crop development. On the other hand, it means that the leaching risk is especially high at the beginning of the growing season when the plants are juvenile and the fertilizers are recently applied, because in this juvenile stage the interception and root water uptake are very low. However, the potential for interrupting lateral subsurface flow due to pressure head gradients depends presumably on the intensity and amount of rainfall. We can relate the occurrence only to the irrigation rates, which equaled moderate rain events of 37 to 45 L m⁻².

Our results suggest that differences between tillage management systems have to be considered when evaluating the impact of agricultural land use on ecological services. The important amount of runoff generated under ridge tillage cultivation with plastic mulching can increase the risk of surface water pollution and soil erosion. In fact, even in the later season, when the crop canopy was well developed, the runoff still constituted one third of the total irrigation in our experiments. Arnhold (personal communication) compared CT, RT, and RT_{pm} plots using the process-based model EROSION 3D (von Werner, 1995) and found the highest runoff and erosion rates under ridge tillage with plastic mulching. Additionally, we assume that the widespread usage of plastic mulching in combination with heavy monsoon events is partly responsible for higher phosphorous leaching in the Haean catchment, which is predominately transported via surface runoff. This is supported by Kim *et al.* (2001) who found that eutrophication and deterioration of water quality in downstream reservoirs in South Korea is associated with discharge of phosphorous.

2.4 Conclusions

Different tillage management practices created typical infiltration zones (i.e. furrows and planting holes) and non-infiltration zones (i.e. plastic covered ridges). However, the impact of ridge cultivation with or without plastic mulch on the predominant subsurface flow processes is relatively low compared to the impact on surface runoff generation. Therefore, to reduce surface runoff, we suggest (i) to encourage crop production in ridge cultivation with perforated plastic mulch. On one hand, perforated plastic mulch should decrease the amount of surface runoff and, thus, diminish the risk of erosion and leaching of agrochemicals, especially in the early season when crops are juvenile. On the other hand, it maintains a positive effect on crop yield and weed control. Furthermore, particular attention should be paid to the lateral leaching risk of agrochemicals and fertilizers above the tillage pan particularly on field sites located directly next to the stream network. Hence, we propose (ii) to promote the establishment of riparian buffer zones between dryland farming fields and the rivers.

2.5 Acknowledgements

We are grateful to Dr. Baltasar Trancón y Widemann for technical assistance and intense discussions. We would like to thank Andreas Kolb for his invaluable technical support during the irrigation experiments. Furthermore, we thank Bora, Heera, and Eunyong for translating and Farmer Shin for giving us the opportunity to carry out the experiments on his fields. This study was carried out as part of the International Research Training Group TERRECO (GRK 1565/1)

funded by the Deutsche Forschungsgemeinschaft (DFG) at the University of Bayreuth, Germany, and the Korean Research Foundation (KRF) at the Kangwon National University, Chuncheon, South Korea.

2.6 References

- Bachmair, S., Weiler, M., Nützmann, G., 2009. Controls of land use and soil structure on water movement: lessons for pollutant transfer through the unsaturated zone. *Journal of Hydrology* **369**(3-4), 241-252.
- Bargar, B., Swan, J. B., Jaynes, D., 1999. Soil water recharge under uncropped ridges and furrows. *Soil Science Society of America Journal* **63**(5), 1290-1299.
- Bogner, C., Gaul, D., Kolb, A., Schmiedinger, I., Huwe, B., 2010. Investigating flow mechanisms in a forest soil by mixed-effects modelling. *European Journal of Soil Science* **61**(6), 1079-1090.
- Bogner, C., Mirzaei, M., Ruy, S., Huwe, B., 2012. Microtopography, water storage and flow patterns in a fine-textured soil under agricultural use. *Hydrological Processes*, DOI: 428 10.1002/hyp.9337.
- Ebeling, W., Poschel, T., Albrecht, K. F., 1995. Entropy - transinformation and word distribution of information-carrying sequences. *International Journal of Bifurcation and Chaos* **5**(1), 51-61.
- Flury, M., Flühler, H., 1995. Tracer characteristics of Brilliant Blue FCF. *Soil Science Society of America Journal* **59**(1), 22-27.
- Gish, T. J., Gimenez, D., Rawls, W. J., 1998. Impact of roots on ground water quality. *Plant and Soil* **200**(1), 47-54.
- Gjettermann, B., Nielsen, K. L., Petersen, C. T., Jensen, H. E., Hansen, S., 1997. Preferential flow in sandy loam soils as affected by irrigation intensity. *Soil Technology* **11**(2), 139-152.
- Hendrickx, J. M. H., Flury, M., 2001. Uniform and preferential flow mechanisms in the vadose zone, in: Council, N. R., (Ed.), *Conceptual models of flow and transport in the fractured vadose zone*. National Academy Press, Washington D.C., pp. 149-187.
- IUSS Working Group WRB, 2006. World reference base for soil resources 2006 - a framework for international classification, correlation and communication. World Soil Resources Reports No. 103, FAO, Rome.
- Jarvis, N. J., 2007. A review of non-equilibrium water flow and solute transport in soil macropores: principles, controlling factors and consequences for water quality. *European Journal of Soil Science* **58**(3), 523-546.
- Kim, B., Park, J., Hwang, G., Jun, M., Choi, K., 2001. Eutrophication of reservoirs in South Korea. *Limnology* **2**(3), 223-229.
- Kulli, B., Gysi, M., Flühler, H., 2003. Visualizing soil compaction based on flow pattern analysis. *Soil and Tillage Research* **70**(3), 29-40.
- Lament Jr., W., 1993. Plastic mulches for the production of vegetable crops. *HortTechnology* **3**(1), 35-39.
- Leistra, M., Boesten, J. J. T. I., 2010. Pesticide leaching from agricultural fields with ridges and furrows. *Water Air and Soil Pollution* **213**(1-4), 341-352.
- Lu, J., Wu, L., 2003. Visualizing bromide and iodide water tracer in soil profiles by spray methods. *Journal of Environmental Quality* **32**(1), 363-367.
- Park, J., Duan, L., Kim, B., Mitchell, M. J., Shibata, H., 2010. Potential effects of climate change and variability on watershed biogeochemical processes and water quality in northeast Asia. *Environment International* **36**(2), 212-225.
- Petersen, C., Jensen, H., Hansen, S., Bender Koch, C., 2001. Susceptibility of a sandy loam soil to preferential flow as affected by tillage. *Soil and Tillage Research* **58**(1-2), 81-89.
- R Core Team, 2012. *R: a language and environment for statistical computing*. R Foundation for Statistical Computing, Vienna. URL <http://www.R-project.org/>. ISBN 3-900051-07-0.
- Saffigna, P. G., Tanner, C. B., Keeney, D. R., 1976. Non-uniform infiltration under potato canopies caused by interception, stemflow, and hilling. *Agronomy Journal* **68**(2), 337-342.
- Shannon, C. E., 1948. A mathematical theory of communication. *Bell System Technical Journal* **27**, 379-423.
- Šimůnek, J., Jarvis, N. J., van Genuchten, M. T., Gärdenäs, A., 2003. Review and comparison of models for describing non-equilibrium and preferential flow and transport in the vadose zone. *Journal of Hydrology* **272**(1-4), 14-35.

- Steger, C., Ulrich, M., Wiedemann, C., 2008. *Machine Vision Algorithms and Applications*. Wiley-VCH, Weinheim.
- Trancón y Widemann, B., Bogner, C., 2012. Image analysis for soil dye tracer infiltration studies, in: *Proceedings of the 3rd International Conference on Image Processing Theory, Tools and Applications*, in press.
- von Werner, M., 1995. GIS-orientierte Methoden der digitalen Reliefanalyse zur Modellierung von Bodenerosion in kleinen Einzugsgebieten. *PhD Thesis*. Free University of Berlin, Department of Earth Sciences.
- Weiler, M., Naef, F., 2003. An experimental tracer study of the role of macropores in infiltration in grassland soils. *Hydrological Processes* **17**(2), 477-493.
- Zhai, P., Sun, A., Ren, F., Liu, X., Gao, B., Zhang, Q., 1999. Changes of climate extremes in China. *Climatic Change* **42**, 203-218.
- Zhai, P., Zhang, X., Wan, H., Pan, X., 2005. Trends in total precipitation and frequency of daily precipitation extremes over China. *Journal of Climate* **18**, 1096-1108.
- Zhang, W., Tian, Z., Zhang, N., Li, X., 1996. Nitrate pollution of groundwater in northern China. *Agriculture, Ecosystems and Environment* **59**, 223-231.

Chapter 3

Plastic covered ridge-furrow systems on mountainous farmland: runoff patterns and soil erosion rates

Sebastian Arnhold ¹, Marianne Ruidisch ¹, Svenja Bartsch ², Christopher L. Shope ³, Bernd Huwe ¹

¹ Department of Soil Physics, University of Bayreuth, Universitätsstraße 30, 95447 Bayreuth, Germany

² Department of Hydrology, University of Bayreuth, Universitätsstraße 30, 95447 Bayreuth, Germany

³ U.S. Geological Survey (USGS), Utah Water Science Center, 2329 W. Orton Circle,
Salt Lake City, UT 84119-2047, United States of America

Abstract

Plastic covered ridge furrow systems can substantially influence runoff and soil erosion on agricultural land. However, the impact of this management practice in combination with a complex farmland topography has not been thoroughly investigated and is still poorly understood. The goal of this study was to identify how topography influences the runoff patterns and erosion rates of plastic covered ridge-furrow systems. We measured runoff and sediment transport on two mountainous fields in South Korea, one with a concave and one with a convex topography, during monsoonal rain events. We used the EROSION 3D model to compare flow and sediment transport differences between the plastic covered system, uncovered ridges, and a smooth soil surface. We found the highest runoff and erosion rates from both of the plastic covered fields, due to the impermeable surface. For the uncovered ridges, we identified a 140% higher erosion compared to the smooth surface on the concave field, although a reduction of 20% on the convex field. The simulated sediment transport patterns showed that the ridge-furrow system concentrated the flow on the concave field resulting in high erosion rates. On the convex field, the ridge-furrow system prevented flow accumulation and erosion. Our results demonstrate that the effect of ridge-furrow systems on erosion is controlled primarily by the topography. These results have practical consequences for watershed conservation planning and the application of large-scale erosion models. Nevertheless, further research is needed to fully understand the impact of this management system on erosion on mountainous farmland.

Keywords: *Complex landscape, Erosion, Furrows, Korea, Plastic mulch, Ridges, Runoff, Topography*

3.1 Introduction

Intensive agriculture in mountainous landscapes can cause severe soil erosion, resulting in irreversible loss of fertile farmland soil and decrease water quality in streams and lakes. Tillage and crop cultivation practice instituted by the farmers has a substantial influence on the amount of erosion on steep farmland areas. Important cultivation practices for vegetable production are ridge-furrow systems covered with plastic films (plastic mulch) accounting for 3 to 4 million hectares worldwide (Dilara, 2000), with an increasing trend, particularly in China (Espí *et al.*, 2006). Plastic mulch has increased crop yields, reduced evaporation losses, reduced nutrient leaching, and limited weeds (Lament Jr., 1993). Plastic mulching is a common management practice on most of the agricultural areas in South Korea (except for rice paddies). Agricultural areas in mountainous landscapes, such as the Kangwon Province in the northeast of South Korea, are cultivated predominantly by cash crops like cabbage, radish, and potato (Kim *et al.*, 2007, Lee *et al.*, 2010a, Park *et al.*, 2010b). These mountainous agricultural areas are characterized by steep slopes and complex field topographies. The ridge-furrow system is predominantly oriented perpendicular to the main slope direction of field sites, but often not parallel with the contours. In many cases, the tillage directions vary across individual field sites. The distance between the centers of two ridges is approximately 70 cm and the ridges are usually between 30 to 40 cm wide and 15 cm higher than the furrows. The ridges are covered with a black plastic film with regularly spaced, 5 cm diameter, planting holes, and the film is buried on either side of the ridge several centimeters deep. Furrows are conventionally treated with herbicides in order to eliminate weeds during the growing season. Therefore, the soil surface between the ridges typically remains uncovered until crops reach their adult stage and start covering parts of the furrows. During rain events, ridge-furrow systems basically drain runoff from ridges into the furrows, producing concentrated overland flow with higher erosive power than without ridges (Wan and El-Swaify, 1999). The impermeable plastic film produces higher surface runoff and can, therefore, intensify the concentrated flow. Even though the plastic cover protects the surface from raindrop impacts and eliminates ridge erosion, the remaining exposed soil surface in the furrows can have significantly increased erosion losses due to elevated runoff amounts (Wolfe *et al.*, 2002).

Several studies have previously investigated the effect of plastic covered ridge-furrow systems on runoff and soil erosion for a variety of different crops. Wan and El-Swaify (1999) analyzed plastic mulch pineapple plantations by using rainfall simulator experiments on field plots. They found substantially higher runoff generation and soil erosion on plastic mulch plots relative to bare plots. Although the authors also observed that plastic mulch in combination with a vegetative crown reduces runoff and soil loss, because water is ponded in the pineapple crowns and funneled into the planting holes. Rice *et al.* (2001) measured the amount of runoff, sediment and pesticides from tomato plots with plastic mulch in comparison to vegetative mulch. They found increased runoff and at least three times higher soil loss for plastic mulch plots. In another example, higher surface runoff contributed to four times higher erosion rates for corn cultivation with plastic mulch than without plastic during field experiments (Gascuel-Odoux *et al.*, 2001). Stevens *et al.* (2009) measured runoff, soil loss, transported pesticides, and nitrogen in plot experiments for a variety of strawberry cultivation practices including plastic mulch. In contrast to the other studies, they did not identify large differences in surface runoff between plastic mulch and uncovered management strategies. Moreover, they found that plastic mulch significantly reduced soil erosion during select rainfall events. In lysimeter plot studies in South Korea, Lee *et al.* (2010b) analyzed the effect of contour farming with plastic mulch on runoff, soil losses, and nutrient losses for cabbage and potato. They found that both runoff and erosion was reduced by plastic mulch compared to the non-covered plots.

These studies showed that plastic mulch can have contrary effects, which may be a result of crop type or different ridge-furrow system design and dimension. In addition, these studies also varied in their experimental design,

particularly in plot size and orientation of the ridge-furrow system in relation to the plot direction. However, each of the described studies used plots or delimited sections of a field site with a defined size and uniform topographical conditions. Complex topography, which dominates in mountainous areas of South Korea, remains particularly absent in the literature. The combination of the ridge-furrow system and the shape of a field with its internal topographical variations influence overland flow patterns and can affect the overall soil loss from a field. Runoff flows along the furrows to lower areas in the field where ridge breakovers can occur (Renard *et al.*, 1997). Wischmeier and Smith (1978) have described that for high slope lengths, the soil loss from a contoured field can exceed that from a field without contouring, because of concentrated flow due to breakovers. Higher erosion damage caused by the breakover of contour ridges has also been reported by Stocking (1972), El-Swaify *et al.* (1982), and Hagmann (1996). Plastic mulch is typically resistant to raindrop impact and overland flow and provides ridge protection. Although, our field observations indicated, that during peak events, concentrated flow can also wash out the plastic film and erode the ridges. Concentrated overland flow and breakovers within a field primarily depend on the topography (convex or concave slopes, plains, depressions) and the orientation of the ridge-furrow system. In order to evaluate those systems in complex landscapes, the entire field site should be considered to take into account all possible flow paths that contribute to concentrated overland flow.

The goal of this study was to investigate the role of plastic covered ridge-furrow management on runoff patterns and soil erosion in two mountainous agricultural fields in South Korea. Therefore, we quantified runoff and erosion from fields with plastic mulch, and subsequently applied a model to simulate the response without plastic and ridges. We implemented a novel measurement method, which is not limited to defined plot dimensions and is able to better represent the complex structure of those fields. We used a process-based erosion model, which describes the spatial runoff and erosion patterns affected by ridge-furrow systems and terrain topography.

3.2 Materials and methods

3.2.1 Study area

This study was conducted in the Haeon-Myeon catchment in the Kangwon Province in the northeast of South Korea (Figure 3.1). The catchment is part of the watershed of Soyang Lake, which is the largest reservoir in South Korea (Kim *et al.*, 2000). The Haeon catchment is a key contributor of agricultural water pollution with substantial impacts on the trophic state of the lake (Park *et al.*, 2010a). Total catchment area is 64 km² with 58% of the catchment classified as forested mountains and 30% as agricultural areas (22% dryland fields and 8% rice paddies). The remaining 12% are residential and seminatural areas including grassland, field margins, riparian areas, small roads and channels. The soil landscape is dominated by *Cambisols* formed from weathered granite. Soils are strongly influenced by human disturbance, especially on cropland through replenishment with excavated soils from nearby mountain slopes (Park *et al.*, 2010a). Haeon average annual precipitation of 1514 mm (2009 and 2010) was approximately 200 mm higher than the average precipitation of the Soyang Lake watershed described in Park *et al.* (2010a). Nearly 65% of the total rainfall in Haeon is concentrated in July, August, and September.

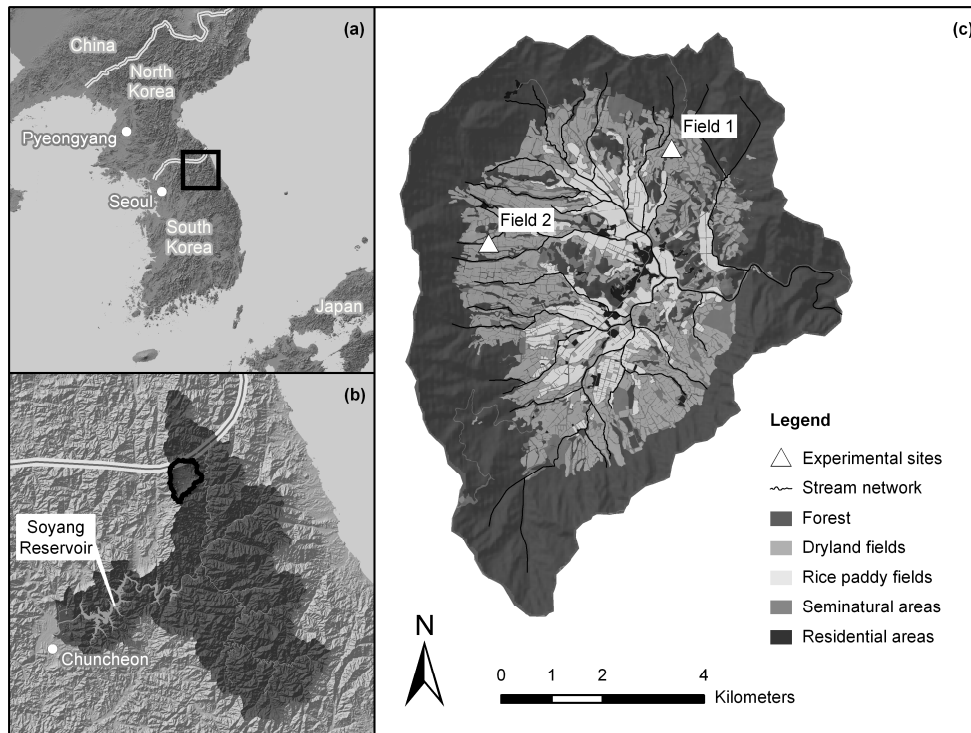


Figure 3.1 Location of the Hae-an-Myeon catchment on the Korean peninsula (a) and within the Soyang Lake watershed (b) with locations of the experimental sites conducted for this study (c) (“seminalural areas” include grassland, field margins, riparian areas, small roads and channels)

We selected two typical dryland fields on steep slopes located in the northeastern and western part of the catchment (Figure 3.1c). The topographical shape of field 1 was concave, characterized by a depression line going through the field’s center and field 2 was convex without topographical depressions. Both fields had an average slope of about 9 degrees. The soil type of field 1 was a *haplic Cambisol* (Ap-Bw-BwC-C) and the soil of field 2 was a *leptic terric Cambisol* (Ap-2Apb-2Bwb-2C), both formed from weathered granite material. The total area of field 1 was 2133 m² and the total area of field 2 1825 m². The crop type planted during our study period for each of the fields was potato (*Solanum tuberosum*), which was conventionally cultivated with plastic mulch.

3.2.2 Observation of runoff and soil erosion

The experimental design for runoff and erosion measurement is shown in Figure 3.2. On each field site, we installed three runoff samplers designed according to Bonilla *et al.* (2006). Each sampler consisted of a runoff collector (RC) connected with a PVC pipe to a multislot flow divider designed by Pinson *et al.* (2004) (Figure 3.2 only shows the positions of the collectors). The runoff collectors were located at positions where large amounts of runoff from the field sites were expected, without artificial enclosure of the contributing areas. The only variations from the Bonilla *et al.* (2006) design were that the collector width was changed to exactly five meters and no mesh at the transition between the collector and the PVC pipe was used to prevent blockage. For the flow divider, the “mid-size-fields” configuration after Bonilla *et al.* (2006) was used, which included four 20-Liter buckets, one with a 1:12 divisor head and two with 1:24 divisor heads and one without a head, resulting in a total runoff sampling capacity of 144 m³ for each collector. The flow dividers were installed in buried wooden boxes similar to those described in Bonilla *et al.* (2006). A PVC pipe was buried and connected to the bottom of the wooden box for removal of excessive water to the field’s edge. After a rainfall period, we measured the water level and calculated the runoff volume for each bucket. We took samples from each bucket (three replicates with 0.12 L) of the homogenized suspension and determined the sediment concentration by

evaporation and weight measurement. The sediment concentration was calculated as the average of three replicates. For very high sediment yields during peak events, the sediment concentration of bucket 1 was estimated from the sediment level. The dry bulk density was estimated through a general relationship between bulk density and organic carbon content for sediments (Avnimelech *et al.*, 2001). Organic carbon content was estimated by measuring the weight loss after organic matter destruction in the laboratory. The total runoff sampled by each collector was calculated by the following equation (modified after Bonilla *et al.*, 2006):

$$R = V_1 + 12 \cdot V_2 + 288 \cdot V_3 + 6912 \cdot V_4 \quad (1)$$

where R is the total runoff volume (L) and V_1 to V_4 the volumes (L) collected in the buckets 1 to 4, respectively. The associated sediment mass was then calculated by (modified after Bonilla *et al.*, 2006):

$$S = V_1 \cdot C_1 + 12 \cdot V_2 \cdot C_2 + 288 \cdot V_3 \cdot C_3 + 6912 \cdot V_4 \cdot C_4 \quad (2)$$

where S is the total sediment mass (kg) and C_1 to C_4 the sediment concentration (kg L^{-1}) measured for bucket 1 to 4, respectively. Observation time was within the Korean summer monsoon period from 5 July to 9 August 2010. We measured seven rainfall periods with different rainfall characteristics over variable time intervals (Figure 3.3). On each of the field sites, we installed rain gauges, which recorded precipitation during all seven rainfall periods at 10 minutes resolution. Due to limited rain gauge malfunctions, gap filling was completed to generate continuous precipitation data sets. The rainfall records of adjacent Haeon weather stations displayed linear correlations to our field data. These records were multiplied by the slope of the linear regression functions and added to our data sets to fill those gaps. Total amount of rainfall, rainfall intensity, and rainfall erosivity (EI_{30}) calculated after Renard *et al.* (1997) for each period were derived.

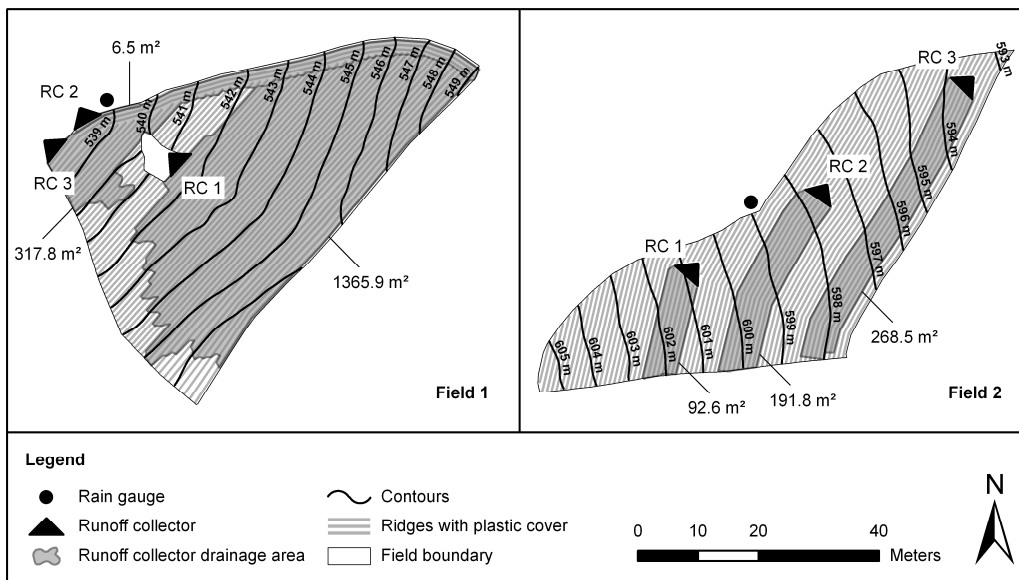


Figure 3.2 Experimental design to measure runoff and soil erosion by installation of three runoff collectors (RC) on field 1 and field 2. Fields topography and runoff collector drainage areas were calculated based on surface elevation measurements and generation of digital terrain models of both fields

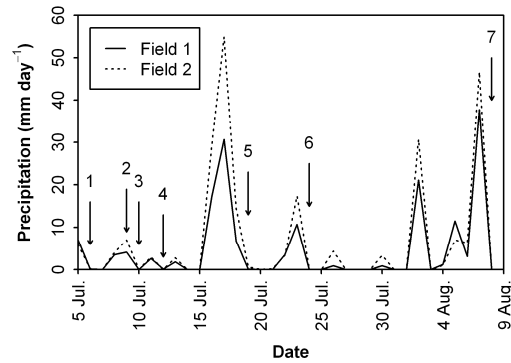


Figure 3.3 Daily precipitation on field 1 and field 2 during the observation time from 5 July to 9 August 2010. The arrows indicate the sampling dates for the associated rainfall periods

To transform the total sediment mass measured at each collector to the soil loss per area, it was necessary to define the size of the drainage area for each collector. We used a tachymeter (Tachymat WILD TC1000) to create a gridded mesh of elevation points at approximately two by two meter intervals over the entire field area. Furthermore, we counted the number of ridges and measured their orientation and dimensions (average height, width, and spacing) on both fields. In a first step, the elevation points were interpolated to create surfaces representing the basic field topography (indicated by the contours in Figure 3.2). In a second step, we added ridges to the interpolated surfaces assuming semicircular ridge profiles with the same dimensions (15 cm high and 40 cm wide) throughout the field area. Finally, we created two digital terrain models (DTMs) with 25 cm spatial resolution for the fields, one representing the basic topography with a smooth surface and one representing the actual field shape with ridges. By using those DTMs, we could delineate the drainage area to each collector and calculate the area (Figure 3.2). The fields were enclosed by elevated mounds and drainage ditches, which minimized the probability of an additional runoff contribution from outside. Nevertheless, in two cases ditch overflow and external runoff contribution was observed. Therefore, the measured runoff and sediment mass during these periods were eliminated from the data set. In all other cases, runoff and soil loss per unit area was quantified by calculating the quotient of runoff volume and sediment mass and the drainage area at each collector. To quantify the mean runoff and soil loss from each field site, the single values for the collectors were averaged and weighted to the drainage area size. The weighted average was used instead of the normal average to account for a higher field representation of RCs covering large areas and for reducing the effect of RCs covering only a small part (e.g. field 1 RC 2). Because of external runoff contributions and additional damages caused by intense rain events, we could not measure all rainfall periods with all three runoff collectors. In those cases, the mean runoff and soil loss rates were calculated only based on the available data of the functioning collectors.

3.2.3 Simulation of runoff and soil erosion

We used the EROSION 3D model (von Werner, 1995) to compare runoff and soil erosion for the plastic covered ridge-furrow management (RP - ridges with plastic) to the runoff and erosion for ridge-furrow cultivation without plastic film covers (RU - ridges uncovered), and cultivation using a smooth soil surface (SS - smooth surface) as it is usually applied for grain crops in many countries. EROSION 3D is a process-based, spatially distributed, erosion model based on the physical principles developed by Schmidt (1991). EROSION 3D describes overland flow distribution and diversion as affected by terrain morphology, as well as the associated erosion and sediment transport. Compared to other process-based erosion models such as WEPP (Nearing *et al.*, 1989) or LISEM (De Roo *et al.*, 1996), EROSION 3D requires a relatively small number of input variables (Wickenkamp *et al.*, 2000), and most of them are directly

related to measured soil, slope and rainfall properties (Schmidt, 1991). Nevertheless, the relatively simple physical approach has some limitations. Soil erodibility and surface roughness, which can vary in the course of rain events, are assumed to be constant throughout the calculations (Wickenkamp *et al.*, 2000). EROSION 3D does not differentiate between rill and interrill detachment and, when applied to small spatial resolutions, can therefore overestimate soil erosion rates (von Werner, 1995).

The EROSION 3D input parameters can be summarized into three groups, relief parameters, precipitation parameters and soil-surface parameters (Schmidt *et al.*, 1999). For the relief parameters, we used the measured 25 cm resolution DTMs. We used the DTM including ridges for the RP and RU scenarios and we used the measured base DTM without ridges to represent a smooth soil surface (SS). Precipitation parameters for each of the seven rainfall periods were provided by the on-site rain gauge records at 10 minutes resolution. Soil and surface parameters used for the simulations are shown in Table 3.1. Layer thickness, texture, bulk density and organic carbon content for the different soil horizons were derived from field measurements and laboratory analysis. For the different management practices, the parameters in Table 3.1 were assigned as follows. For RP, parameters specified for “plastic film” were applied for ridges, and parameters specified for “soil surface” were used for the furrows. For RU and SS, the parameters specified for “soil surface” were applied to the entire field area (ridges, furrows as well as the smooth surface). The initial soil moisture at the beginning of each rainfall period was derived from HYDRUS 2D/3D (Šimůnek *et al.*, 2011) simulations. The HYDRUS 2D/3D model was calibrated to pressure heads measured from May to August 2010 on field 1 and field 2 and used to analyze soil water dynamics due to plastic mulch management. Surface roughness (Manning’s n) was obtained from recommended literature values. Huggins and Monke (1966) (cited in Vieux, 2001) give Manning’s n values for row crops of 0.07 to $0.2 \text{ s m}^{-1/3}$ and the EROSION 3D parameter catalogue (Michael *et al.*, 1996) recommend values for potato fields of 0.08 to $0.09 \text{ s m}^{-1/3}$. These recommendations represent average field conditions including the roughness of the soil surface and the roughness caused by plant stems and leaves. To take into account the different surface conditions between the plastic covered ridges and the uncovered furrows, plastic film and soil surface were treated separately. For the plastic film cover, a Manning’s n value of $0.01 \text{ m s}^{-1/3}$ was selected (Montes, 1998, Chanson, 2004). Potato stems are embedded in small planting holes within the plastic film on the top of the ridges and rarely influence flow along the ridge flanks. For the bare sandy soil surface, Engman (1986) (cited in Vieux, 2001) recommend values of 0.01 to $0.016 \text{ s m}^{-1/3}$. Nevertheless, due to the fact that potatoes were at a mature stage during our observations and their leaves partially touched the ground, we used a Manning’s n value for the soil surface of $0.035 \text{ s m}^{-1/3}$ (Chow, 1959, cited in Sturm, 2001, Vieux, 2001). Percentage soil cover during each rainfall period was estimated by photographs taken during the field measurements. Plastic covered ridges were considered to cover the soil to 100%. Although the plastic film contains planting holes, it was assumed that they were completely covered by crop leaves.

Table 3.1 Soil and surface parameter values used for the EROSION 3D simulations, divided into uncovered parts of the field (soil surface) and covered parts (plastic film). The third row shows the horizon names of the soil profiles of both fields (according to FAO, 2006)

Input parameters	Field 1						Field 2					
	Soil surface			Plastic film			Soil surface			Plastic film		
	Ap	Bw	BwC	Ap	Bw	BwC	Ap	2Apb	2Bwb	Ap	2Apb	2Bwb
Soil parameters:												
Layer thickness (m)	0.20	0.80	0.10	0.20	0.80	0.10	0.20	0.08	0.62	0.20	0.08	0.62
Clay (%)	9	9	9	9	9	9	11	24	25	11	24	25
Silt (%)	33	55	38	33	55	38	36	59	57	36	59	57
Sand (%)	58	36	53	58	36	53	53	17	18	53	17	18
Bulk density (kg m ⁻³)	1279	1178	1183	1279	1178	1183	1269	1146	1309	1269	1146	1309
Organic carbon (%)	1.8	0.0	0.0	1.8	0.0	0.0	1.7	2.0	0.0	1.7	2.0	0.0
Initial moisture (%):												
Period 1	33	36	37	26	36	37	32	44	44	29	40	44
Period 2	27	36	36	23	36	36	28	39	44	26	37	44
Period 3	28	36	37	23	36	36	29	40	44	26	38	44
Period 4	27	36	36	23	35	36	28	39	44	26	37	44
Period 5	24	35	36	22	35	36	27	37	43	24	35	43
Period 6	27	36	36	23	35	36	29	41	46	28	41	46
Period 7	25	35	36	23	35	36	29	42	46	28	40	46
Surface parameters:												
Roughness (s m ^{-1/3}) ^[a]	0.035			0.010			0.035			0.010		
Soil cover (%):												
Period 1	65			100			90			100		
Period 2	73			100			95			100		
Period 3	75			100			95			100		
Period 4	79			100			95			100		
Period 5	85			100			95			100		
Period 6	75			100			98			100		
Period 7	50			100			90			100		
Skin factor (-) ^[b]	0.00250			0.00003			0.01000			0.00013		
Erodibility (N m ⁻²) ^[b]	0.07			1000.00			0.11			1000.00		

^[a] Manning's roughness coefficient derived from literature values (Chow, 1959, Montes, 1998, Vieux, 2001, Chanson, 2004)

^[b] Skin factor and erodibility values optimized after model calibration to total observed runoff volume and sediment mass

EROSION 3D was calibrated to observed runoff and erosion rates for the plastic covered ridge-furrow system and then used to simulate runoff and erosion for the other management practices (RU and SS). The two last parameters in Table 3.1 (skin factor and erodibility) were used for the calibration. The skin factor is used in EROSION 3D to manipulate the infiltration capacity, as predicted by an empirical approach after Campbell (1985) in order to take into account preferential flow and soil surface conditions, such as crusting. The skin factor for plastic film was defined as 1.3% of the soils value to consider the planting holes which made up approximately 1.3% of the ridge's area. The plastic itself was considered as impermeable. The erodibility parameter is defined as the critical momentum flux, which has to be exceeded by the momentum flux of rainfall and overland flow to generate erosion (Schmidt, 1991) and was calibrated only at the soil surface. The plastic film material was considered as non-erodible (1000 N m⁻²). We used three performance statistics as evaluation criteria for the quality of model calibration, the Nash-Sutcliffe efficiency (*NSE*), the *RMSE*-observations standard deviation ratio (*RSR*) and the Percent bias (*PBIAS*). According to Moriasi *et al.* (2007), satisfactory model performance can be assumed if *NSE* is larger than 0.5, *RSR* smaller or equal to 0.7, and if *PBIAS* $\pm 25\%$ or less. Positive values of *PBIAS* indicate model underestimation, and negative values indicate model overestimation (Gupta *et al.*, 1999).

3.3 Results and discussion

3.3.1 Observed runoff and soil erosion

The measured runoff and soil erosion was highly variable during the observation time due to the rainfall characteristics and varied strongly between field 1 and field 2 (Table 3.2). Precipitation amounts ranged from 2.6 mm to 76.5 mm on field 1 and from 3.0 mm to 102.5 mm on field 2. Total precipitation over all periods of field site 2 (242.7 mm) was higher than field site 1 (165.2 mm). The highest precipitation was recorded for the periods 5 and 7 on both fields. Even though precipitation amounts were similar in both periods, rainfall erosivity was much higher in period 7, due to higher rainfall intensities. On both fields, two of the seven rainfall periods (2 and 3) did not produce appreciable runoff and sediment and the associated soil loss rate for those periods was zero. As expected, runoff and transported sediment correlated positively with precipitation and the highest amounts of runoff and sediment were found on both field sites in periods 5 and 7. The soil loss rate predominantly corresponded with rainfall erosivity within each field, although, the magnitude of difference between fields was large. Even though erosivity was usually higher on field 2, soil loss was always higher on field 1, except during period 3 (Table 3.2). The largest difference between both field sites was observed for period 7. The total observed runoff over all seven rainfall periods was 80.3 L m⁻² on field 1 and 94.1 L m⁻² on field 2. The ratio of total runoff to the amount of rainfall was higher on field 1 (0.49) compared to field 2 (0.39), indicating a lower infiltration capacity of field 1. Total soil loss was 3646.7 kg ha⁻¹ on field 1 and 626.5 kg ha⁻¹ on field 2. The large differences in soil loss may not be explained by the soil characteristics, slope, and crop conditions only, which were relatively similar for both fields. It is expected that soil loss may be affected primarily by the differences in the field topography and the orientation of the ridge-furrow system.

Table 3.2 Observed data for field 1 and field 2. Rainfall characteristics, runoff volume, and sediment mass measured by the runoff collectors (RC 1, RC 2, RC 3), and derived mean runoff and soil loss rates of the whole field

Site	Period	Rainfall		Rainfall erosivity ^[a] (MJ mm ha ⁻¹ h ⁻¹)	RC 1		RC 2		RC 3		Mean runoff ^[b] (L m ⁻²)	Mean soil loss ^[b] (kg ha ⁻¹)
		Rainfall (mm)	intensity (mm h ⁻¹)		Runoff (L)	Sediment (kg)	Runoff (L)	Sediment (kg)	Runoff (L)	Sediment (kg)		
Field 1	1	7.2	7.2	19.4	-	-	10.9	0.1	246.2	4.2	0.8	132.2
	2	3.5	1.4	0.8	0.1	0.0	0.3	0.0	0.5	0.0	0.0	0.0
	3	4.2	2.3	1.3	3.7	0.0	1.1	0.0	9.1	0.0	0.0	0.2
	4	2.6	1.0	0.2	0.0	0.0	0.0	0.0	0.0	0.0	0.0	0.0
	5	56.8	2.4	40.9	-	-	84.5	0.2	6457.6	10.7	20.2	333.3
	6	14.3	2.7	8.1	2245.4	0.9	33.4	0.1	1935.4	2.0	2.5	17.5
	7	76.5	4.3	293.3	-	-	150.4	0.2	18268.7	102.4	56.8	3163.5
Field 2	1	6.2	7.4	13.9	41.2	0.4	126.6	0.7	165.7	0.2	0.6	21.9
	2	4.2	1.7	1.2	1.8	0.0	0.2	0.0	0.0	0.0	0.0	0.0
	3	6.9	4.1	4.8	14.9	0.0	64.4	0.1	4.6	0.0	0.2	1.7
	4	3.0	1.2	0.3	1.1	0.0	3.1	0.0	0.0	0.0	0.0	0.0
	5	102.1	3.3	167.0	4635.7	2.4	-	-	-	-	50.1	254.2
	6	20.9	3.6	27.5	148.0	0.2	634.1	0.5	101.1	0.0	1.6	11.9
	7	99.5	4.5	373.4	5393.8	3.0	6457.6	6.5	-	-	41.7	336.8

^[a] Rainfall erosivity calculated after Renard *et al.* (1997)

^[b] Mean runoff and soil loss calculated as average of the runoff collector values weighted to their drainage area size

3.3.2 Simulated runoff and soil erosion

The optimized values for the skin factor resulting in the best fit between observed and simulated runoff were 0.0025 for field 1 and 0.01 for field 2 for soil surface, and 0.00003 and 0.00013 for plastic film, respectively (Table 3.1). The optimized values for soil surface erodibility with the best fit between observed and simulated soil loss was 0.07 N m⁻²

for field 1 and 0.11 N m^{-2} for field 2 (Table 3.1). The optimized values of erodibility were relatively high and out of the range suggested by Michael *et al.* (1996). These high values indicate a strong erosion overestimation of the model due to the high DTM resolution (von Werner, 1995), which had to be compensated during the calibration. However, the comparison between simulated and observed runoff (Figure 3.4) and soil loss (Figure 3.5) shows acceptable results. For runoff, the model performance was slightly better for field 1 ($NSE = 0.943$, $RSR = 0.239$) than for field 2 ($NSE = 0.914$, $RSR = 0.293$). The model overestimated runoff for both fields with higher magnitude for field 2 ($PBIAS = -13.462$) compared to field 1 ($PBIAS = -1.275$). Also for soil loss, the model performed better for field 1 ($NSE = 0.976$, $RSR = 0.154$) than for field 2 ($NSE = 0.803$, $RSR = 0.444$). The percent bias values showed an overestimation of soil loss for field 1 ($PBIAS = -14.571$) and an underestimation of soil loss for field 2 ($PBIAS = 12.879$). Satisfactory representations were achieved for both runoff and soil loss for field 1 and field 2 (Moriassi *et al.*, 2007).

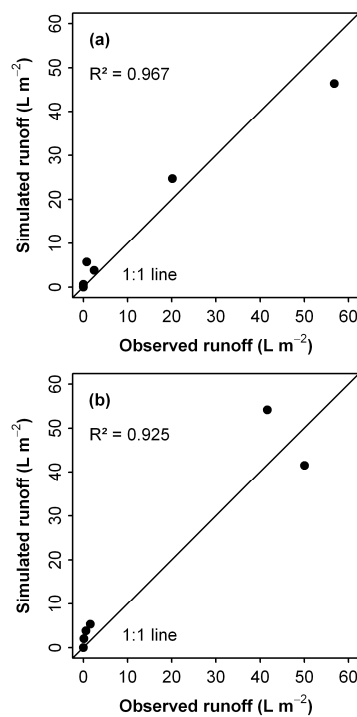


Figure 3.4 Simulated and observed runoff for field 1 (a) and field 2 (b)

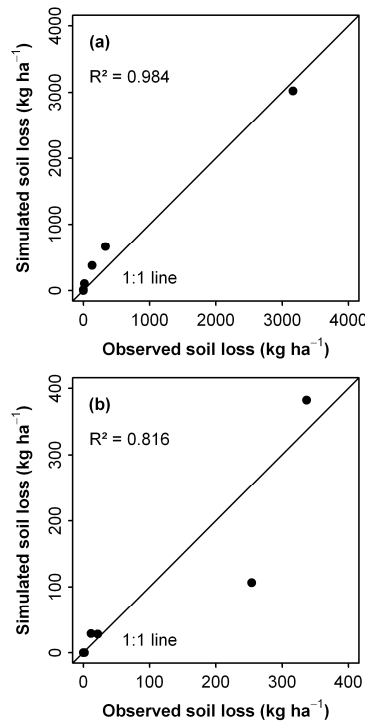


Figure 3.5 Simulated and observed soil loss for field 1 (a) and field 2 (b)

Among the three different management practices, we found the highest simulated runoff for both fields for the ridges with plastic cover (RP) over each rainfall period (Figure 3.6). The total runoff simulated for RP for field 1 and field 2 over all seven rainfall periods was 81.3 L m⁻² and 106.8 L m⁻², respectively. Without plastic cover, the total runoff was reduced to 52.1 L m⁻² (36%) on field 1 and 60.2 L m⁻² (44%) on field 2. The higher runoff amounts for RP are a direct result of the high spatial area associated with the impermeable plastic film. This was also found by HYDRUS 2D/3D simulations at both fields, which calculated up to 70% more runoff for plastic mulch than without plastic cover. For all periods, EROSION 3D predicted the same runoff amount for RU and SS, because soil properties were not changed between the management practices. For both RU and SS, the model estimated the same hydraulic conductivity, resulting in the same runoff amount from the entire field. Only the runoff distribution changed due to different surface conditions. The amount of runoff reduction by removal of the plastic cover largely varied between the different rainfall periods, and corresponded with the rainfall intensity. The lowest runoff reduction was simulated for period 1 (10% reduction for field 1 and 21% reduction for field 2). Period 1 was characterized by one very short rain event with average intensities of 7.2 mm h⁻¹ and 7.4 mm h⁻¹ on field 1 and field 2, respectively. For period 7 with average intensities of 4.3 mm h⁻¹ (field 1) and 4.5 mm h⁻¹ (field 2), runoff was reduced by 23% on field 1 and 28% on field 2. The highest runoff reduction was predicted for field 1 (79%) for period 6 (average intensity of 2.7 mm h⁻¹) and for field 2 (61%) for period 5 (average intensity of 3.3 mm h⁻¹). For small rainfall intensities lower than the infiltration capacity of the soil, the impermeable plastic cover largely increases the total runoff of the field sites. For high intensities exceeding the soil's infiltration capacity, this effect is much smaller, because of high runoff generation on both, plastic and bare soil. This effect was previously described also by Wolfe *et al.* (2002). Nevertheless, canopy interception and stem flow were not considered in the simulations, because we did not have information about the infiltration amounts caused by stem flow on plastic covered ridge-furrow systems. After plant emergence, stem flow leads to local infiltration of precipitation water around the stems (Leistra and Boesten, 2010). Saffigna *et al.* (1976) and Jefferies and MacKerron (1985) (cited in Leistra and Boesten, 2010) found that for potato plants, the percentage of stem flow of the

above-crop rainfall can account for up to 46% and 87%, respectively. During the mature crop stage, stem flow could potentially result in higher infiltration and less soil erosion (Wan and El-Swaify, 1999). Therefore, the runoff effect of plastic mulch may be slightly overestimated for the rainfall periods throughout this study. However, stem flow is only relevant for infiltration rates, when a high covering crop crown is developed. For the time between field preparation and maturity and after senescence, when most of the above-ground biomass is dead, the stem flow effect is negligible. Therefore, we believe that the model assumptions are reasonable for evaluating the principle effects of plastic mulch on runoff and erosion over the season.

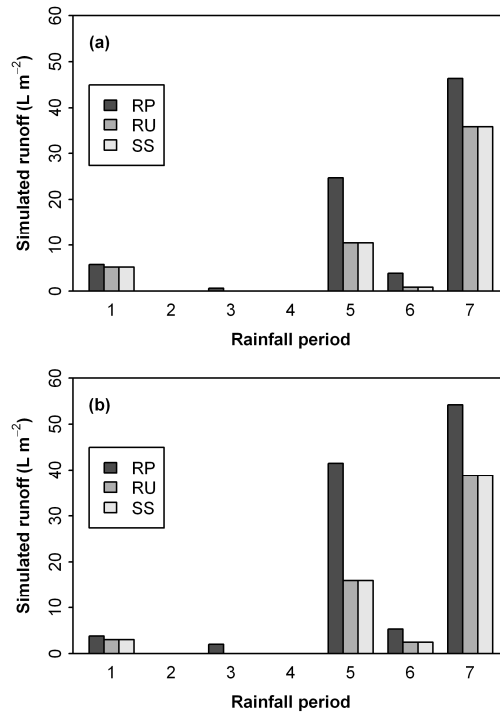


Figure 3.6 Simulated runoff for all rainfall periods for field 1 (a) and field 2 (b) for different management practices (RP: ridges with plastic cover, RU: uncovered ridges, SS: smooth soil surface)

The highest soil loss was simulated for ridges with plastic cover (RP) at both fields caused by the higher rate of surface runoff compared to RU, but for SS, we found contrary effects between the fields (Figure 3.7). The total soil loss simulated for RP for field 1 and field 2 over all seven rainfall periods was 4178.1 kg ha⁻¹ and 545.8 kg ha⁻¹, respectively. Total soil loss was reduced to 2469.9 kg ha⁻¹ (41%) on field 1 and 371.7 kg ha⁻¹ (32%) on field 2 by removal of plastic from the ridges (RU). The highest reduction was predicted for both fields for period 6 with 79% on field 1 and 82% on field 2. The lowest soil loss reduction was simulated for field 1 for period 1 (30%) and field 2 for period 7 (25%). For smooth soil surface conditions (SS), the model predicted an additional soil loss reduction for field 1 to 1017.3 kg ha⁻¹ (76% reduction compared to RP), but for field 2 an increase in soil loss compared to RU to 467.5 kg ha⁻¹, which is only 14% reduction compared to RP. Soil loss reduction by SS on field 1 and the soil loss increase on field 2 compared to RU was predicted for all periods. The highest soil loss reduction for SS occurred during period 6 at both fields with 89% reduction compared to RP on field 1 and 42% reduction compared to RP on field 2. The lowest soil loss reduction for field 1 was period 1 (72% compared to RP) and for field 2 period 5 (9% compared to RP). Correlation between measured rainfall characteristics and the effects of the three management practices as described for surface runoff and rainfall intensity were not detected.

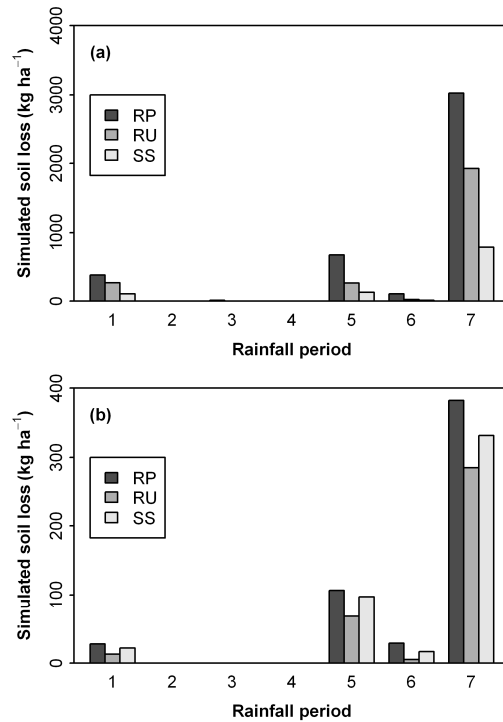


Figure 3.7 Simulated soil loss for all rainfall periods for field 1 (a) and field 2 (b) for different management practices (RP: ridges with plastic cover, RU: uncovered ridges, SS: smooth soil surface)

Due to field topography and ridge orientation, both fields show totally different flow characteristics, which caused the differences in soil loss for RP, RU, and SS. Figure 3.8 shows the flow patterns and spatial distribution of the simulated sediment concentrations. The magnitude of increase in sediment concentration represents the amount of erosion at a particular location. Runoff flow direction (indicated by the arrows) for RP and RU is primarily controlled by the ridges. Therefore, water is routed in the furrows parallel to ridges instead of moving along the steepest flow paths. The spatial patterns of erosion for RP and RU are basically the same. With increasing flow length, sediment concentration becomes higher. The reason is the increasing runoff rate, which provides higher erosive energy in the furrows (Wolfe *et al.*, 2002). The RU scenario shows slightly higher sediment concentration than RP because of additional soil erosion from the uncovered ridges. The total sediment mass transported from the field sites was higher for RP because of higher amounts of runoff. Water is flowing along the furrows until it reaches the field's edge or a topographical depression. On field 1, runoff is trapped and accumulating in such depressions due to the field concavity and routed across the ridges. As a consequence, lines of concentrated flow are formed perpendicular to the ridge orientation, especially in the field's center and on the bottom (Figure 3.8). For those concentrated flow lines, the model predicted much higher soil erosion rates than for the surrounding areas. During our field measurements, we observed ridge breakovers with a deep erosion rill formed by concentrated flow in the center of field 1 (Figure 3.9). The plastic film was washed out and ridges were destroyed by water flow, forming a permanent channel partially deeper than 10 cm. On field 2, such concentrated flow lines were not formed because of its convex shape. Water was routed along the furrows and leaving the field at its edge without accumulation. Row lengths are relatively high especially at the field bottom, which results in higher erosion rates at the lower parts of the furrows. Nevertheless, the predicted sediment concentration at those locations remained lower than for the concentrated flow lines on field 1. Management without ridges (SS) produced entirely different runoff flow patterns and erosion rates. For the SS scenario, water was routed directly along the steepest flow paths and solely controlled by field topography. Runoff was more evenly distributed over the surface without high flow

concentration. For field 1, part of the runoff was still accumulating in the field's center and at the edges, although with less erosive power than predicted for RP and RU, as indicated by lower sediment concentrations for SS throughout the field. The absence of ridges on field 2 resulted in routing along a steeper slope and flow accumulation at field's edges where higher erosion was predicted.

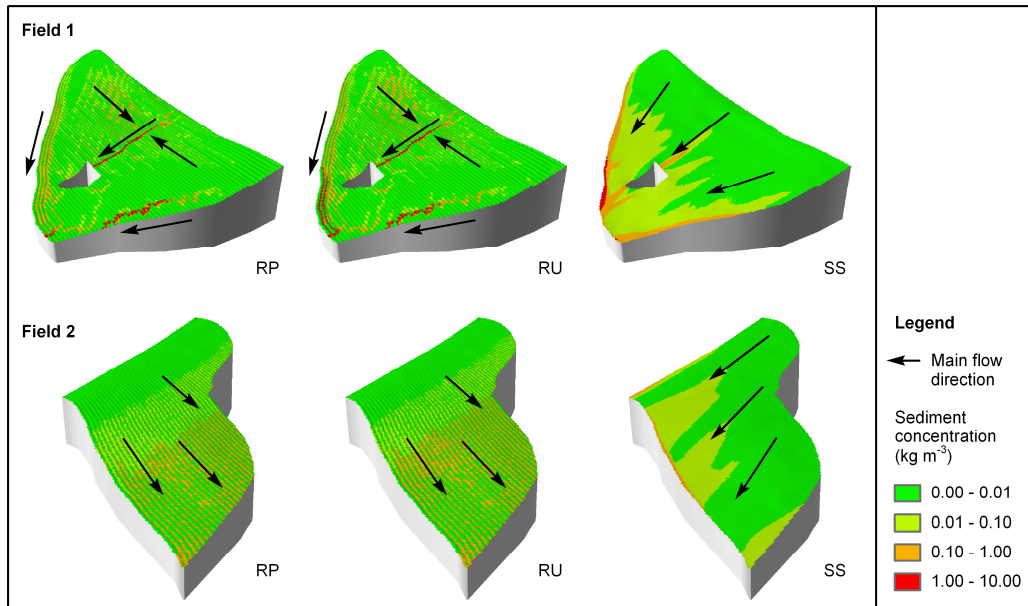


Figure 3.8 Simulated sediment concentration over all rainfall periods for field 1 and field 2 for different management practices including main flow directions (RP: ridges with plastic cover, RU: uncovered ridges, SS: smooth soil surface)



Figure 3.9 Observed erosion rill formed by ridge breakovers and concentrated flow in the depression line in the center of field 1

These results demonstrate that the effect of the ridge-furrow system on erosion is controlled primarily by the topography of the fields. Because of its concave shape, field 1 generated a 140% higher erosion for the ridge-furrow system compared to a smooth surface due to ridge breakovers, as previously described (Wischmeier and Smith, 1978,

Stocking, 1972, El-Swaify *et al.*, 1982, Haggmann, 1996). The ridge-furrow system on the convex field 2 separated runoff and constrained flow to the furrows, which prevented flow accumulation and resulted in 20% lower soil erosion rates.

3.4 Summary and conclusions

In this study, we analyzed the effect of plastic covered ridge-furrow systems on runoff and erosion in combination with the complex field topography of a mountainous landscape in South Korea. We installed runoff collectors on two field sites managed with plastic mulch and measured runoff and sediment loss during monsoonal rain events in 2010. The measured differences in soil loss between both fields suggested that soil erosion may be primarily affected by the field's topography and the orientation of the ridge-furrow system. We used observed field data to calibrate the EROSION 3D model and subsequently applied the model to investigate runoff and erosion for an uncovered ridge-furrow system and a smooth soil surface on the same fields. Model performance statistics demonstrate that EROSION 3D can be applied successfully on high spatial resolutions when calibrated to available measured data.

The model results for different management practices showed much higher surface runoff produced by plastic film covers. The percent difference between plastic mulch and uncovered management was strongly influenced by the average intensities of the rain events. Simulated soil loss was also highest on both fields for plastic mulch ridges as a result of higher runoff rate produced by the impermeable plastic film. The effect of the plastic film on surface runoff may be slightly overestimated for the rainfall periods throughout this study, because stem flow effects on the infiltration rate were not considered. However, for evaluating the principle effects of plastic mulch on runoff and erosion, we believe that the model assumptions were reasonable. Nevertheless, additional research is necessary in order to identify the effect of interception and stem flow on the infiltration rate in plastic mulch systems for different crops during the growing season.

The effect of the ridge-furrow system on soil erosion compared to the smooth soil surface was very different between fields. The ridge-furrow system increases soil erosion of field 1, however, it potentially prevents erosion on field 2 when not covered with plastic film. The predicted flow patterns and spatial distribution of sediment concentration demonstrated that the effect is primarily controlled by the field topography. Because of the concave shape of field 1, ridges lead to flow accumulation causing breakovers and concentrated flow with high erosive power and resulting in higher total erosion from the field. Although ridges on the convex field 2 prevent runoff routing along the steepest slope and accumulation at the edges, which resulted in reduced total erosion from the field. These results show that ridge-furrow systems can increase soil erosion dramatically on one field, but have contrary effects on another field, simply depending on the topography.

Our results have practical consequences for planning and implementation of best management practices for watersheds. Especially in mountainous areas, where the topography within and between fields can be strongly variable, ridge-furrow cultivation should be performed carefully. The ridge-furrow system should be preferable located parallel with the contours, or oriented towards the edges in order to drain runoff away from depressions and to prevent concentrated flow within fields. To prevent flow accumulation and high erosion rates at the field edges, also the transition zones between the field and the surrounding margins have to be considered. Our results show that in any case the furrows between the ridges need to be better protected against soil erosion. Conventional herbicide applications eliminate the development of a plant cover in the furrows. Even though the vegetative cover of adult crops can protect soil from raindrop impact, the furrows remain susceptible to erosion by overland flow during the entire growing season.

In order to reduce soil erosion on crop fields in South Korea, we recommend organic farming practices without herbicide application, which supports the development of weeds in the furrows. Another effective erosion control measure can be cereal grass cultivation in the furrows as suggested by Rice *et al.* (2007). Vegetative-covered furrows are functioning as “in-field buffers”, which can increase infiltration capacity and reduce runoff flow velocity due to higher surface roughness (Rice *et al.*, 2007). Reducing the runoff flow rate along the furrows could also help to prevent the severe damages caused by ridge breakovers.

Another important issue is the application of large-scale erosion models to those areas dominated by ridge-furrow cultivation. Erosion prediction on watershed-scale is usually conducted on the basis of relatively coarse digital elevation models and does often not account for special tillage and cropping systems and their orientation. The models can strongly over- and underestimate soil erosion rates especially for complex landscapes and should be corrected for ridge-furrow systems. However, this study analyzed only two field sites with a specific topography and ridge orientation. In order to identify general patterns, which can be used for large-scale model applications, additional research studies are necessary to account for a variety of different field topographies and ridge-furrow systems.

3.5 Acknowledgements

This study was carried out within the framework of the International Research Training Group TERRECO, funded by the German Research Foundation (DFG) and the Korea Science and Engineering Foundation (KOSEF). The authors thank Andreas Kolb, Steve Lindner, and Bongjae Kwon for their technical support during the field installations.

3.6 References

- Avnimelech, Y., Ritvo, G., Meijer, L. E., Kochba, M., 2001. Water content, organic carbon and dry bulk density in flooded sediments. *Aquacultural Engineering* **25**, 25-33.
- Bonilla, C. A., Kroll, D. G., Norman, J. M., Yoder, D. C., Molling, C. C., Miller, P. S., Panuska, J. C., Topel, J. B., Wakeman, P. L., Karthikeyan, K. G., 2006. Instrumentation for measuring runoff, sediment, and chemical losses from agricultural fields. *Journal of Environmental Quality* **35**, 216-223.
- Campbell, G. S., 1985. *Soil physics with BASIC. Transport models for soil-plant systems*. Elsevier, Amsterdam.
- Chanson, H., 2004. *The hydraulics of open channel flow. An introduction*, second ed. Elsevier Butterworth Heinemann, Oxford.
- Chow, V. T., 1959. *Open-channel hydraulics*. McGraw-Hill, New York.
- De Roo, A. P. J., Wesseling, C. G., Ritsema, C. J., 1996. LISEM: a single-event physically based hydrological and soil erosion model for drainage basins. I: theory, input and output. *Hydrological Processes* **10**, 1107-1117.
- Dilara, P. A., Briassoulis, D., 2000. Degradation and stabilization of low-density polyethylene films used as greenhouse covering materials. *Journal of Agricultural Engineering Research* **76**(4), 309-321.
- El-Swaify, S. A., Dangler, E. W., Armstrong, C. L., 1982. *Soil erosion by water in the tropics*. College of Tropical Agriculture and Human Resources, University of Hawaii, Honolulu.
- Engman, E. T., 1986. Roughness coefficients for routing surface runoff. *Journal of Irrigation and Drainage Engineering* **112**(1), 39-53.
- Espí, E., Salmerón, A., Fontecha, A., García, Y., Real, A. I., 2006. Plastic films for agricultural applications. *Journal of Plastic Film and Sheeting* **22**(2), 85-102.
- Food and Agriculture Organization of the United Nations (FAO). 2006. *Guidelines for soil description*, fourth ed. Rome.
- Gascuel-Oudou, C., Garnier, F., Heddadj, D., 2001. Influence of cultural practices on sheetflow, sediment and pesticide transport: the case of corn cultivation under plastic mulching, in: Stott, D. E., Mohtar, R. H., Steinhardt, G. C.

- (Eds.), *Sustaining the global farm. Selected papers from the 10th International Soil Conservation Organization Meeting*. International Soil Conservation Organization, pp. 300-304.
- Gupta, H. V., Sorooshian, S., Yapo, P. O., 1999. Status of automatic calibration for hydrologic models: comparison with multilevel expert calibration. *Journal of Hydraulic Engineering* **4**(2), 135-143.
- Hagmann, J., 1996. Mechanical soil conservation with contour ridges: cure for, or cause of, rill erosion? *Land Degradation and Development* **7**, 145-160.
- Huggins, L. F., Monke, E. J., 1966. *The mathematical simulation of the hydrology of small watersheds*. Technical Report 1. Purdue University Water Resources Research Center, West Lafayette.
- Jefferies, R. A., MacKerron, D. K. L., 1985. Stemflow in potato crops. *Journal of Agricultural Science* **105**, 205-207.
- Kim, B., Choi, K., Kim, C., Lee, U., Kim, Y., 2000. Effects of the summer monsoon on the distribution and loading of organic carbon in a deep reservoir, Lake Soyang, Korea. *Water Research* **34**(14), 3495-3504.
- Kim, S., Yang, J., Park, C., Jung, Y., Cho B., 2007. Effects of winter cover crop of ryegrass (*Lolium multiflorum*) and soil conservation practices on soil erosion and quality in the sloping uplands. *Journal of Applied Biological Chemistry* **55**(1), 22-28.
- Lament Jr., W. J., 1993. Plastic mulches for the production of vegetable crops. *HortTechnology* **3**(1), 35-39.
- Lee, G., Lee, J., Ryu, J., Hwang, S., Yang, J., Joo, J., Jung, Y., 2010a. Status and soil management problems of highland agriculture of the main mountainous region in the South Korea, in: Gilkes, R. J., Prakongkep, N. (Eds.), *Proceedings of the 19th World Congress of Soil Science. Soil solutions for a changing world*. International Union of Soil Sciences, pp. 154-157.
- Lee, G., Lee, J., Ryu, J., Zhang, Y., Jung, Y., 2010b. Loss of soil and nutrient from different soil managements in highland agriculture, in: Gilkes, R. J., Prakongkep, N. (Eds.), *Proceedings of the 19th World Congress of Soil Science. Soil solutions for a changing world*. International Union of Soil Sciences, pp. 78-81.
- Leistra, M., Boesten, J. J. T. I., 2010. Pesticide leaching from agricultural fields with ridges and furrows. *Water, Air and Soil Pollution* **213**, 341-352.
- Michael, A., Schmidt, J., Schmidt, W. A., 1996. *EROSION 2D/3D. A computer model for the simulation of soil erosion by water. Parameter catalog application (2D)*. Freiberg.
- Montes, S., 1998. *Hydraulics of open channel flow*. ASCE Press, Reston
- Moriasi, D. N., Arnold, J. G., van Liew, M. W., Bingner, R. L., Harmel, R. D., Veith, T. L., 2007. Model evaluation guidelines for systematic quantification of accuracy in watershed simulations. *Transactions of the ASABE* **50**(3), 885-900.
- Nearing, M. A., Foster, G. R., Lane, L. J., Finkner, S. C., 1989. A process-based soil erosion model for USDA-Water Erosion Prediction Project technology. *Transactions of the ASAE* **32**(5), 1587-1593.
- Park, J., Duan, L., Kim, B., Mitchell, M. J., Shibata, H., 2010a. Potential effects of climate change and variability on watershed biogeochemical processes and water quality in Northeast Asia. *Environment International* **36**, 212-225.
- Park, Y., Kim, J., Kim, N., Kim, S., Jeon, J., Engel, B. A., Jang, W., Lim, K., 2010b. Development of new R, C and SDR modules for the SATEEC GIS system. *Computers and Geosciences* **36**(6), 726-734.
- Pinson, W. T., Yoder, D. C., Buchanan, J. R., Wright, W. C., Wilkerson, J. B., 2004. Design and evaluation of an improved flow divider for sampling runoff plots. *Applied Engineering in Agriculture* **20**(4), 433-438.
- Renard, K. G., Foster, G. R., Weesies, G. A., McCool, D. K., Yoder, D. C., 1997. *Predicting soil erosion by water. A guide to conservation planning with the Revised Universal Soil Loss Equation (RUSLE)*. Agriculture Handbook 703. USDA, Washington D.C.
- Rice, P. J., Harman-Fetcho, J. A., Sadeghi, A. M., McConnell, L. L., Coffman, C. B., Teasdale, J. R., Abdul-Baki, A. A., Starr, J. L., McCarty, G. W., Herbert, R. R., Hapeman, C. J., 2007. Reducing insecticide and fungicide loads in runoff from plastic mulch with vegetative-covered furrows. *Journal of Agricultural and Food Chemistry* **55**(4), 1377-1384.
- Rice, P. J., McConnell, L. L., Heighton, L. P., Sadeghi, A. M., Isensee, A. R., Teasdale, J. R., Abdul-Baki, A. A., Harman-Fetcho, J. A., Hapeman, C. J., 2001. Runoff loss of pesticides and soil: a comparison between vegetative mulch and plastic mulch in vegetable production systems. *Journal of Environmental Quality* **30**, 1808-1821.

- Saffigna, P. G., Tanner, C. B., Keeney, D. R., 1976. Non-uniform infiltration under potato canopies caused by interception, stemflow, and hilling. *Agronomy Journal* **68**(2), 337-342.
- Schmidt, J., von Werner, M., Michael, A., 1999. Application of the EROSION 3D model to the CATSOP watershed, The Netherlands. *Catena* **37**, 449-456.
- Schmidt, J., 1991. A mathematical model to simulate rainfall erosion, in: Bork, H. R., De Ploey, J., Schick, A. P. (Eds.), *Erosion, transport and deposition processes. Theories and models*. Catena Supplement 19. Catena, Cremlingen, pp. 101-109.
- Šimůnek, J., Šejna, M., van Genuchten, M., 2011. *The HYDRUS software package for simulating two- and three-dimensional movement of water, heat, and multiple solutes in variably-saturated media*. Technical manual, version 2.0. PC Progress, Prague
- Stevens, M. D., Black, B. L., Lea-Cox, J. D., Sadeghi, A. M., Harman-Fetcho, J. A., Pfeil, E., Downey, P., Rowland, R., Hapeman, C. J., 2009. A comparison of three cold-climate strawberry production systems: environmental effects. *HortScience* **44**(2), 298-305.
- Stocking, M. A., 1972. Aspects of the role of man in erosion in Rhodesia. *Zambezia* **2**(2), 1-10.
- Sturm, T. W., 2001. *Open channel hydraulics*. McGraw-Hill, Boston.
- Vieux, B. E., 2001. *Distributed hydrologic modeling using GIS*. Kluwer Academic Publishers, Dordrecht.
- von Werner, M., 1995. GIS-orientierte Methoden der digitalen Reliefanalyse zur Modellierung von Bodenerosion in kleinen Einzugsgebieten. *PhD Thesis*. Free University of Berlin, Department of Earth Sciences.
- Wan, Y., El-Swaify, S. A., 1999. Runoff and soil erosion as affected by plastic mulch in a Hawaiian pineapple field. *Soil and Tillage Research* **52**, 29-35.
- Wickenkamp, V., Duttmann, R., Mosimann, T., 2000. A multiscale approach to predicting soil erosion on cropland using empirical and physically based soil erosion models in a geographic information system, in: Schmidt, J. (Ed.), *Soil erosion. Application of physically based models*. Springer, Berlin, pp. 109-134.
- Wischmeier, W. H., Smith, D. D., 1978. *Predicting rainfall erosion losses. A guide to conservation planning*. Agriculture Handbook 537. USDA, Washington D.C.
- Wolfe, M. L., Ross, B. B., Diem, J. F., Dillaha, T. A., Flahive, K. A., 2002. *Protecting water quality: best management practices for row crops grown on plastic mulch in Virginia*. Virginia Cooperative Extension, Blacksburg.

Chapter 4

Conventional and organic farming:

soil erosion and conservation potential for row crop cultivation

Sebastian Arnhold¹, Steve Lindner², Bora Lee², Emily Martin³, Janine Kettering⁴, Trung Thanh Nguyen⁵, Thomas Koellner⁵, Yong Sik Ok⁶, Bernd Huwe¹

¹ Department of Soil Physics, University of Bayreuth, Universitätsstraße 30, 95447 Bayreuth, Germany

² Department of Plant Ecology, University of Bayreuth, Universitätsstraße 30, 95447 Bayreuth, Germany

³ Biogeographical Modelling, University of Bayreuth, Universitätsstraße 30, 95447 Bayreuth, Germany

⁴ FLAD & FLAD Communication GmbH, Thomas-Flad-Weg 1, 90562 Heroldsberg, Germany

⁵ Professorship of Ecological Services, University of Bayreuth, Universitätsstraße 30, 95447 Bayreuth, Germany

⁶ Department of Biological Environment, Kangwon National University, 192-1 Hyoja-Dong, Kangwon-Do, Chuncheon 200-701, Republic of Korea

Abstract

The cultivation of row crops on mountainous farmland can generate severe soil erosion due to low ground cover, especially in the early growth stages. Organic farming, due to the absence of herbicides, can support the development of weeds and increase the ground cover compared to conventional farming. However, the benefits towards soil erosion, and the conservation potential of organic farming systems, in terms of herbicide application and weed growth, have not been investigated. Aim of this study was to identify how conventional and organic farming influence the erosion rate of soil, due to row crops cultivated on mountainous farmland in the presence or absence of agricultural chemicals. We measured multiple vegetation parameters of crops and weeds of conventional and organic farms cultivated with bean, potato, radish, and cabbage in a mountainous watershed in South Korea. We simulated the long-term soil erosion rates with the Revised Universal Soil Loss Equation (RUSLE) by using 13 years of recorded rainfall data in order to account for the temporal variability of monsoonal rainfall. We determined average annual erosion rates for the study area to be between $30.6 \text{ t ha}^{-1} \text{ yr}^{-1}$ and $54.8 \text{ t ha}^{-1} \text{ yr}^{-1}$, with maximum values for those areas where radish was grown, due to the shorter growing period, higher soil disturbance at harvest, and low amounts of residue. Organic farming reduced soil loss for radish by 18% as a result of a high weed biomass density and cover at the end of the growing season. For potato, organic farming increased soil loss by 25% due to a reduced crop coverage, which is suspected to have been a consequence of crop-weed competition or increased herbivory associated with the absence of agricultural chemicals. Our results demonstrate that organic farming can potentially decrease the soil erosion risk for row crops because it supports weed development in the furrows, but it can also produce higher erosion rates when crop yields are reduced as a consequence, outweighing the protective effect of the weeds. However, the simulated erosion rates under both farming systems exceed by far any tolerable soil loss. We conclude that organic farming alone cannot be used to effectively control erosion, and that both farming systems require additional conservation measures, such as winter cover crops and residue mulching, to sufficiently prevent soil loss for row crop cultivation.

Keywords: *Farming system, Herbicide, Korea, Row crop, Soil erosion, Weed cover*

4.1 Introduction

Intensive agriculture in mountainous landscapes can cause high soil erosion with negative impacts on farmland productivity and sustainability, as well as downstream water quality. The severity of erosion is strongly affected by the specific nature of cultivation within such areas. Vegetation above the surface protects the soil from the impact of raindrops and runoff, while the root system contributes to the internal stabilization of the soil (Morgan, 2005). Therefore, the crop type and management system applied by farmers plays a critical role in erosion control on steep agricultural land. The cultivation of row crops generally results in more serious erosion problems due to the high ratio of exposed ground, especially in the early growth stages, and due to the need for seedbed preparations (Morgan, 2005). More extensive groundcover can be provided by weeds, helping to further reduce soil erosion (Bennett, 1939), and Brock (1982) reported that weed control by the use of herbicides significantly increases soil erosion rates. Several other studies have also shown that a developed weed cover can effectively reduce soil loss compared to manual weeding or the application of herbicides (Weil, 1982, Afandi *et al.*, 2002, García-Orenes *et al.*, 2009, Blavet *et al.*, 2009). Environmentally friendly farming systems rely on the minimization of chemical use, such as herbicides and pesticides, and can, therefore, play an important role in erosion control. Especially for row crops, the percentage of ground cover can be altered by weed growth, which could provide additional soil protection on organic farmland. Nevertheless, organic farming can also result in reduced crop yields due to crop-weed competition and herbivory.

Several authors have already described the potential effects of organic versus conventional farming on soil erosion control (Lotter *et al.*, 2003, Erhart and Hartl, 2010, Goh, 2011, Gomiero *et al.*, 2011). However, the individual studies used different methodologies to assess the erosion potential, and they observed very different impacts of the two farming systems. Lockeretz *et al.* (1981) calculated potential soil loss of organic and conventional farms by using the Universal Soil Loss Equation (Wischmeier and Smith, 1978) and found about one-third less erosion where organic farming is practiced, due to the different crop rotation systems in place. Reganold *et al.* (1987) investigated the long-term effects by comparing erosion measurements and topsoil thickness of two farms, and found an almost four times lower erosion on the organic farm as a result of different crop rotation and less tillage operations. Fleming *et al.* (1997) used soil samples from organic and conventional fields and calculated the soil erodibility, finding that organic farming can potentially reduce erosion for some soils. Also Siegrist *et al.* (1998) found, in a long-term field experiment, that organic farming increases the aggregate stability of the soil. However, organic farming did not sufficiently reduce soil erosion in their study. Also during a long-term field experiment, Eltun *et al.* (2002) observed lower erosion on plots with organic arable crops, but higher erosion on plots with organic forage crops. Auerswald *et al.* (2003) investigated the soil erosion potential also by using the Universal Soil Loss Equation, based on cropping statistics of conventional and organic farms, finding a slightly lower soil loss where organic farming was practiced, but concluding that there is no general effect, due to the large variability within both farming systems. Pacini *et al.* (2003) modeled soil erosion using GLEAMS (Leonard *et al.*, 1987) on different farms, and they found that organic farming dramatically increased erosion compared to conventional farming, because of different crops and more intense tillage operations. In another study using rainfall simulations, Kuhn *et al.* (2012) reported lower erosion rates from organic compared to conventional soils.

Although the erosion control potential of organic farming could be identified in many of these studies, a general conclusion of the impact of the farming systems can still not be drawn. Soil stabilization might be an effect of long-term organic farming and may not apply for recently established organic farms. Large differences between both farming systems were primarily observed where farms used different crops and tillage operations. The effects of weed

development associated with the two farming systems for the same crop as a specific consequence of the application or absence of agricultural chemicals has not been investigated.

The aim of this study was to identify the erosion control potential of conventional and organic farming systems on mountainous farmland in South Korea, which is highly susceptible to soil erosion due to the steep slopes and the cultivation of row crops. In the Kangwon Province in the northeast of South Korea, for instance, primarily radish and cabbage are cultivated (Kim *et al.*, 2007), having short growing periods, thus leaving the farmland with low protection against rainfall and runoff (Park *et al.*, 2010b). Conventional farmland management in South Korea is characterized by an intensive use of agricultural chemicals, including herbicides and pesticides (Kang and Kim, 2000, Kim and Kim, 2004). However, environmentally friendly farming systems (organic farming and no-chemical farming), which do not use agricultural chemicals are becoming more popular (Kim *et al.*, 2001, Choo and Jamal, 2009). Due to governmental support, the number of organic farms in South Korea has strongly increased within recent years (Kim and Kim, 2004, Kim *et al.*, 2012). The effect of different row crops on soil erosion in Korea has previously been studied over many years by the National Academy of Agricultural Science (NAAS) (Jung *et al.*, 2003). Other studies investigated the effect of planting time and vegetation cover (Cho *et al.*, 2010) or the erosion control potential of cover crop cultivation together with row crops (Kim *et al.*, 2008, Ryu *et al.*, 2010), but the impact of vegetation development associated with conventional and organic farming needs further investigation.

We formulated the following hypotheses: (1) organic farming increases weed coverage for row crops due to the absence of herbicides, and (2) the protective effects of weeds control soil erosion for organic farming. To test the hypotheses, we measured multiple vegetation parameters of four major row crops and the associated weeds on both conventional and organic farms in a watershed in the Kangwon Province of South Korea, and we determined the potential resultant soil loss amounts using the Revised Universal Soil Loss Equation (RUSLE) (Renard *et al.*, 1997). To better understand the long-term effects of the farming systems, we considered the regional climate development, as soil loss rates associated with crops and farming systems are highly variable depending on the planting and harvest times and the occurrence of erosive rainstorm events. The majority of annual rainfall on the Korean peninsula is concentrated in the summer monsoon between June and August (Park *et al.*, 2010a) and hence, the annual soil erosion rate may be dependent on only a few extreme events. Choi *et al.* (2008) observed an intensification of extreme rainfall events in Korea, and found a strong change in temporal distribution over the years, and Kim *et al.* (2009) reported a large variability in precipitation during the monsoon season. Hence, the variation in rainfall patterns and intensities can therefore result in highly variable erosion rates for similar crops and farming systems between different years. The severity of erosion is also controlled by other factors, such as the level of soil disturbance during harvest and the amount of residue remaining on the field (Toy *et al.*, 2002). Therefore, we used long-term weather station data to account for the variability of monsoonal rainstorm events, and we simulated different scenarios to include variable planting dates and harvest operations for the different row crops and farming systems.

4.2 Materials and methods

4.2.1 Study area

This study was conducted in the Haeon-Myeon catchment in the Kangwon Province of South Korea (Figure 4.1). The catchment is located within the watershed of the Soyang Lake, which is the largest reservoir in South Korea (Kim *et al.*, 2000). The reservoir is affected by high amounts of nutrients from the Soyang River largely due to eroded soils from agricultural areas within the watershed (Kim and Jung, 2007, Park *et al.*, 2010a). The Haeon catchment is a major

agricultural hotspot area, which substantially affects the trophic state of the reservoir (Park *et al.*, 2010a). The total area of the catchment is 64 km², of which 58% is covered with forest and 30% by agricultural lands (22% dryland fields, 8% rice paddies). The remaining 12% consists of residential areas and seminatural areas, which include grassland, field margins, riparian areas, and farm roads. The topography of the study area is characterized by flat areas and moderately steep slopes in the center of the catchment, and high slopes at the forest edges. The terrain is highly complex with a variety of different hill slopes and flow directions. The soils of the Haeon catchment are dominated by *Cambisols* formed from weathered granite. They are highly influenced by human disturbances. Especially dryland fields are modified by the replenishment of excavated material from nearby mountain slopes in order to compensate for annual erosion losses (Park *et al.*, 2010a). The average annual precipitation in the Haeon catchment is 1599 mm (1999 to 2011), of which more than 65% are concentrated in July, August, and September.

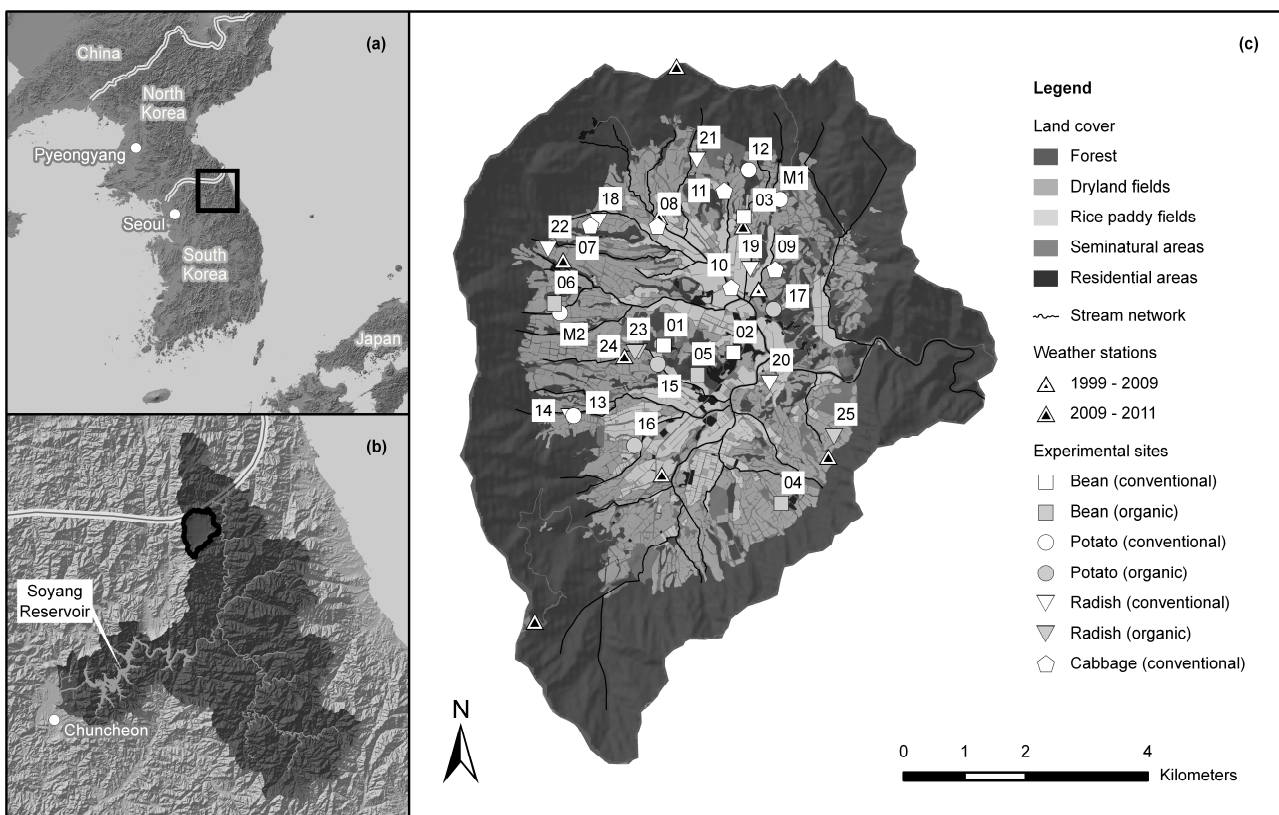


Figure 4.1 Location of the study area (Haean-Myeon catchment) on the Korean peninsula (a) and within the watershed of the Soyang Lake (b) with the locations of the weather stations and 25 experimental sites (01 to 25) selected for this study (c). The sites M1 and M2 indicate the position of two additional fields where soil loss was measured in 2010, which was used to evaluate model plausibility

For this study, 25 field sites were selected, which included the four major dryland row crops, bean (*Glycine max*), potato (*Solanum tuberosum*), radish (*Raphanus sativus*), and cabbage (*Brassica rapa* and *Brassica oleracea*) cultivated by conventional and organic farmers in this region (Figure 4.1c). Organic cabbage fields were not available for this study. Therefore, we could only differentiate between organic and conventional management for bean, potato, and radish. For both potato and bean, six fields were selected, each with three conventional and three organic sites. For radish, five conventional and three organic field sites were used, and for cabbage only five conventional sites were available. The field sites were distributed over the entire Haean catchment, some of which were located in the center, and some upon steep slopes at the forest edges. They represent the variety of different field sizes, hillslopes, and soil

conditions of the mountainous agricultural land in this region. For all crops investigated, the fields are cultivated by a ridge-furrow system covered with plastic film (plastic mulch). The spacing between two ridges is approximately 70 cm, and the ridge height is about 15 cm. The plastic film covers approximately 50% of the soil surface.

4.2.2 Erosion simulation with the Revised Universal Soil Loss Equation

We used the Revised Universal Soil Loss Equation (RUSLE) (Renard *et al.*, 1997) to calculate the average annual soil erosion rates for the 25 selected field sites, and to compare the effects of the four row crops and the applied farming systems. RUSLE is a widely used empirical soil erosion model founded on the Universal Soil Loss Equation (USLE) described by Wischmeier and Smith (1978) (Renard *et al.*, 1997). The factor approach of the model allows us to identify and directly compare the effects of crop management on soil erosion. RUSLE provides the possibility to enter multiple parameters that can be measured in the field, to describe the crop conditions and surface properties associated with a specific management practice. RUSLE calculates the average annual erosion from a given field slope as follows (Renard *et al.*, 1997):

$$A = R \cdot K \cdot L \cdot S \cdot C \cdot P \quad (1)$$

where A is the average annual soil loss ($\text{t ha}^{-1} \text{ yr}^{-1}$), R the rainfall and runoff erosivity factor ($\text{MJ mm ha}^{-1} \text{ h}^{-1} \text{ yr}^{-1}$), K the soil erodibility factor ($\text{t h MJ}^{-1} \text{ mm}^{-1}$), L and S the slope length and slope steepness factors (-), C the cover-management factor (-), and P the support practice factor (-). The calculation of the individual factors requires different input parameters, which were obtained from field measurements on the 25 sites in 2009. The methods of data collection and the calculation procedures are described in the following sections.

4.2.2.1 Rainfall and runoff erosivity factor (R)

The R -factor quantifies the effect of raindrop impact on soil erosion and reflects the amount and rate of runoff associated with the rainfall (Wischmeier and Smith, 1978, Renard *et al.*, 1997). The R -factor for a given year is computed from recorded weather station data sets by adding the total kinetic energy multiplied by the maximum 30-minute intensity of erosive rainstorm events (EI_{30}) within that year (Renard *et al.*, 2011). The total energy of a rainstorm event is the sum of the rainfall energies of all individual recording time intervals. The energy for each time interval is the product of the unit energy and the rainfall amount within that interval. The unit energy is calculated as follows (Brown and Foster, 1987):

$$e = 0.29 \cdot [1 - 0.72 \cdot \exp(-0.05 \cdot i)] \quad (2)$$

where e is the unit energy ($\text{MJ ha}^{-1} \text{ mm}^{-1}$), and i the rainfall intensity (mm h^{-1}) for each time interval.

For the Haean catchment, two types of weather station data sets were available, providing a total of 13 years of recorded precipitation and temperature data. The first data set was derived from a weather station located in the center of the Haean catchment (Figure 4.1c), which recorded precipitation and temperature from January 1999 to May 2009 with 1 hour resolution. The second data set was derived from nine weather stations installed in May 2009 in Haean (Figure 4.1c) recording weather data with 30 minutes resolution until December 2011. Due to technical problems, only four of the weather stations in 2010, and only two weather stations in 2011 could be used for the R -factor calculations. We developed an algorithm by using the R programming language that automatically identifies the erosive events and calculates R -factor and rainfall erosivity for every half-month period from the weather station data sets. According to Renard *et al.* (1997), small rain showers with less than 12.7 mm of rain and rainfall intensities of less 25.4 mm h^{-1} were excluded from the calculations, and periods with six hours of less than 1.27 mm of rainfall were used to divide one rain

event into two (Meusburger *et al.*, 2012b). Precipitation occurring at temperatures of less than or equal to 0.0°C were considered as snow, or solid precipitation, and hence, were excluded from calculations (Leek and Olsen, 2000, Meusburger *et al.*, 2012b).

By using this algorithm (performed by RStudio ver. 0.95.258), we calculated the *R-factors* for the years 1999 to 2011 and the temporal distribution of the rainfall erosivity in half-month periods, which was required for the calculation of the *C-factor* (see section 4.2.2.4). Subsequently, we corrected the *R-factors* for 1999 to 2009 data sets, as the maximum 30-minute intensity was underestimated due to the lower resolution. Therefore, we calculated the rainfall erosivity for the 2009 to 2011 data sets, first by using the original 30 minutes resolution, and second by using aggregated 1 hour resolution data sets. We correlated the calculated erosivity values and derived the slope of the regression line, which was used as a correction factor for the data sets of 1999 to 2009. Finally, the average annual *R-factor* was calculated as the mean of the 13 years individual *R-factors*.

4.2.2.2 Soil erodibility factor (*K*)

The *K-factor* represents the effects of soil properties and soil profile characteristics on soil erosion (Renard *et al.*, 2011). It is obtained from the soil erodibility nomograph of Wischmeier *et al.* (1971) as a function of the soil texture (content of clay, silt, sand, and very fine sand), the organic matter content, and the soil structure and permeability. An algebraic approximation of the nomograph is given by the following equation for those cases where the silt content of the soil does not exceed 70% (López-Vicente *et al.*, 2008, modified after Renard *et al.*, 1997):

$$K = 0.1317 \cdot \left[0.00021 \cdot (12 - OM) \cdot M^{1.14} + 3.25 \cdot (s - 2) + 2.5 \cdot (p - 3) \right] / 100 \quad (3)$$

where *K* is the soil erodibility factor (t h MJ⁻¹ mm⁻¹), *OM* the content of organic matter (%), *M* the product of the primary particle size fractions (-), *s* the soil structure code (-), and *p* the soil permeability code (-). The factor 0.1317 is used for unit conversion to SI units (Foster *et al.*, 1981). *M* is calculated as (modified after Renard *et al.*, 1997):

$$M = (silt + vfs) \cdot (silt + sand) \quad (4)$$

where *silt* is the percentage of silt (0.002 - 0.05 mm) (%), *vfs* the percentage of very fine sand (0.05 - 0.1 mm) (%), and *sand* the percentage of sand (0.05 - 2 mm) (%).

We took samples of top soils (0 to 30 cm depth) of the 25 sites (mixed samples from five sampling locations distributed over the field) and determined soil texture (wet sieving for sand, and laser particle measurement for silt and clay), and the organic matter contents in the laboratory. The soil structure code was estimated from field observations. The dominant portion of the dryland fields in the study area is characterized by structureless, sandy top soil horizons, and was, therefore, set to 1 (very fine granular). Profile descriptions and tracer experiments on dryland fields in the study area indicated a relatively low infiltration capacity of most of the subsoil horizons. The permeability code for all 25 fields was therefore set to 4 (moderate to slow). By using the analyses data of the soil samples and the assumptions for *s* and *p*, we calculated the *K-factor* with equation (3). Potential seasonal variations of the *K-factor* due to soil freezing, soil water, and soil surface conditions (López-Vicente *et al.*, 2008) were not considered in this study.

4.2.2.3 Slope length and steepness factors (*L* and *S*), and support practice factor (*P*)

The *L-factor* and the *S-factor* describe the effect of the field topography on soil erosion. The *L-factor* considers the higher erosion potential with increasing slope length and the *S-factor* reflects the influence of the slope steepness on erosion (Renard *et al.*, 1997). The *L-factor* is calculated as (modified after Renard *et al.*, 1997):

$$L = (3.2808 \cdot \lambda / 72.6)^{\beta / (1 + \beta)} \quad (5)$$

where L is the slope length factor (-), λ the slope length (m), and β the ratio of rill erosion to interrill erosion, which itself is calculated as (Renard *et al.*, 1997):

$$\beta = (\sin \theta / 0.0896) / [3.0 \cdot (\sin \theta)^{0.8} + 0.56] \quad (6)$$

where θ is the slope angle ($^{\circ}$). The factor 3.2808 in equation (5) is used to insert slope length as SI unit. The S -factor is calculated as (modified after Renard *et al.*, 1997):

$$S = 10.8 \cdot \sin \theta + 0.03 \quad \theta < 5.14^{\circ} \quad (7)$$

$$S = 16.8 \cdot \sin \theta - 0.50 \quad \theta \geq 5.14^{\circ} \quad (8)$$

where S is the slope steepness factor (-), and θ the slope angle ($^{\circ}$).

The P -factor reflects the positive impact of management through the control of runoff by practices such as contour tillage, strip cropping, terracing, or subsurface drainage etc. (Renard *et al.*, 2011). The ridge-furrow cultivation system on the dryland fields in South Korea can be regarded as contouring support practice. The effectiveness for a given ridge height is controlled by the field slope steepness and the steepness along the furrows when ridges are not parallel to the contours. First, the P -factor for on-grade contouring (P_0) is calculated and subsequently adjusted for off-grade contouring (Renard *et al.*, 2011). For the high ridges (approximately 15 cm) on Korean row crop fields, P_0 is calculated as (modified after Renard *et al.*, 1997):

$$P_0 = 18051 \cdot (0.0797 - \sin \theta)^4 + 0.27 \quad \sin \theta < 0.0797 \quad (9)$$

$$P_0 = 10.24 \cdot (\sin \theta - 0.0797)^{1.5} + 0.27 \quad \sin \theta \geq 0.0797 \quad (10)$$

$$P_0 = 1.0 \quad \sin \theta \geq 0.2516 \quad (11)$$

where P_0 is the on-grade contouring support practice factor (-), and θ the slope angle ($^{\circ}$). The adjusted contouring P -factor is calculated as (modified after Renard *et al.*, 1997):

$$P = P_0 + (1 - P_0) \cdot (\sin \theta_f / \sin \theta)^{0.5} \quad (12)$$

where P is the off-grade contouring P -factor (-), P_0 the on-grade contouring P -factor (-), θ_f the slope angle along the furrows, and θ the average slope angle of the field ($^{\circ}$).

For the highly complex terrain found in the study area, where fields can have various flow paths in different directions, it is difficult to identify the representing hill slope profiles and to determine slope lengths and the slope angles of the field and along the furrows. Motivated by the work of Cochrane and Flanagan (2003), we developed an algorithm using the R programming language that automatically identifies all possible flow paths within one field site and extracts the mean slope length and slope angle from three provided ArcGIS raster grids of a given field site. From an available 30 m resolution digital elevation model of the study area, we developed a 0.25 m resolution DEM by using bilinear interpolation (performed by ArcGIS ver. 10.0), from which we extracted individual digital terrain models for the 25 field sites. Based on our field observations in 2009 and from photographs taken from all field sites, we created 25 additional digital terrain models, which included the height, dimension, and orientation of the ridges and furrows. For each of those 50 DTMs, we developed three raster grids, which were used for the R algorithm: a depression-filled elevation raster, a flow direction raster, and a flow accumulation raster (performed by ArcGIS ver. 10.0). The depression-filled elevation raster contains the elevation model of the field site without topographical sinks. The flow direction raster contains for each cell the information to which neighboring cell water would flow. The flow accumulation raster contains for each cell the number of cells that would drain into it, and is used to identify the starting cells of flow paths (cell value equals 0). We extracted the mean slope length and slope angle by using the R algorithm (performed by RStudio ver. 0.95.258) for the raster grids without ridges and furrows, and calculated L -factor and

S-factor for the 25 fields with equation (5) to (8) and P_0 with equations (9) to (11). Subsequently, we used the same algorithm for the raster grids including ridges and furrows to extract the mean slope angle along the furrows, which was used to calculate the off-grade contouring *P-factor* with equation (12). Finally, we changed the *P-factor* to 1.0 for those field sites, for which the slope length considerably exceeded the critical slope length according to the slope steepness, as described by Wischmeier and Smith (1978). When slope length increases a critical length, ridge breakovers can occur resulting in a higher erosion rate that makes contouring ineffective (Wischmeier and Smith, 1978).

4.2.2.4 Cover-management factor (*C*)

The cover-management factor represents the effects of crop and management practices on soil erosion and is used to compare the relative impacts of the different crops and management types (Renard *et al.*, 1997). It includes the impact of previous management, the soil surface protection of vegetation cover, and the reduction in erosion due to surface cover and surface roughness (Renard *et al.*, 1997). Because these conditions change over the course of the year, a time-varying *C-factor* approach is used in RUSLE based on half-month time steps (Renard *et al.*, 1997). For each of the half-month periods within the year, a soil loss ratio (*SLR*) is calculated, for which the conditions are assumed to remain constant, and is weighted by the percentage of rainfall erosivity associated with that period (see section 2.2.1) to obtain the annual *C-factor* (modified after Renard *et al.*, 1997):

$$C = (SLR_1 \cdot EI_1 + SLR_2 \cdot EI_2 + \dots + SLR_{24} \cdot EI_{24}) / 100 \quad (13)$$

where *C* is the cover-management factor (-), SLR_i the soil loss ratio for the half-month period *i*, and EI_i the percentage of the total rainfall erosivity (EI_{30}) within the half-month period *i* (%).

The soil loss ratio for each half-month period is calculated as the product of five subfactors (Renard *et al.*, 1997):

$$SLR = PLU \cdot CC \cdot SC \cdot SR \cdot SM \quad (14)$$

where *SLR* is the soil loss ratio (-), *PLU* the prior land use subfactor (-), *CC* the canopy cover subfactor (-), *SC* the surface cover subfactor (-), *SR* the surface roughness subfactor (-), and *SM* the soil moisture subfactor (-).

The prior land use subfactor is calculated as (modified after Renard *et al.*, 1997 and López-Vicente *et al.*, 2008):

$$PLU = C_f \cdot C_b \cdot \exp\left[-\left(c_{ur} \cdot 8.9219 \cdot B_{ur}\right) + \left(c_{us} \cdot 8.9219 \cdot B_{us} / C_f^{c_{uf}}\right)\right] \quad (15)$$

where *PLU* is the prior land use subfactor (-), C_f the surface-soil consolidation factor (-), C_b represents the relative effectiveness of subsurface residue in consolidation, B_{ur} is the mass density of live and dead roots in the upper 2.54 cm of soil (g m^{-2}), B_{us} is the mass density of incorporated surface residue in the upper 2.54 cm of soil (g m^{-2}), c_{ur} and c_{us} are coefficients indicating the impact of the subsurface residues, and c_{uf} represents the impact of soil consolidation on the effectiveness of incorporated residue. The factor 8.9219 is used to insert root and residue mass density as SI units. The soil consolidation factor for freshly tilled soil is 1.0 and decreases to 0.45 when soil is left undisturbed for seven years (Renard *et al.*, 1997). Because in the study area fields are usually tilled every year, soils are disturbed by harvest activities, and short-term consolidation rates were not known, we used a value of 1.0 for all 24 half-month periods throughout the year. For the coefficients C_b , c_{ur} , c_{us} , and c_{uf} , the values 0.951, 0.00199, 0.000416, and 0.5 were used, respectively (Renard *et al.*, 1997).

The canopy cover subfactor is calculated as (modified after Renard *et al.*, 1997):

$$CC = 1 - F_c \cdot \exp(-0.1 \cdot H \cdot 3.2808) \quad (16)$$

where *CC* is the canopy cover subfactor (-), F_c the fraction of the land area covered by canopy (-), and *H* the distance that raindrops fall after striking the canopy (m), calculated as (modified after USDA, 2008):

$$H = H_b + 0.29 \cdot (H_t - H_b) \quad (17)$$

where H is the raindrop fall height (m), H_b the height to the bottom of the canopy (m), and H_t the height to the top of the canopy (m), assuming a round canopy shape and a uniformly distributed canopy density. The factor 3.2808 in equation (16) is used to insert H as SI unit. The height to the bottom of the canopy was assumed to be 0.15 m (ridge height).

The surface cover subfactor is calculated as (modified after Renard *et al.*, 1997):

$$SC = \exp\left\{-b \cdot S_p \cdot [0.24 / (0.3937 \cdot R_u)]^{0.08}\right\} \quad (18)$$

where SC is the surface cover subfactor (-), b an empirical coefficient, which is 0.035 for typical cropland erosion conditions (Renard *et al.*, 1997), S_p the percentage of land area covered by surface cover (%), and R_u is the surface roughness (cm).

The surface roughness subfactor is calculated as follows (modified after Renard *et al.*, 1997):

$$SR = \exp[-0.66 \cdot (0.3937 \cdot R_u - 0.24)] \quad (19)$$

where SR is the surface roughness subfactor (-), and R_u the surface roughness (cm). The factor 0.3937 in equation (18) and (19) is used to insert surface roughness as SI unit.

The soil moisture subfactor is only used in the Northwest Wheat and Range Region of the USA (Renard *et al.*, 2011) and was therefore set to 1.0 for this study.

To obtain the relevant crop and management parameters for calculating the soil loss ratios for each half-month period, we measured the development of biomass density, cover, and canopy height for the four major crops and the associated weeds during the growing season of 2009 on four of the 25 sites (site 03, 07, 16, and 18). At three (radish and cabbage) and four (bean and potato) different dates between planting and harvest, we sampled the crops and weeds from nine subplots, separated the different plant parts of crops (roots with radishes or potatoes, stems or cabbage cores, leaves, seeds, and dead plant material) and weeds (below-ground, and above-ground), and determined the dry biomass of the different components. Based on the number of crops and weeds per m², we calculated the average biomass density of each component. From photographs of the different subplots taken on the day of sampling, we estimated the associated crop cover, weed cover, and the canopy height for the different sampling dates. We created growth charts of the four major crops, including weeds, for biomass density (separated by plant components), canopy cover, and canopy height. The growth charts were completed by biomass, cover, and height measurements of the four sites before harvest. From three subplots, we further sampled all crops and weeds, separated the different plant parts, determined their biomass densities, and estimated crop cover, weed cover, and canopy height either in the field, or from additional photographs. Subsequently, we adjusted those growth charts to fit to the real planting and harvest dates, as the last biomass sampling was carried out before harvest.

On the remaining 21 field sites including organic and conventional farming, we also sampled all crops and weeds from three subplots before harvest, and determined the biomass density of the different plant parts. We additionally estimated crop cover, weed cover, and canopy height from three subplots in the field, and from additional photographs. Based on this data, we calculated the average yield, cover, and canopy height of all four row crops and both farming systems at harvest. The four base growth charts were finally adjusted to those values, resulting in growth charts containing the crop and weed biomass density separated by plant parts, crop cover, weed cover, and canopy height for conventional and organic bean, potato, radish, as well as for conventional cabbage production.

The associated soil loss ratios for the 24 individual half-month periods of 2009 were then calculated with the equations (14) to (19) underlying the following assumptions. Because farmers did not cultivate their crops according to fixed rotation systems, we had no information of potential residual biomass and cover from previous crops. To compare

the farming system for the individual crops, we decided to focus only on the current growing season without considering effects of previous years. Prior to planting, it was therefore assumed that fields did not contain plastic covers, and that the biomass density of roots and residues, as well as crop cover, surface cover and canopy height, were zero. The surface roughness R_u was estimated as 1.65 cm, by comparing soil surface photographs of dryland fields in the study area to roughness plot photographs by Renard *et al.* (1997). During the growing season, between planting and harvest, only root biomass density of the weeds is relevant (assuming 10 cm rooting depth), because weeds are growing in the furrows, whereas crop roots are only concentrated in the ridges, which are covered by plastic film. The application of plastic mulch provides 50% surface cover for the entire growing season, but surface roughness is also reduced to 0.83 cm, assuming that the roughness of the plastic sheet covering 50% of the soil surface is 0.0 cm. Canopy cover is the combination of crop cover and the cover of weeds, assuming that weeds cover both, ridges and furrows, and crops cover primarily ridges. Canopy cover of crops is reduced by the amount of dead biomass (as the ratio of dead biomass to total biomass), because dead plant parts fall to the ground, become residues, and were therefore add to the surface cover. After harvest, all crop biomass dies and becomes residue, and the canopy cover is then only determined by weed cover. The canopy height was set to zero. The amount of biomass density remaining in the field depends on the crop type. For bean, the crop yield accounts only for a relatively small fraction of the plant, and almost the whole biomass remains on the field, and for potato, only the potatoes are harvested, whereas for radish, most of the biomass is harvested, and for cabbage, everything except the roots and the outer leaves (approximately 15% of the leaf biomass) is harvested. The density of incorporated root and residue biomass after harvest, as well as the percentage of canopy and surface cover depends on the degree of soil disturbance at harvest. Bean and cabbage can be harvested above the soil surface without plastic removal and soil disturbance. The harvesting of potato requires the removal of the plastic film and a complete disturbance and mixing of the soil in the ridges (50% of the field surface-soil). Also radish is harvested by the removal of at least 50% of the plastic film and soil disturbance and mixing of the underlying ridges (25% of the field surface-soil). However, the different farmers in the study area use different techniques and machinery for harvesting their crops, which can produce different levels of disturbance and mixing. To include the variety of those different harvesting procedures, two scenarios were simulated: a low disturbance scenario representing the minimum required disturbance for manual harvest (described above), and a high disturbance scenario representing a maximum disturbance such as that created by using machinery. For bean and cabbage, 50% of the plastic is removed and 25% of the surface-soil is mixed. For potato, 100% of the plastic is removed and 100% of the surface-soil is mixed, and for radish 100% of the plastic is removed and 50% of the surface-soil is mixed. According to those ratios of plastic removal and soil surface-mixing, the canopy cover and surface cover was reduced, surface roughness was increased, and the biomass density of incorporated roots and residue was calculated based on the remaining biomass density of dead crops and weeds. The average depth of disturbance was assumed to be 10 cm, which was estimated from field observations. For the periods after harvest, it was assumed that the cover and biomass density status remained stable. Additional growth of weeds after harvest and the decomposition of residue could not be included in this study because we did not have data of growth and decomposition rates after the cropping period.

In order to account for different schedules of planting and harvesting over different years, we simulated two additional scenarios, one scenario representing an early planting year by shifting all calculated *SLR* values to the previous half-month period, and one scenario representing a late planting year shifting all *SLR* values to the next half-month period. Subsequently, we calculated the *C-factor* for the major crops, for conventional and organic farming, and for each of the 13 years of available rainfall data and each of the scenarios by using equation (13). Finally, we

calculated the average annual *C-factor* for conventional and organic bean, potato, radish, as well as conventional cabbage, as the mean *C-factor* over all years and scenarios.

4.2.2.5 Calculation of soil erosion rates

The average annual soil erosion rates associated with the four major crops and two different farming systems were calculated according to equation (1) by using the average annual *C-factors* and combining them with all 25 field sites. Using the average annual *R-factor*, and the field individual factors *K*, *L*, *S* and *P*, we calculated the average annual erosion rate for conventional and organic bean, potato, radish, as well as conventional cabbage, for each field site.

4.2.3 Model plausibility

In order to verify the simulated erosion rates with RUSLE, the soil loss for two additional field sites, M1 and M2 (Figure 4.1c) were calculated, where sediment was measured for a one month period during the monsoon season of 2010. Between the 5 July and 9 August 2010, the amount of eroded sediment was measured with three runoff collectors designed according to Bonilla *et al.* (2006) within both field sites. The amount of rainfall was continuously measured with two rain gauges, soil samples of both fields were analyzed, and the cover and dimensions of the crop (*Solanum tuberosum*) canopy were measured. Additionally, we developed digital terrain models with 0.25 m resolution of both fields, both with and without ridges and furrows. Based on this information, we calculated the individual RUSLE factors and the soil loss rates for both fields for the observation period from 5 July to 9 August 2010, using the methods described above. The calculated soil loss rate was then compared to the observed erosion.

Because the observation period in 2010 was relatively short and only two field sites were measured, we additionally compared the average annual erosion rates computed with RUSLE to the long-term annual erosion rates estimated using the fallout radionuclide caesium-137 (¹³⁷Cs) for two sloping dryland fields in the Haeen catchment (Meusburger *et al.*, 2012a). One site was located in an area of the catchment, which was recently converted from forest to farmland, and the other site was characterized by long-term agricultural use. Soil core samples were taken from three locations within each site and were analyzed for ¹³⁷Cs activity. Fallout ¹³⁷Cs was generated as a product of nuclear weapons tests between the mid 1950s and the early 1970s (Meusburger *et al.*, 2012a). It is redistributed in soils by processes like erosion and deposition, and can be used for assessing the amount of soil loss (Mabit *et al.*, 2008).

4.3 Results and discussion

4.3.1 Rainfall and runoff erosivity factor (*R*)

As expected, the rainfall and runoff erosivity for the period May 2009 to December 2011, calculated on the basis of 30 minutes resolution records, was higher than for the aggregated 1 hour resolution data sets (Figure 4.2). Both data sets exhibited a high linear correlation ($R^2 = 0.998$). The slope of the regression line was 1.391, which was used as correction factor for rainfall erosivity calculated on the basis of the 1 hour resolution records between January 1999 and May 2009. The resulting corrected rainfall erosivity factor for the years 1999 to 2011 is shown in Figure 4.3. It was estimated to be highly variable over the 13 year period with a maximum in 2006 and minima in the years 2000 and 2002. The erosive rain events are concentrated in the monsoon season between June and September, but the temporal distribution within the individual years shows very different seasonal rainfall patterns (Figure 4.4). In the years 2001, 2009, and 2011, erosive rain events were found relatively early in June and July, whereas in the years 2000, 2003, 2007, and 2010, most of the erosive rainfall was calculated for August and September. In the years 1999 and 2006, almost all

of the erosive rain events were concentrated within one single month, whereas in the years 2004 and 2005, the erosive rainfall is spread over a relatively long period from June to September.

The average annual *R-factor* for the Haean catchment is 6599.1 MJ mm ha⁻¹ h⁻¹ yr⁻¹, which is about 50% higher than the *R-factor* found in previous studies of this region (Chuncheon) (Jung *et al.*, 1983, Park *et al.*, 2000). This might be as a result of recent extreme years, for example that of 2006 with Typhoon Ewiniar, which saw the highest daily rainfall recorded in Korea (Park *et al.*, 2011), and which could not be considered by these authors. These studies, additionally, used hourly precipitation data with limited utility to calculate the actual rainfall erosivity (Park *et al.*, 2000, Lee and Heo, 2011). In another study, Lee and Heo (2011) presented an *R-factor* for Chuncheon of 6076 MJ mm ha⁻¹ h⁻¹ yr⁻¹ based on long-term high resolution rainfall data. It indicates that our calculations are plausible, although only 13 years of weather station data were available in the Haean catchment, instead of the 20 to 25 years recommended by Wischmeier and Smith (1978).

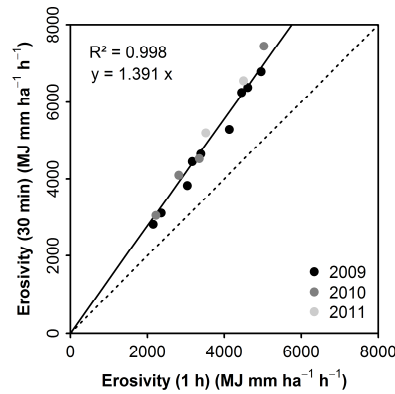


Figure 4.2 Correlation between rainstorm erosivity calculated on the basis of 1 hour and 30 minutes resolution rainfall records of nine weather stations in the Haean catchment from May 2009 to December 2011. The solid line shows the line of the linear regression through the origin, and the 1:1 line (dotted) is included as reference

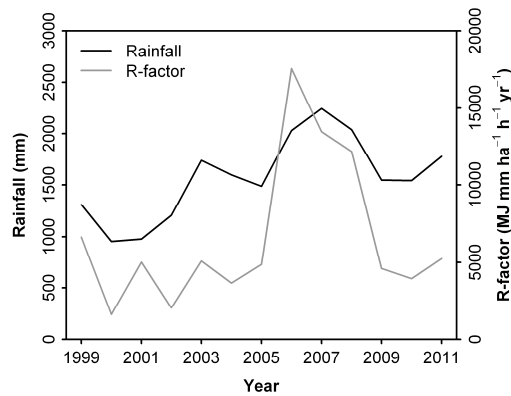


Figure 4.3 Annual rainfall and *R-factor* for the Haean catchment for the years 1999 to 2011

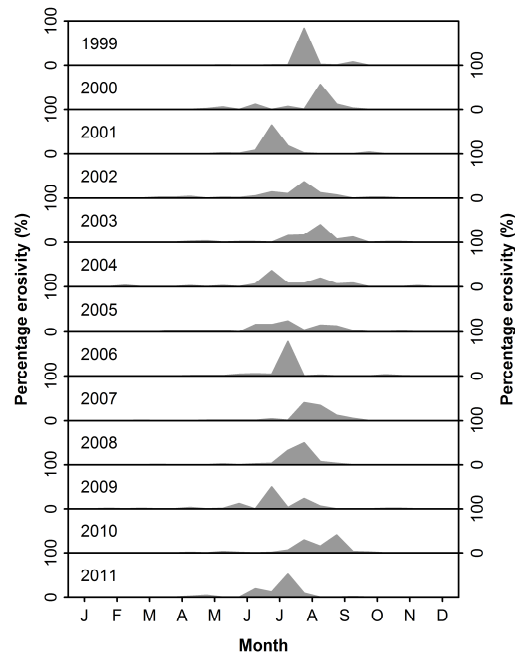


Figure 4.4 Temporal distribution of rainstorm erosivity (percentage of the half-month period erosivity) within the individual years from January to December for 1999 to 2011

4.3.2 Soil erodibility factor (*K*)

The soils of the 25 field sites selected for this study were characterized by a high sand content (41% to 90%) and a low amount of organic matter (0.3% to 2.2%) resulting in an average soil erodibility of $0.0211 \text{ t h MJ}^{-1} \text{ mm}^{-1}$ (Table 4.1). Soil texture was predominantly sandy loam or loamy sand. The minimum *K-factor* was calculated for site 06 ($0.0092 \text{ t h MJ}^{-1} \text{ mm}^{-1}$), which had the highest sand content among the 25 fields. The maximum *K-factor* was calculated for site 2 ($0.0367 \text{ t h MJ}^{-1} \text{ mm}^{-1}$), which was characterized by a finer texture (loam) compared to the other field sites.

The average *K-factor* for fields under conventional farming management systems (chemical usage) was $0.0219 \text{ t h MJ}^{-1} \text{ mm}^{-1}$, and $0.0199 \text{ t h MJ}^{-1} \text{ mm}^{-1}$ for the organic fields. The lower calculated soil erodibility for the organic fields was primarily due to higher sand and lower silt contents. The average organic matter content was slightly higher for soils of conventionally managed fields (1.1%) than for organic fields (0.7%). The high variability of texture and organic matter within conventional and organic fields indicate that the different erodibility factors result from the spatial variation of soil properties within the study area, and not from the farming systems employed, as described by Fleming *et al.* (1997). Organic farming is still a relatively new management practice in the study area. The positive effects on soil properties, for example, the increased infiltration capacity and improved soil stability by the addition of organic matter (Erhart and Hartl, 2010), may only become visible after many years of organic management.

Table 4.1 Soil characteristics (organic matter and texture) and topography (slope angle and slope length) of the 25 field sites with the calculated *K*-factors, *L*-factors, *S*-factors, and contouring *P*-factors for the Revised Universal Soil Loss Equation

Site	Area (m ²)	Org. matter (%)	Clay (%)	Silt (%)	Sand (%)	<i>K</i> -factor (t h MJ ⁻¹ mm ⁻¹)	Slope angle (°)	Slope length (m)	<i>L</i> -factor (-)	<i>S</i> -factor (-)	<i>P</i> -factor (-)
01	2246	2.2	5.2	18.3	76.5	0.0155	7.0	47.7	1.525	1.539	1.000
02	6228	1.1	16.9	41.9	41.2	0.0367	3.6	36.4	1.244	0.701	0.949
03	3056	0.6	3.6	17.1	79.3	0.0219	4.6	21.8	0.992	0.898	0.742
04	5787	1.6	9.3	26.6	64.1	0.0251	8.6	106.5	2.479	2.000	1.000
05	5447	1.1	4.9	21.0	74.1	0.0225	1.9	16.7	0.911	0.393	0.994
06	5712	0.3	1.6	8.3	90.1	0.0092	14.9	57.1	1.845	3.828	1.000
07	11347	0.8	2.2	12.4	85.3	0.0153	3.7	54.0	1.489	0.729	0.858
08	10536	2.1	5.6	22.1	72.4	0.0230	0.0	15.7	0.996	0.036	1.094
09	1767	1.3	6.2	23.0	70.9	0.0246	7.5	24.4	1.056	1.687	0.730
10	4878	0.4	4.1	13.0	82.8	0.0155	0.0	11.3	0.998	0.031	1.049
11	13764	1.2	5.0	20.6	74.4	0.0220	5.6	124.6	2.440	1.153	1.000
12	6452	0.7	5.4	21.1	73.5	0.0262	5.8	35.5	1.280	1.207	0.832
13	2711	1.3	7.6	25.0	67.3	0.0247	5.1	31.3	1.188	0.984	0.901
14	5643	1.3	6.4	23.5	70.1	0.0250	10.9	45.6	1.553	2.683	1.000
15	1143	0.3	2.8	13.3	83.8	0.0173	0.0	6.3	1.000	0.030	1.000
16	10981	0.4	3.4	16.6	80.0	0.0212	6.9	50.7	1.572	1.509	1.000
17	72	0.3	2.8	15.9	81.3	0.0204	12.0	4.7	0.380	3.005	1.009
18	3779	0.8	3.3	15.3	81.4	0.0180	6.4	37.1	1.318	1.369	1.148
19	3967	0.7	2.5	13.6	83.8	0.0182	2.5	24.6	1.041	0.497	1.088
20	2408	1.2	6.3	23.6	70.1	0.0243	10.1	22.0	0.996	2.452	0.999
21	14843	1.0	4.1	16.7	79.2	0.0181	11.8	44.5	1.540	2.923	1.000
22	16578	1.3	6.4	19.8	73.9	0.0204	11.4	52.1	1.693	2.816	1.000
23	1913	0.4	4.3	18.7	77.0	0.0216	0.0	9.0	1.000	0.030	1.000
24	1978	0.4	3.6	17.0	79.4	0.0201	0.0	10.6	1.000	0.030	1.000
25	11652	1.7	5.7	21.6	72.7	0.0217	10.6	68.9	1.990	2.584	1.000
Mean	6196	1.0	5.2	19.4	75.4	0.0211	6.0	38.4	1.341	1.405	0.976

4.3.3 Slope length and steepness factors (*L* and *S*), and support practice factor (*P*)

The 25 field sites were highly variable in their slope length and steepness (Table 4.1) representing the topographical variability of the agricultural land in the study area (see section 4.2.1). The slope length varies from 4.7 to 124.6 m, resulting in *L*-factors between 0.380 and 2.479. The average slope length among all 25 fields was 38.4 m and the average *L*-factor was 1.341. Slope steepness ranged from 0.0° (sites 08, 10, 15, 23, and 24) to 14.9° (site 06). The associated *S*-factors were 0.030 and 3.828, respectively. The average slope steepness among all 25 field sites was 6.0° resulting in an average *S*-factor of 1.405. The calculated slope angle along the furrows ranged from 0.9° to 12.9°. For most of the sites, the slope along the furrows was smaller than the average steepness of the hill slope. However, the slope angle along the furrows was still relatively high, or the slope length exceeded the critical length, which resulted in *P*-factors close to 1 for most of the sites. The smallest *P*-factor was calculated for site 09 (0.730). For some field sites, the slope calculation for the ridge-furrow system resulted in higher slope angles along the furrows compared to the steepness of the hill-slope resulting in *P*-factors larger than 1. The highest *P*-factor was calculated for site 18 (1.148). The average *P*-factor among all 25 field sites was 0.976. The high *P*-factors show that the contouring control effect provided by the ridge-furrow system in the study area is not very effective, because the ridges are generally not oriented along the contours.

4.3.4 Cover-management factor (C)

The growth charts of the four major dryland row crops in 2009 show a highly variable development of biomass, cover, and canopy height (Figure 4.5). The main difference is the duration of the growing period between bean (157 days, planted on 27 May and harvested on 31 October 2009), potato (123 days, planted on 30 April and harvested on 31 August 2009), radish (82 days, planted on 2 June and harvested on 23 August 2009) and cabbage (61 days, planted on 20 May and harvested on 20 July 2009). The highest leaf biomass at the end of the individual growing periods was measured for bean (253.3 g m^{-2}) and cabbage (134.0 g m^{-2}), resulting in a higher crop cover compared to potato and radish. For potato and radish, the highest portion of crop biomass is represented by the below-ground parts, and for potato, approximately after the first half of the growing period, we observed a strong decrease in leaf biomass and crop cover. At the same time, weed biomass and weed cover increased until the end of the growing period to 184.8 g m^{-2} and 44%, respectively. For the other three crops, weed biomass and cover remained negligible compared to crop biomass and cover throughout the growing season. The canopy height curves show a similar shape to the curves of crop cover development. Radish and cabbage have their maximum canopy height at the end of the growing period. For bean and potato, canopy height is decreasing at the end of the growing period.

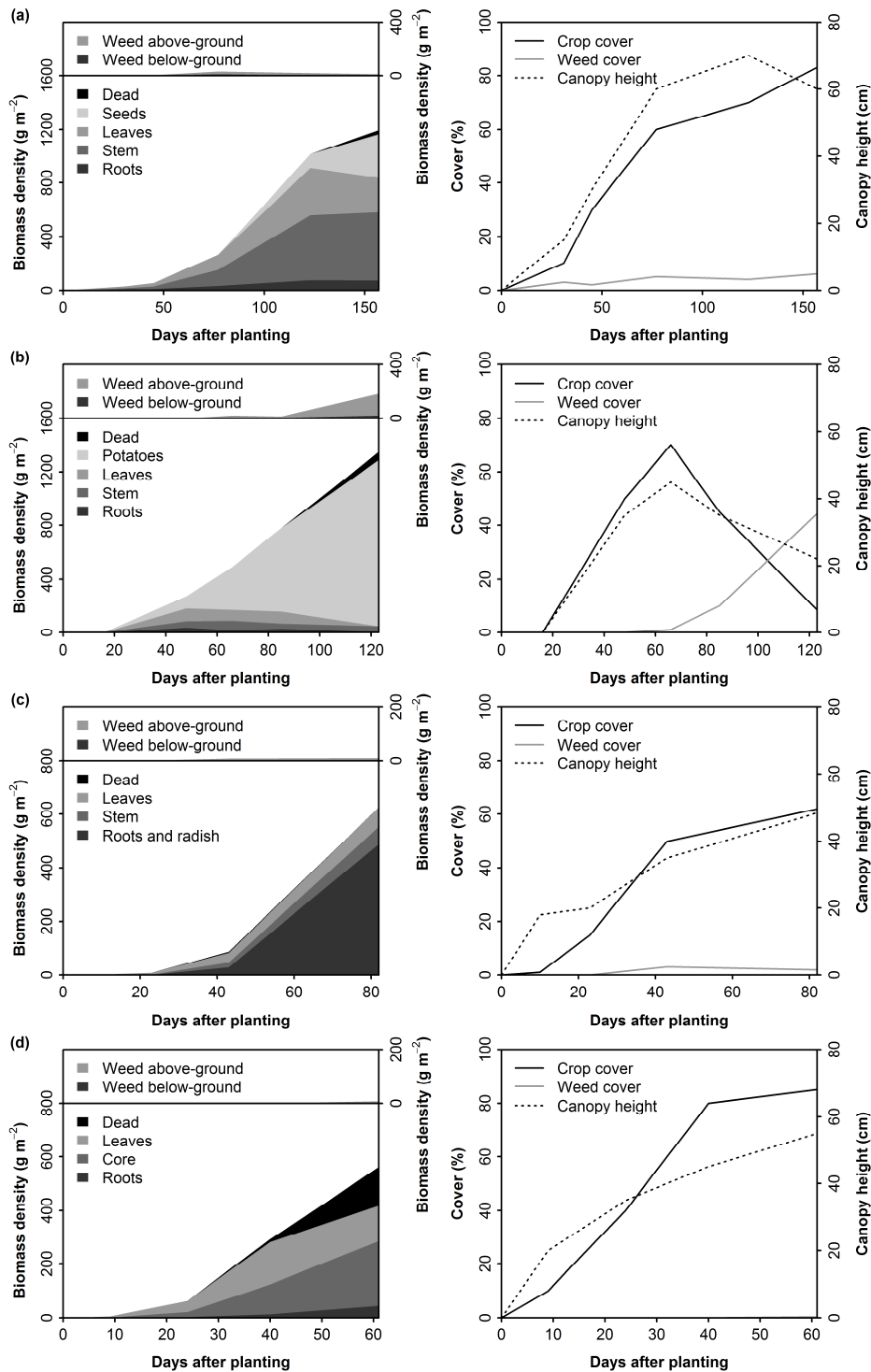


Figure 4.5 Growth charts of the four major row crops, bean (a), potato (b), radish (c), and cabbage (d) with crop and weed biomass density (left), and crop cover, weed cover, and canopy height (right). The lower segment of the biomass density plot shows the development of the different crop components and the upper segment shows the development of the associated weeds

The yield measurements of the 25 fields before harvest show a higher total crop biomass density for conventional management compared to organic management for bean and potato (Figure 4.6a). The mean crop biomass density for conventional farming for bean and potato was 1205.5 g m⁻² and 1976.0 g m⁻², respectively. The mean crop biomass density for organic farming was 995.3 g m⁻² and 1270.9 g m⁻², respectively. In contrast, radish shows a slightly higher mean crop biomass for organic farming (669.7 g m⁻²) compared to conventional farming (568.0 g m⁻²). The mean crop

cover at harvest for radish was also higher for organic (71.2%) than for conventional farming (61.7%) (Figure 4.6c). However, the crop cover for potato was much higher for conventional (26.8%) than for organic farming (12.1%). Bean showed approximately the same values under both management systems. Weed biomass and cover was consistently higher for organic than conventional farming, except for bean, which shows similar values for weed development under both farming systems (Figure 4.6b and 4.6d). For potato, the mean weed biomass density for conventional and organic farming was 96.1 g m^{-2} and 127.2 g m^{-2} , respectively. Mean weed cover for conventional and organic potato was 21.3% and 43.0%, respectively. Radish showed a high difference in weed biomass densities between conventional (19.1 g m^{-2}) and organic (127.1 g m^{-2}) farming methods. Weed cover for conventional radish farming was 3.3%, and 14.0% for organic radish farming. Conventionally grown cabbage shows the lowest values for weed biomass density and weed cover among all four crops. The canopy height did not change much between both farming systems (Figure 4.6e). For bean, the canopy height was slightly lower for organic (70.0 cm) compared to conventional farming (77.8 cm), and for radish the canopy height was higher for organic (61.7 cm) than for conventional farming (50.8 cm). Potato showed approximately the same canopy height for both systems.

These results demonstrate that weed biomass and especially the ground cover provided by weeds can be highly increased by the absence of herbicides associated with organic farming. For bean, the low weed biomass and cover under organic farming might be explained by the high crop coverage of the plant throughout the growing period, and the resultant constriction of weed development. Although organic farming supports the development of weeds, we also found that for potato, organic farming resulted in a lower crop yield and crop cover, which might be a consequence of crop-weed competition or herbivory due to the absence of herbicides and pesticides.

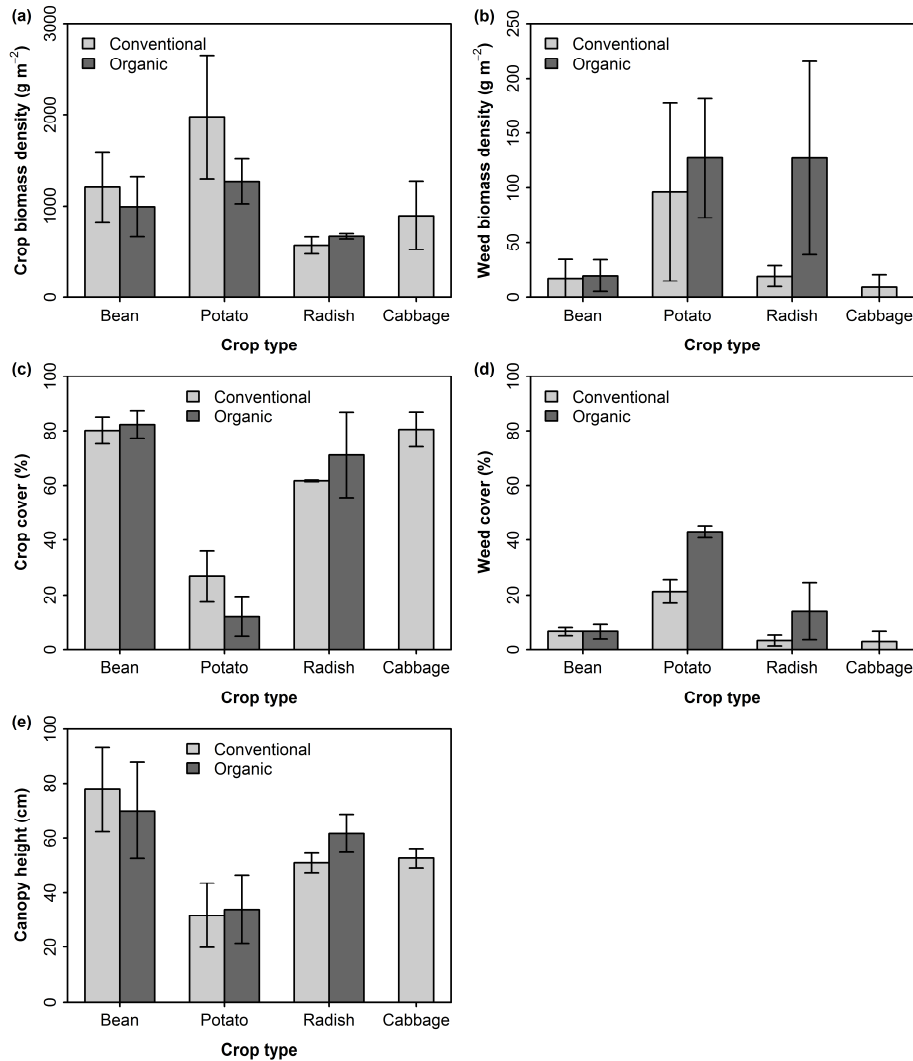


Figure 4.6 Vegetation parameters of crops and weeds measured before harvest for conventional and organic farming of four major row crops. Crop and weed biomass density (a and b), crop and weed cover (c and d), and canopy height (e). The bars show the mean value and the error bars the standard deviation of the associated field sites

The calculated *C-factors* for the four main crops and the two management types show a high variability over the 13 year period in terms of the level of disturbance, and the timing of planting and harvesting (Figure 4.7).

For bean (Figure 4.7a), maximum *C-factors* were calculated for the years 2002, 2009, and 2011, when rain events occurred in April and May. Bean did not show a considerably different *C-factor* between low and high levels of disturbance at harvest, as it is harvested at the end of October when the monsoon season is already over. Bean fields are more susceptible to erosive rain events early in the year, when fields are not yet cultivated. For all 13 years, a higher *C-factor* was therefore calculated for late planting and harvesting, rather than for an earlier schedule. No difference between conventional and organic bean farming was detected, in accordance with the similar measured crop and weed parameters.

For potato (Figure 4.7b), maximum *C-factors* were calculated for the years 2000, 2003, 2007, and 2010, when erosive rain events occurred late in the year, at which stage the potato is already harvested. For a high level of disturbance at harvest, a higher *C-factor* was calculated, affecting primarily the early planting and harvest scenario. Potato is generally planted early in the year, which makes potato fields more susceptible to late rainstorm events. Therefore, early planting and harvest resulted in much higher *C-factors* for all 13 years than a late schedule. Organic

farming generally showed slightly higher *C-factors* than conventional farming, which can be explained by the lower crop biomass and surface cover by crop residue, which has a stronger effect than the higher weed cover and biomass of the organic system. The difference between organic and conventional farming was higher where a low level of disturbance occurred at harvest, as less crop residue, which can act as surface cover, is incorporated.

For radish (Figure 4.7c), the years with maximum *C-factors* were different for the early and late planting and harvest scenarios. For early planting and harvest, peaks were calculated for the same years as for potato (2000, 2003, 2007, and 2010). For late planting and harvest, the highest *C-factors* were calculated for the years 2005, 2009, and 2011, when erosive rain events occurred early in the year. Also for radish, a high level of disturbance resulted in higher *C-factors*, affecting primarily the early planting and harvest scenario. Radish has a relatively short growing period compared to bean and potato, which makes radish fields susceptible for those years with late rain events, if planting and harvesting occurs earlier, as well as for those years with early rain events, if planting and harvesting occurs late. On average, early planting and harvesting resulted in higher *C-factors* than a later planting and harvesting schedule. Contrary to potato, for radish, lower *C-factors* were calculated for organic than for conventional farming for all 13 years, due to the higher weed biomass and cover, but also as a result of the slightly higher crop biomass and cover. The difference between organic and conventional farming was considerably higher where a high level of disturbance occurred at harvest and for the early planting and harvesting scenarios. The advantage of higher weed cover for organic farming is reduced by a high disturbance, but at the same time a large amount of residue is added to the soil from the high weed biomass pool, which increases the soil stability. Additionally, by the removal of plastic associated with the higher disturbance, a larger amount of soil is exposed, but the ratio of the remaining surface cover for organic farming becomes higher than before, due to higher residue coverage. For early planting and harvesting, this has a much stronger impact on the *C-factor*, because it affects only the late rainstorm events. On the contrary, for low disturbance levels in combination with late planting and harvesting, the differences between organic and conventional farming practices were almost negligible.

For cabbage (Figure 4.7d), the years with the highest *C-factors* were also different between the early and late planting and harvesting scenarios. Cabbage has the shortest growing period of all, and is therefore affected by both early and late rain events. To what degree the rain events affect the *C-factor* depends again on the planting and harvesting schedule. For early planting and harvesting, the highest values were calculated for the years 2002 and 2003, when rain events occurred late in the year. For late planting and harvesting, the maximum values were found for 2000, 2002, 2004, and 2009, when rain events occurred earlier (similar to bean). On average, the scenarios of early and late planting and harvest did not result in considerably different *C-factors*. The higher level of disturbance at harvest resulted in higher *C-factors* for cabbage as a result of the reduced surface cover.

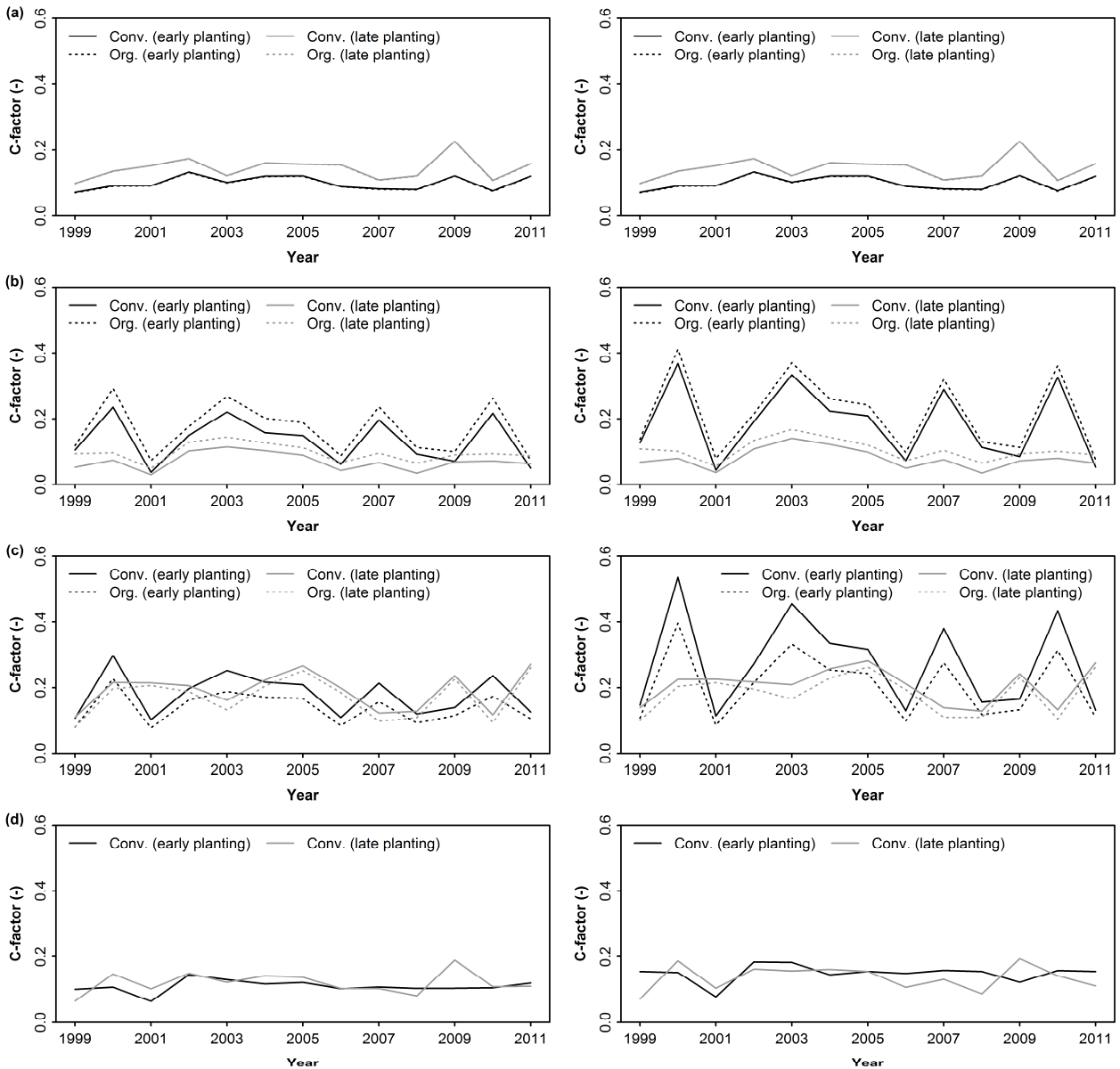


Figure 4.7 Variation of the *C-factor* between 1999 and 2011 for conventional (conv.) and organic farming (org.) of the four major row crops, bean (a), potato (b), radish (c), and cabbage (d) for a low degree of disturbance (left) and a high degree of disturbance at harvest (right), and variable planting and harvest times. Early planting means two weeks before, and late planting two weeks after the observed planting and harvest dates of 2009

The average annual *C-factor* calculated over all scenarios and years was highest for radish with 0.202 for conventional farming, and 0.166 for organic farming. For bean, average annual *C-factors* of 0.121 and 0.120 were calculated for conventional and organic farming, respectively. For potato, the calculated *C-factors* were 0.113 for conventional, and 0.141 for organic farming. For conventional cabbage, the average annual *C-factor* was 0.128.

4.3.5 Soil erosion rates

According to the highest *C-factor*, radish also showed the highest average annual soil erosion rate over all 25 field sites (Table 4.2). The high erosion for radish can be explained by the relatively short growing period, the higher disturbance and lower amount of crop residue remaining on the field after harvest compared to the other crops. The growing period of cabbage is shorter than that for radish, but less disturbance takes place due to above-ground harvesting, and a higher

residue cover reduces the erosion risk. Potato requires the highest disturbance at harvest, but due to the longer growing period, it provides a better soil protection than radish. Bean provides a high coverage due to a very long growing period, but because of the relatively late planting, fields are still vulnerable to early rainstorm events, which results in soil loss rates similar to those of potato and cabbage.

The mean annual soil loss of radish was reduced by 18% by organic farming ($45.0 \text{ t ha}^{-1} \text{ yr}^{-1}$) compared to conventional farming ($54.8 \text{ t ha}^{-1} \text{ yr}^{-1}$) due to the higher weed biomass density and weed cover at the end of the growing season, as a consequence of the absence of agricultural chemicals. Also the slightly higher crop biomass and coverage contributed to the lower soil loss rate. Nevertheless, our results demonstrate that the protective effect of weeds can not sufficiently counteract the negative effects of the short growing period in combination with low residue and high disturbance, because the average erosion for organic radish is still higher than those of the other three crops. For potato, the soil loss rate was increased by 25% by organic farming ($38.2 \text{ t ha}^{-1} \text{ yr}^{-1}$) compared to conventional farming ($30.6 \text{ t ha}^{-1} \text{ yr}^{-1}$) due to a reduced crop biomass density and cover. Although, weed biomass and cover was increased by the absence of agricultural chemicals, the negative effects of a reduced crop yield had a more significant impact. However, our results also demonstrate that a reduced crop yield for potato as a possible consequence of crop-weed competition or herbivory associated with organic farming, does not dramatically increase erosion, because the average soil loss does not strongly exceed those of bean or cabbage, and is still lower than those of radish. For bean, no considerable difference between organic farming ($32.5 \text{ t ha}^{-1} \text{ yr}^{-1}$) and conventional farming ($32.8 \text{ t ha}^{-1} \text{ yr}^{-1}$) could be identified according to similar vegetation characteristics of crops and weeds for both farming systems.

The highest soil erosion rates among the 25 field sites were calculated for site 04 with values between $93.0 \text{ t ha}^{-1} \text{ yr}^{-1}$ (conventional potato) and $166.4 \text{ t ha}^{-1} \text{ yr}^{-1}$ (conventional radish). Site 04 is characterized by a relatively steep hillslope in combination with a high slope length (Table 4.1). The lowest erosion was calculated for site 10 with rates between $0.4 \text{ t ha}^{-1} \text{ yr}^{-1}$ and $0.7 \text{ t ha}^{-1} \text{ yr}^{-1}$. Also the sites 08, 15, 23 and 24 showed similarly low soil loss rates. These sites are located in the center of the catchment and do not have considerable slope angles (Table 4.1).

Table 4.2 Simulated average annual soil loss for conventional and organic farming of the four major row crops in the Haeen catchment. Mean, maximum and minimum refer to the simulated soil loss over all 25 field sites

Crop type	Management system	Average annual soil loss ($\text{t ha}^{-1} \text{ yr}^{-1}$)		
		Mean	Maximum	Minimum
bean	conventional	32.8	99.6	0.4
	organic	32.5	98.7	0.4
potato	conventional	30.6	93.0	0.4
	organic	38.2	116.1	0.5
radish	conventional	54.8	166.4	0.7
	organic	45.0	136.7	0.6
cabbage	conventional	34.7	105.4	0.4

4.3.6 Model plausibility

The comparison between the simulated and observed soil loss amounts from July to August 2010 showed a strong underestimation for site M1 and a slight overestimation for site M2 (Table 4.3). The rainfall erosivity calculated from rain gauge records during the measuring period in 2010 was lower for site M1 ($363.9 \text{ MJ mm ha}^{-1} \text{ h}^{-1}$) than for site M2 ($588.2 \text{ MJ mm ha}^{-1} \text{ h}^{-1}$). However, the simulated soil loss for site M1 (1.27 t ha^{-1}) was almost twice as much as the simulated soil loss of site M2 (0.71 t ha^{-1}) as a result of the higher *S-factor* and *C-factor*. Both observation sites had similar soil conditions, and soil texture was sandy loam, and organic matter content was 3.0% for both sites. The

average slope lengths were also very similar for site M1 and M2 with 23.9 m and 25.1 m, respectively. Therefore, the calculated *K-factor* and *L-factor* were very similar for both sites. Site M1 (9.6°) was slightly steeper than M2 (8.1°), which resulted in a higher *S-factor*. The main difference between both sites was the lower crop cover during the observation period on site M1 (72%) compared to M2 (94%), which resulted in highly varying *C-factors*, and therefore a higher simulated soil loss for site M1. However, even though the RUSLE model produced a much higher erosion rate for site M1 compared to M2, the actual soil loss on M1 was still highly underestimated. This insufficient performance might be partially explained by the higher runoff generation associated with the plastic mulch, which cannot be adequately modeled by RUSLE. The model does not contain parameters that can be used to control the infiltration capacity as a result of an impermeable surface cover. Effects of the plastic mulch cultivation could be therefore only incorporated in the surface cover subfactor (*SC*) and roughness subfactor (*SR*). Our field observations, however, showed that plastic mulch can considerably increase runoff generation and soil erosion. On site M1, we observed severe gully erosion generated by ridge breakovers as a consequence of accumulated surface runoff. Runoff was concentrated in the furrows and drained to the center of the field, where it formed a gully that produced this high observed erosion rate of 3.65 t ha⁻¹.

Table 4.3 Rainfall erosivity, factors for the Revised Universal Soil Loss Equation, and simulated soil loss for the sites M1 and M2 in comparison to the observed soil loss measured during the monsoon season of 2010

Site	<i>EI₃₀</i> (MJ mm ha ⁻¹ h ⁻¹)	<i>K-factor</i> (t h MJ ⁻¹ mm ⁻¹)	<i>L-factor</i> (-)	<i>S-factor</i> (-)	<i>C-factor</i> (-)	<i>P-factor</i> (-)	Simulated soil loss (t ha ⁻¹)	Observed soil loss (t ha ⁻¹)
M1	363.9	0.0286	1.047	2.310	0.055	0.917	1.27	3.65
M2	588.2	0.0275	1.075	1.856	0.024	0.911	0.71	0.63

The ¹³⁷Cs analyses carried out by Meusburger *et al.* (2012a) revealed long-term soil loss rates of 9.1 t ha⁻¹ yr⁻¹ on the recently deforested site, and 41.8 t ha⁻¹ yr⁻¹ on the long-term farmland site. Although, this study was carried out on different fields, our simulated erosion rates (Table 4.2) reflect the average observed erosion rate of the long-term farmland site. Also other erosion studies on dryland fields in the Kangwon Province show similar values. Jung *et al.* (2003) found an average erosion rate of 47.5 t ha⁻¹ yr⁻¹, and Choi *et al.* (2005) reported erosion rates between 4.2 and 29.6 t ha⁻¹ yr⁻¹ for potato, and 3.3 and 81.6 t ha⁻¹ yr⁻¹ for radish.

Although, the RUSLE model can not accurately reproduce erosion processes associated with plastic mulch cultivation, the comparison to other studies in the Haean catchment and Kangwon Province show that the long-term simulated erosion rates are plausible. We had to assume a number of simplifications during the model parameterization, most notable prior and after the growing season. However, the simulated soil loss rates adequately reflect the actual annual erosion in this region, as erosive rain events are concentrated only in the monsoon season, and hence, the effects of weed growth and residue decomposition play only a marginal role after harvest.

4.4 Summary and conclusions

In this study, we analyzed the effect of conventional and organic farming on soil erosion of row crop cultivation on mountainous farmland in South Korea. We measured multiple vegetation parameters of four major row crops (bean, potato, radish, and cabbage), as well as those of weeds from different fields of conventional and organic farms, and simulated the long-term soil loss using the Revised Universal Soil Loss Equation (RUSLE). The comparison of the model results to the observed soil erosion rates demonstrated an acceptable performance of RUSLE for row crop

cultivation in this region. We found the highest erosion rate for radish due to the shorter growing period in combination with high soil disturbance at harvest and low amounts of remaining residue. Nevertheless, the simulated erosion rates for the other three crops were not considerably lower. Organic farming reduced soil loss for radish due to higher weed coverage, but increased erosion for potato due to lower crop yield.

These results demonstrate that the absence of agricultural chemicals, especially herbicides, in organic farming systems can reduce soil erosion for row crops due to the development of weeds in the furrows. However, our results also show that a reduced crop yield associated with crop-weed competition or herbivory outbalances the positive effects of weeds, and can therefore produce higher erosion rates in organic farming systems.

Nevertheless, in both cases the difference in soil loss between the farming systems is relatively small, and the effects of weed coverage and crop yield are highly variable depending on the timing of planting and harvest in relation to the occurrence of rainstorm events, and the degree of soil disturbance. The simulated average annual soil loss for both management systems exceeds, by far, any tolerable soil loss rates. The OECD (2001) defined soil loss as tolerable when it is less than $6.0 \text{ t ha}^{-1} \text{ yr}^{-1}$, and severe when it exceeds $33.0 \text{ t ha}^{-1} \text{ yr}^{-1}$. The average annual erosion rate for all four row crops in this study is at least at the limit of severe erosion, and well above in many cases. Our results also show that the maximum erosion rates can be three to four times higher than the average values depending on field topography.

We can therefore conclude that neither farming system sufficiently lowers the amount of soil erosion of row crop cultivation on mountainous farmland. Although we identified a protective effect of a high weed coverage associated with the absence of herbicides, organic farming alone cannot be used to effectively control soil erosion. Both farming systems require additional conservation measures to prevent soil loss from row crop fields in this region. Especially after harvest, when soil is disturbed and ground cover is low, fields are very susceptible to erosion. The work of Kim *et al.* (2007) suggests that winter crop cultivation with ryegrass can be used to protect the soil after the growing season. However, the development of a high coverage that effectively reduces soil loss takes time and requires early sowing (Morgan, 2005). Soil protection may, therefore, be more effective in the following year, before seed bed preparation is carried out. The incorporation of ryegrass residue into the soil may provide additional beneficial effects on soil properties and crop yields, but requires further investigation (Kim *et al.*, 2007). To improve the protection of the furrows during the growing period, Rice *et al.* (2007) suggested cereal grass cultivation to increase the infiltration capacity and reduce runoff flow velocity. However, cultivating cover crops during the growing season could involve competition with the main crop, which could result in lower yields. Another very effective measure to prevent erosion is mulching with plant residues (Morgan 2005). Our results show that surface cover by plant residue is more effective than the canopy cover provided by weeds. Plant residue can therefore be used to cover furrows instead of cultivating cover crops that may have negative impact on crop yield. Also Kim *et al.* (2007) found in their study that ryegrass residue mulching significantly reduces soil loss on row crop fields. We recommend residue mulching during the growing season in combination with winter cover crops after harvest for conventional and organic farming to prevent soil erosion for row crop cultivation on mountainous farmland.

4.5 Acknowledgements

This study was carried out within the framework of the International Research Training Group TERRECO funded by the German Research Foundation (DFG) and the Korea Science and Engineering Foundation (KOSEF), and with the support of the Cooperative Research Program for Agricultural Science and Technology Development (Project no. PJ9070882012) of the Rural Development Administration in Korea. The authors thank especially Heera Lee, Miyeon

Park, Marianne Ruidisch, Melanie Hauer, Balint Jakli, Feelgeun Song, and Hoyun Jang for their help during the field measurements and sample preparation, Bumsuk Seo for his invaluable support in programming the R algorithms, and Eunyong Jung for translation and for negotiating the permissions to carry out this study.

4.6 References

- Afandi, G., Manik, T. K., Rosadi, B., Utomo, M., Senge, M., Adachi, T., Oki, Y., 2002. Soil erosion under coffee trees with different weed managements in humid tropical hilly area of Lampung, South Sumatra, Indonesia. *Journal of the Japanese Society of Soil Physics* **91**, 3-14.
- Auerswald, K., Kainz, M., Fiener, P., 2003. Soil erosion potential of organic versus conventional farming evaluated by USLE modelling of cropping statistics for agricultural districts in Bavaria. *Soil Use and Management* **19**, 305-311.
- Bennett, H. H., 1939. *Soil conservation*. McGraw-Hill, New York.
- Blavet, D., De Noni, G., Le Bissonnais, Y., Leonard, M., Maillou, L., Laurent, J. Y., Asseline, J., Leprun, J. C., Arshad, M. A., Roose, E., 2009. Effect of land use and management on the early stages of soil water erosion in French Mediterranean vineyards. *Soil and Tillage Research* **106**(1), 124-136.
- Bonilla, C. A., Kroll, D. G., Norman, J. M., Yoder, D. C., Molling, C. C., Miller, P. S., Panuska, J. C., Topel, J. B., Wakeman, P. L., Karthikeyan, K. G., 2006. Instrumentation for measuring runoff, sediment, and chemical losses from agricultural fields. *Journal of Environmental Quality* **35**, 216-223.
- Brock, B. G., 1982. Weed control versus soil erosion control. *Journal of Soil and Water Conservation* **37**(2), 73-76.
- Brown, L. C., Foster, G. R., 1987. Storm erosivity using idealized intensity distributions. *Transactions of the ASAE* **30**(2), 379-386.
- Cho, H., Ha, S., Hur, S., Han, K., Jeon, S., Hyun, S., Kim, E., Lee, D., 2010. Red pepper coverage effect on soil erosion by different transplanting dates, in: Gilkes, R. J., Prakongkep, N. (Eds.), *Proceedings of the 19th World Congress of Soil Science. Soil solutions for a changing world*. International Union of Soil Sciences, pp. 62-64.
- Choi, G., Kwon, W., Boo, K., Cha, Y., 2008. Recent spatial and temporal changes in means and extreme events of temperature and precipitation across the Republic of Korea. *Journal of the Korean Geographical Society* **43**(5), 681-700.
- Choi, J., Choi, Y., Lim, K., Shin, Y., 2005. Soil erosion measurement and control techniques, in: Chung, N., Kim, W., Kim, H., Kim, J., Eom, K., Lee, I. (Eds.), *Proceedings of the International Workshop on Newly Developed Innovative Technology for Soil and Water Conservation*. Rural Development Administration.
- Choo, H., Jamal, T., 2009. Tourism on organic farms in South Korea: a new form of ecotourism? *Journal of Sustainable Tourism* **17**(4), 431-454.
- Cochrane, T. A., Flanagan, D. C., 2003. Representative hillslope methods for applying the WEPP model with DEMs and GIS. *Transactions of the ASAE* **46**(4), 1041-1049.
- Eltun, R., Korsæth, A., Nordheim, O., 2002. A comparison of environmental, soil fertility, yield, and economical effects in six cropping systems based on an 8-year experiment in Norway. *Agriculture, Ecosystems and Environment* **90**, 155-168.
- Erhart, E., Hartl, W., 2010. Soil protection through organic farming: a review, in: Lichtfouse, E. (Ed.), *Sustainable agriculture reviews. Organic farming, pest control and remediation of soil pollutants*. Springer, Dordrecht, pp. 203-226.
- Fleming, K. L., Powers, W. L., Jones, A. J., Helmers, G. A., 1997. Alternative production systems' effects on the K-factor of the Revised Universal Soil Loss Equation. *American Journal of Alternative Agriculture* **12**(2), 55-58.
- Foster, G. R., McCool, D. K., Renard, K. G., Moldenhauer, W. C., 1981. Conversion of the Universal Soil Loss Equation to SI metric units. *Journal of Soil and Water Conservation* **36**(6), 355-359.
- García-Orenes, F., Cerdà, A., Mataix-Solera, J., Guerrero, C., Bodí, M. B., Arcenegui, V., Zornoza, R., Sempere, J. G., 2009. Effects of agricultural management on surface soil properties and soil-water losses in eastern Spain. *Soil and Tillage Research* **106**(1), 117-123.

- Goh, K. M., 2011. Greater mitigation of climate change by organic than conventional agriculture: a review. *Biological Agriculture and Horticulture* **27**, 205-230.
- Gomiero, T., Pimentel, D., Paoletti, M. G., 2011. Environmental impact of different agricultural management practices: conventional vs. organic agriculture. *Critical Reviews in Plant Sciences* **30**(1-2), 95-124.
- Jung, K., Son, Y., Hur, S., Ha, S., Jang, Y., Jung, P., 2003. *Estimation of nationwide soil loss with soil type*. National Academy of Agricultural Science (NAAS), Research Report.
- Jung, P., Ko, M., Im, J., Um, K., Choi, D., 1983. Rainfall erosion factor for estimating soil loss. *Korean Journal of Soil Science and Fertilizer* **16**(2), 112-118.
- Kang, J., Kim, C., 2000. Technical change and policy implications for developing environmentally-friendly agriculture in Korea. *Journal of Rural Development* **23**, 163-182.
- Kim, B., Choi, K., Kim, C., Lee, U., Kim, Y., 2000. Effects of the summer monsoon on the distribution and loading of organic carbon in a deep reservoir, Lake Soyang, Korea. *Water Research* **34**(14), 3495-3504.
- Kim, B., Jung, S., 2007. Turbid storm runoffs in Lake Soyang and their environmental effect. *Journal of the Korean Society of Environmental Engineers* **29**(11), 1185-1190.
- Kim, C., Jeong, H., Moon, D., 2012. *Production and consumption status and market prospects for environment-friendly agri-foods*. Korea Rural Economic Institute (KREI), Research Report.
- Kim, C., Kim, T., 2004. Economics of conversion to environmentally friendly practices of rice production. *Journal of Rural Development* **27**, 91-112.
- Kim, K., Ahn, J., Lee, J., Hong, S., Hwang, S., Kim, C., 2008. Evaluation of companion crop for conservation of soil in highland cultivation of Chinese cabbage. *Journal of Bio-Environment Control* **17**(1), 1-8.
- Kim, M., Flanagan, D. C., Frankenberger, J. R., Meyer, C. R., 2009. Impact of precipitation changes on runoff and soil erosion in Korea using CLIGEN and WEPP. *Journal of Soil and Water Conservation* **64**(2), 154-162.
- Kim, P., Chung, D., Malo, D., 2001. Characteristics of phosphorus accumulation in soils under organic and conventional farming in plastic film houses in Korea. *Soil Science and Plant Nutrition* **47**(2), 281-289.
- Kim, S., Yang, J., Park, C., Jung, Y., Cho, B., 2007. Effects of winter cover crop of ryegrass (*Lolium multiflorum*) and soil conservation practices on soil erosion and quality in the sloping uplands. *Journal of Applied Biological Chemistry* **55**(1), 22-28.
- Kuhn, N. J., Armstrong, E. K., Ling, A. C., Connolly, K. L., Heckrath, G., 2012. Interrill erosion of carbon and phosphorus from conventionally and organically farmed Devon silt soils. *Catena* **91**, 94-103.
- Lee, J., Heo, J., 2011. Evaluation of estimation methods for rainfall erosivity based on annual precipitation in Korea. *Journal of Hydrology* **409**(1-2), 30-48.
- Leek, R., Olsen, P., 2000. Modelling climatic erosivity as a factor for soil erosion in Denmark: changes and temporal trends. *Soil Use and Management* **16**, 61-65.
- Leonard, R. A., Knisel, W. G., Still, D. A., 1987. GLEAMS: Groundwater Loading Effects of Agricultural Management Systems. *Transactions of the ASAE* **30**(5), 1403-1418.
- Lockeretz, W., Shearer, G., Kohl, D. H., 1981. Organic farming in the Corn Belt. *Science* **211**, 540-547.
- López-Vicente, M., Navas, A., Machín, J., 2008. Identifying erosive periods by using RUSLE factors in mountain fields of the Central Spanish Pyrenees. *Hydrology and Earth System Sciences* **12**, 523-535.
- Lotter, D. W., Seidel, R., Liebhardt, W., 2003. The performance of organic and conventional cropping systems in an extreme climate year. *American Journal of Alternative Agriculture* **18**(3), 146-154.
- Mabit, L., Bernard, C., Makhlof, M., Laverdière, M. R., 2008. Spatial variability of erosion and soil organic matter content estimated from ¹³⁷Cs measurements and geostatistics. *Geoderma* **145**, 245-251.
- Meusburger, K., Jeong, J., Mabit, L., Park, J., Sandor, T., Alewell, C., 2012a. Effect of deforestation on soil erosion rates using fallout radionuclides - a case study in a mountainous catchment, South Korea, *in preparation*.
- Meusburger, K., Steel, A., Panagos, P., Montanarella, L., Alewell, C., 2012b. Spatial and temporal variability of rainfall erosivity factor for Switzerland. *Hydrology and Earth System Sciences* **16**(1), 167-177.
- Morgan, R. P. C., 2005. *Soil erosion and conservation*, third ed. Blackwell, Malden.

- Organization for Economic Cooperation and Development (OECD), 2001. *Environmental indicators for agriculture*. OECD Publications, Paris.
- Pacini, C., Wossink, A., Giesen, G., Vazzana, C., Huirne, R., 2003. Evaluation of sustainability of organic, integrated and conventional farming systems: a farm and field-scale analysis. *Agriculture, Ecosystems and Environment* **95**(1), 273-288.
- Park, J., Duan L., Kim, B., Mitchell, M. J., Shibata, H., 2010a. Potential effects of climate change and variability on watershed biogeochemical processes and water quality in Northeast Asia. *Environment International* **36**, 212-225.
- Park, J., Woo, H., Pyun, C. K., Kim, K., 2000. A study of distribution of rainfall erosivity in USLE / RUSLE for estimation of soil loss. *Journal of Korea Water Resources Association* **33**(5), 603-610.
- Park, S., Oh, C., Jeon, S., Jung, H., Choi, C., 2011. Soil erosion risk in Korean watersheds, assessed using the Revised Universal Soil Loss Equation. *Journal of Hydrology* **399**(3-4), 263-273.
- Park, Y., Kim, J., Kim, N., Kim, S., Jeon, J., Engel, B. A., Jang, W., Lim, K., 2010b. Development of new R, C and SDR modules for the SATEEC GIS system. *Computers and Geosciences* **36**(6), 726-734.
- Reganold, J. P., Elliott, L. F., Unger, Y. L., 1987. Long-term effects of organic and conventional farming on soil erosion. *Nature* **330**, 370-372.
- Renard, K. G., Foster, G. R., Weesies, G. A., McCool, D. K., Yoder, D. C., 1997. *Predicting soil erosion by water. A guide to conservation planning with the Revised Universal Soil Loss Equation (RUSLE)*. Agriculture Handbook 703. USDA, Washington D.C.
- Renard, K. G., Yoder, D. C., Lightle, D. T., Dabney, S. M., 2011. Universal Soil Loss Equation and Revised Universal Soil Loss Equation, in: Morgan, R. P. C., Nearing, M. A. (Eds.), *Handbook of erosion modelling*. Wiley-Blackwell, Chichester, pp. 137-167.
- Rice, P. J., Harman-Fetcho, J. A., Sadeghi, A. M., McConnell, L. L., Coffman, C. B., Teasdale, J. R., Abdul-Baki, A. A., Starr, J. L., McCarty, G. W., Herbert, R. R., Hapeman, C. J., 2007. Reducing insecticide and fungicide loads in runoff from plastic mulch with vegetative-covered furrows. *Journal of Agricultural and Food Chemistry* **55**(4), 1377-1384.
- Ryu, J., Lee, J., Lee, G., Jin, Y., Zhang, Y., Jung, Y., 2010. Hairy vetch and rye as cover crops to reduce soil erosion from sloped land in highland agriculture, in: Gilkes, R. J., Prakongkep, N. (Eds.), *Proceedings of the 19th World Congress of Soil Science. Soil solutions for a changing world*. International Union of Soil Sciences, pp. 41-43.
- Siegrist, S., Schaub, D., Pfiffner, L., Mäder, P., 1998. Does organic agriculture reduce soil erodibility? The results of a long-term field study on loess in Switzerland. *Agriculture, Ecosystems and Environment* **69**, 253-264.
- Toy, T. J., Foster, G. R., Renard, K. G., 2002. *Soil erosion. Processes, prediction, measurement, and control*. John Wiley and Sons, New York.
- United States Department of Agriculture (USDA), 2008. *Revised Universal Soil Loss Equation version 2. Science documentation*. USDA, Washington D.C.
- Weil, R. R., 1982. Maize-weed competition and soil erosion in unweeded maize. *Tropical Agriculture (Trinidad)* **59**(3), 207-213.
- Wischmeier, W. H., Johnson, C. B., Cross, B. V., 1971. A soil erodibility nomograph for farmland and construction sites. *Journal of Soil and Water Conservation* **26**(5), 189-193.
- Wischmeier, W. H., Smith, D. D., 1978. *Predicting rainfall erosion losses. A guide to conservation planning*. Agriculture Handbook 537. USDA, Washington D.C.

Appendix

List of other publications

Ruidisch, M., Kettering, J., Arnhold, S., Huwe, B., 2012. Modeling water flow in a plastic mulched ridge cultivation system on hillslopes affected by South Korean summer monsoon. *Agricultural Water Management*, *in press*.

Declaration / Erklärung

I hereby declare, to the best of my knowledge and belief, that this thesis does not contain any material previously published or written by another person, except where due reference has been made in the text. This thesis contains no material, which has been previously accepted or definitely rejected for award of any other doctoral degree at any university or equivalent institution.

Bayreuth, 09.10.2012

Sebastian Arnhold

Hiermit erkläre ich, dass ich die vorliegende Promotionsarbeit selbständig verfasst und keine anderen als die angegebenen Quellen und Hilfsmittel benutzt habe.

Bayreuth, 09.10.2012

Sebastian Arnhold

Hiermit erkläre ich, dass ich nicht bereits anderweitig versucht habe, diese Dissertation ohne Erfolg einzureichen oder mich einer Doktorprüfung zu unterziehen.

Bayreuth, 09.10.2012

Sebastian Arnhold

Hiermit erkläre ich, dass ich die Hilfe von gewerblichen Promotionsberatern bzw. -vermittlern weder bisher in Anspruch genommen habe, noch künftig in Anspruch nehmen werde.

Bayreuth, 09.10.2012

Sebastian Arnhold